RECLAMATION

Managing Water in the West

Technical Memorandum No. 86-68210-2016-01

West-Wide Climate Risk Assessments: Hydroclimate Projections

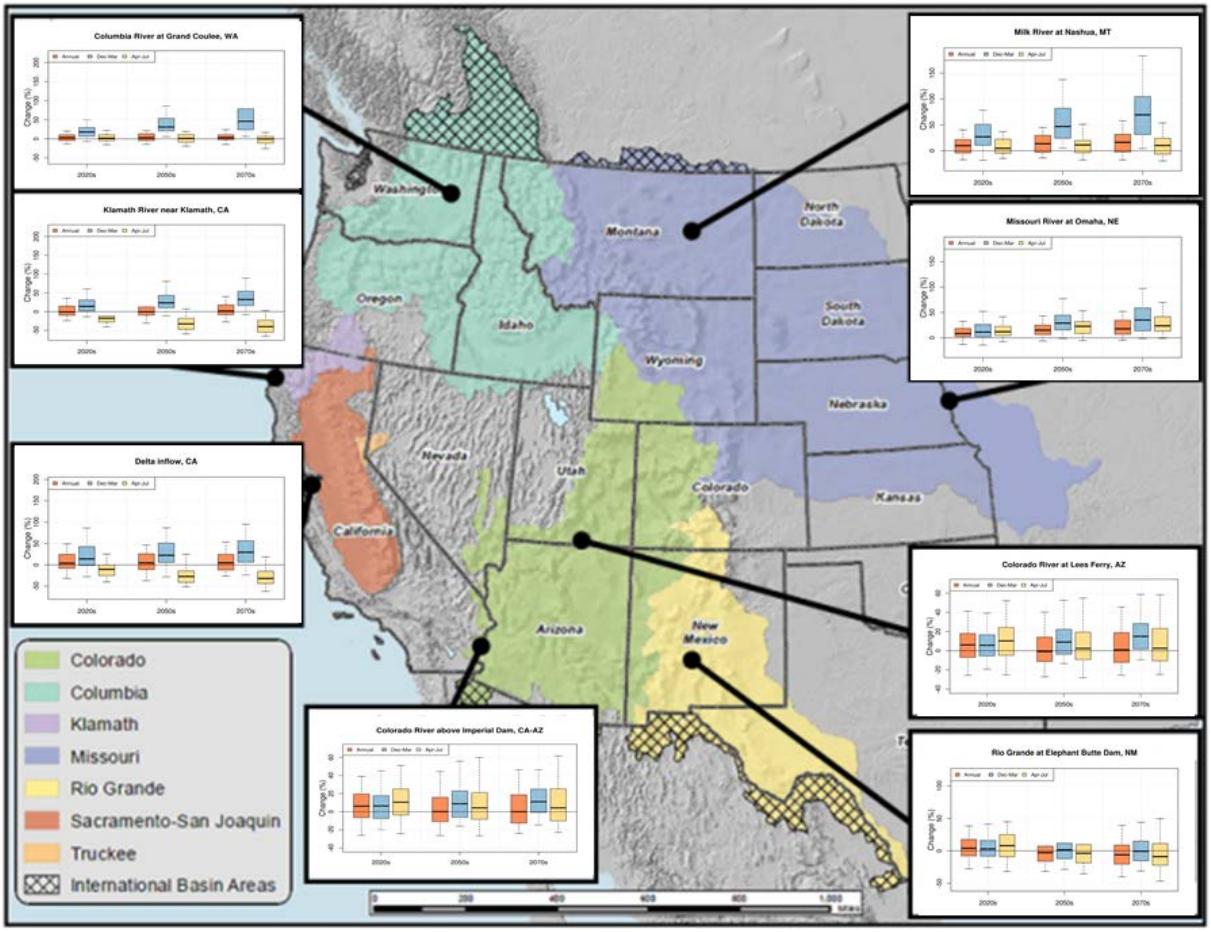

U.S. Department of the Interior
Bureau of Reclamation
Technical Service Center
Denver, Colorado

March 2016

Mission Statements

U.S. DEPARTMENT OF THE INTERIOR

The U.S. Department of the Interior protects America's natural resources and heritage, honors our cultures and tribal communities, and supplies the energy to power our future.

U.S. BUREAU OF RECLAMATION

The mission of the Bureau of Reclamation is to manage, develop, and protect water and related resources in an environmentally and economically sound manner in the interest of the American public.

Technical Memorandum No. 86-68210-2016-01

West-Wide Climate Risk Assessments: Hydroclimate Projections

Prepared by Bureau of Reclamation:

Technical Service Center

Water and Environmental Resources Division
Water Resources Planning and Operations Support Group
Subhrendu Gangopadhyay
Tom Pruitt

Policy and Administration

Water Resources and Planning Division
Katharine G. Dahm

Review and contributions in alphabetical order:
Pamela S. Adams, Bureau of Reclamation
Donald M. Anderson, Bureau of Reclamation
Jeff Arnold, U.S. Army Corps of Engineers
Levi D. Brekke, Bureau of Reclamation
Martyn P. Clark, National Center for Atmospheric Research
Jennifer E. Cuhaciyan, Bureau of Reclamation
Patrick J. Erger, Bureau of Reclamation
Timothy R. Green, U.S. Department of Agriculture, Agricultural Research Service
Ethan Gutmann, National Center for Atmospheric Research
Lauren E. Hay, U.S. Geological Survey
Shih-Chieh Kao, Oak Ridge National Laboratories
Dagmar K. Llewellyn, Bureau of Reclamation
Gregory T. Pederson, U.S. Geological Survey
James R. Prairie, Bureau of Reclamation
Eric L. Rothwell, Bureau of Reclamation
Noe I. Santos, Bureau of Reclamation
Andy W. Wood, National Center for Atmospheric Research
Christopher P. Weaver, U.S. Global Change Research Program

U.S. Department of the Interior
Bureau of Reclamation
Technical Service Center
Denver, Colorado

March 2016

This page intentionally left blank.

Executive Summary

Public Law 111-11, Title IX, Subtitle F (SECURE Water Act), Section (§) 9503 authorizes the U.S. Department of the Interior's Bureau of Reclamation (Reclamation) to assess climate change risks for water and environmental resources in major Reclamation river basins. Section 9503 also includes the authorities to evaluate potential climate change impacts on water resource management and development of strategies to either mitigate for or adapt to impacts. The major Reclamation river basins listed within the SECURE Water Act are the Colorado, Columbia, Klamath, Missouri, Rio Grande, Sacramento, San Joaquin, and Truckee River Basins. Reclamation is accomplishing the SECURE Water Act authorities through activities within its WaterSMART Basin Study Program.

This technical assessment report provides an analysis of changes in hydroclimate variables—namely, precipitation, temperature, snow-water equivalent, and streamflow—across the major Reclamation river basins, and it is the technical foundation for Chapter 2 of the 2016 SECURE Water Act Report to Congress and the SECURE Water Act Report Data Visualization Tool. This technical report updates the 2011 SECURE Water Act Report assessment using the most current hydrologic projections developed as part of the World Climate Research Programme's Coupled Model Intercomparison Project Phase 5 (CMIP5). Overall, the difference between these CMIP5 projections and the earlier Phase 3 (CMIP3) projections is relatively minor when assessing the range of basin-scale potential future climate and hydrologic conditions.

The following summary statements of future hydrologic impacts are consistent with the mean changes in temperature and precipitation derived from these projections, characterized generally across the western United States:

- Temperature increases have already resulted in decreased snowpack, differences in the timing and volume of spring runoff, and an increase in peak flows for some western U.S. basins. The impacts to snowpack and runoff affect the timing and availability of water supplies.
- Warming is expected to continue, causing further impacts to supplies, increasing agricultural water demands, and affecting the seasonal demand for hydropower electricity.
- Precipitation patterns are also expected to change, interacting with warming to cause longer-term and more frequent droughts and larger and more numerous floods, varying by basin.
- Cool-season runoff is projected to increase over the West Coast basins, from California to Washington, and over the North-Central U.S., but little change

to slight decreases are projected over the southwestern U.S. and the Southern Rockies.

- Warm-season runoff is projected to decrease substantially over a region spanning southern Oregon, the southwestern U.S., and the Southern Rockies. However, north of this region, warm-season runoff is projected to change little or to slightly increase.
- Projected increasing precipitation in the northern tier of the western U.S. could counteract warming-related decreases in warm-season runoff, whereas projected decreases in precipitation in the southern tier of the western U.S. could amplify warming-related decreases in warm season runoff.

Collectively, the impacts of climate change to water resources give rise to difficult questions about how best to operate Reclamation facilities to meet growing demands for water and hydropower now and how to upgrade and maintain infrastructure to optimize operations in the future. More-extreme variations in climate will make it difficult for Reclamation to meet competing demands for water. Warming is expected to continue, causing further impacts on supplies, increasing agricultural water demands, and affecting the seasonal demand for hydropower electricity. The projected increased intensity of droughts and floods also raises concerns about infrastructure safety, the resiliency of species and ecosystems in adapting to these changes, and the ability to maintain adequate levels of hydropower production.

Acronyms and Abbreviations

BCSD	Bias-correction and spatial disaggregation
CMIP	Coupled Model Intercomparison Project (CMIP3 and CMIP5 refer to CMIP phases 3 and 5, respectively)
CONUS	Contiguous United States (the U.S. excluding Alaska and Hawaii)
DCHP	Downscaled climate and hydrology projections
GCM	Global climate model
GHG	greenhouse gas
GIS	Geographic Information System
HCDN	Hydro-Climatic Data Network
ICAR models	Intermediate complexity atmospheric research models
IPCC	Intergovernmental Panel on Climate Change
km	kilometer
LCCs	Landscape Conservation Cooperatives
NARCCP	North American Regional Climate Change Assessment Program
NCA	National Climate Assessment
NOAA	National Oceanic and Atmospheric Administration
PDFs	Probability Density Functions
PET	Potential Evapotranspiration
RCP	Representative Concentration Pathways
Reclamation	Bureau of Reclamation
SECURE	Science and Engineering to Comprehensively Understand and Responsibly Enhance
SWA	SECURE Water Act
SWE	Snow-water equivalent
USGCRP	U.S. Global Change Research Program
VIC	Variable infiltration capacity hydrologic model
WaterSMART	WaterSMART (Sustain and Manage America's Resources for Tomorrow)
WCRP	World Climate Research Programme
WWCRA	West-Wide Climate Risk Assessments

°C	degrees Celsius
°F	degrees Fahrenheit

Table of Contents

Figures

Tables

This page intentionally left blank.

1. Introduction

The Bureau of Reclamation (Reclamation), established in 1902, is best known for the dams, powerplants, and canals it constructed within the 17 western states of the United States. Today, Reclamation is the largest wholesaler of water in the Nation. Reclamation's mission is to manage, develop, and protect water and related resources in an environmentally and economically sound manner in the interest of the American public. As the largest manager and wholesaler of Western water, Reclamation has a responsibility to consider potential risks to water supplies, and to help implement measures that ensure water will be managed as effectively and sustainably as possible.

A growing risk to effective Western water management is climate change. In recent decades, climate science has highlighted a broad suite of future challenges for managing water, in addition to risks already posed by natural variations in climate and pressures associated with growing populations. These challenges include impacts to water supplies, water demands, and environmental conditions that may affect Reclamation's ability to fulfill its mission. In light of these challenges, Reclamation is working with its Western partners to identify appropriate forward-looking adaptive actions that add resiliency and reliability to water-management planning and practices.

The Omnibus Public Land Management Act of 2009 (Public Law 111-11) was enacted on March 30, 2009. Subtitle F of Title IX of that legislation, known as the SECURE[1] Water Act, recognizes that climate change poses a significant challenge to the protection of adequate and safe supplies of water, which are fundamental to the health, economy, security, and ecology of the United States. Section 9503 of the SECURE Water Act authorizes Reclamation to coordinate and partner with others to ensure the use of best available science, to assess specific risks to water supply, to analyze the extent to which water supply risks will impact various water-related benefits and services, to develop appropriate mitigation strategies, and to monitor water resources to support these analyses and assessments.[2]

Section 9503 (Reclamation Climate Change and Water Program) authorizes Reclamation to assess climate change risks for water and environmental resources in major Reclamation river basins. Section 9503 also includes the authorities to

[1] SECURE is the acronym for Science and Engineering to Comprehensively Understand and Responsibly Enhance.

[2] The SECURE Water Act also authorizes the Department of Energy (Section 9505) and the Department of Interior's United States Geological Survey (Sections 9507 and 9508) to assess and report on the impacts of climate change on national hydropower production and water data enrichment, respectively.

evaluate potential climate change impacts on water resource management, and to develop strategies to either mitigate for or adapt to impacts. The major Reclamation river basins listed within the SECURE Water Act include the Colorado, Columbia, Klamath, Missouri, Rio Grande, Sacramento, San Joaquin, and Truckee River Basins. The SECURE Water Act also directs Reclamation to submit reports to Congress 2 years after enactment and every 5 years thereafter, describing progress in carrying out those activities. This assessment is the technical companion document to the 2016 SECURE Water Act report to Congress.

1.1. Reclamation's WaterSMART Program and Activities Addressing the SECURE Water Act

WaterSMART (Sustain and Manage American Resources for Tomorrow) was established in February 2010 by the Department of the Interior as a broad framework for Federal collaboration with states, tribes, local governments, and non-governmental organizations to work toward secure and sustainable water supply. Reclamation has implemented the climate change adaptation activities authorized under Section 9503 of the SECURE Water Act through the **Basin Study Program**, which is part of WaterSMART. The Basin Study Program includes three complementary activities that represent a comprehensive approach to incorporate the best available science into planning activities for climate change adaptation:

- **Basin Studies:** Reclamation partners with basin stakeholders to conduct comprehensive studies to define options for meeting future water demands in river basins in the West where imbalances in supply and demand exist or are projected. Reclamation also works with stakeholders to develop adaptation strategies through the Basin Studies, which are comprehensive technical assessments that identify current or future imbalances between water supply and demand resulting from climate change and other stressors. In response to the identified imbalances, the studies assess options and strategies for meeting future water demands.
- **Landscape Conservation Cooperatives (LCCs):** LCCs provide tools for analyzing and addressing climate change impacts for use in Basin Studies. The LCCs are partnerships of governmental (Federal, state, tribal, and local) and non-governmental entities. The primary goal of the LCCs is to bring together science and resource management to inform climate adaptation strategies to address climate change and other stressors within an ecological region or landscape. Each LCC functions in a specific geographic area; the series of LCCs together form a national network.

Reclamation and the U.S. Fish and Wildlife Service (USFWS) co-lead the Desert and Southern Rockies LCCs. [3]

- **West-Wide Climate Risk Assessments (WWCRAs):** WWCRAs complement the Basin Studies by developing key data on climate-induced risks and impacts to Reclamation's operations (including climate projections and analyses of baseline water supply, water demand, water management operations, and environmental responses). These data provide a foundation for future Basin Studies, as well as for project-specific applications. WWCRAs also generate important information, tools, and guidance that support the integration of climate information into planning activities, consistent with Reclamation's Climate Change Adaptation Strategy.

Reclamation coordinates with the U.S. Geological Survey (USGS), National Oceanic and Atmospheric Survey (NOAA), and the Natural Resources Conservation Service (NRCS) on climate monitoring activities through the **WWCRA Implementation Team**. Climate monitoring objectives for the Implementation Team include:

- Sustain active communication between agencies on monitoring activities, climate and water resources data, and science tools for water management decisions;
- Understand data availability, accessibility, and applicability for direct use and implementation in Reclamation's climate change impact and planning studies; and
- Identify opportunities to improve climate monitoring data available for water management decisions.

Reclamation is using climate monitoring data networks in a broad set of studies to determine impacts and risks to water resources due to climate change. Inter-agency coordination to acquire and maintain water resources data aids in strengthening the understanding of water supply trends and assists in the assessments and analyses conducted by Reclamation. Information generated through WWCRA provides a foundation of climate change data, information, and tools that partners can build from to develop adaptation strategies.

Reclamation is also actively engaged with research partners to develop and share information for a common understanding of climate change impacts to water resources in the West. The **Science and Technology Program** is a Reclamation-

[3] Reclamation also participates in the other LCCs located in the 17 Western states, which include the Great Northern LCC, North Pacific LCC, Great Basin LCC, California LCC, Plains and Prairie Potholes LCC, Great Plains LCC, and Gulf Coast Prairie LCC. Currently, Reclamation is a steering committee member on the Great Northern LCC.

wide competitive, merit-based applied research and development program focused on innovative solutions for water and power challenges in the Western U.S. Reclamation partners with the U. S. Army Corps of Engineers (Corps), USGS, NOAA, and others through the **Climate Change and Water Working Group** (CCAWWG) to identify mutual science needs for short-term water management decisions and long-term planning. These programs are fundamental to developing new information for adapting to climate change by assessing the current state of knowledge, identifying where gaps exist, and finding opportunities to address those gaps.

1.2. The 2011 SECURE Water Act Report

In 2011, Reclamation published the initial *SECURE Water Act Section 9503(c) – Reclamation Climate Change and Water 2011 Report to Congress* (Reclamation, 2011a). That report assessed climate change risks and how those risks could impact water operations, hydropower, flood control, and fish and wildlife in the western U.S. It represented the first consistent and coordinated assessment of risks to future water supplies across eight major Reclamation river basins, and identified several increased risks to western U.S. water resources during the 21st century. Specific projections cited in the report include:

- A temperature increase of 5 to 7 degrees Fahrenheit (°F) during the 21st century;
- A precipitation increase over the northwestern and north-central portions of the western U.S., and a decrease over the southwestern and south-central areas; and
- A decrease across much of the West in April 1st snowpack.

The report noted that projected changes in temperature and precipitation are expected to impact the timing and quantity of stream flows in all western basins, which would impact the amount of water available for farms and cities, hydropower generation, fish and wildlife, and other uses such as recreation.

1.3. WWCRA: Hydroclimate Projections

Beginning in 2010, the WWCRAs developed surface water hydrologic projections over the western United States from contemporary climate projections. These projections are intended to provide risk assessment information for metrics described in the SECURE Water Act 9503(b)(2), including climate change risks to snowpack, changes in the timing of streamflow, and changes in the quantity of runoff. The 2011 SECURE Water Act Report to Congress used the World Climate Research Programme (WCRP) global climate projections developed through its Coupled Model Intercomparison Project (CMIP), which are released

roughly every 5 to 7 years. The 2011 SECURE Water Act assessment was based on hydrologic projections featured in the Fourth Assessment of the Intergovernmental Panel on Climate Change (IPCC). These projections, considered the best available in 2011, had been developed as part of the WCRP CMIP Phase 3 and are referred to here as CMIP3 projections.

This companion technical assessment to the 2016 SECURE Water Act Report to Congress has relied upon the most current hydrologic projections featured in the IPCC's Fifth Assessment, which were developed as part of the WCRP CMIP Phase 5 and are referred to here as CMIP5 Projections. This assessment provides projections of future water supplies in the eight major Reclamation river basins listed in the SECURE Water Act, characterized in a manner consistent with the approach used in the 2011 SECURE Water Act Report to Congress. The evaluation includes an assessment of future climate conditions over the basin (i.e., precipitation and temperature), as well as the surface water hydrologic response (i.e., snow-water equivalent, or the water available from snowpack) and runoff.

1.4. Report Organization

The focus of this report is to describe the development of hydroclimate projections and to provide a summary evaluation of climate change implications for surface water hydrology in the eight major Reclamation river basins listed in the SECURE Water Act. The report is organized as follows:

Chapter 2 provides background on the global climate projections used in the study, including the downscaled climate projections and hydrologic projections presented in this report.

Chapter 3 presents the summary overview of hydrologic projections in the eight major Reclamation river basins listed above. The overview focuses on annual climate projections and the decadal changes in temperature and precipitation, April 1st snowpack, and mean monthly and mean seasonal runoff, specific to each basin.

Chapter 4 summarizes the findings of climate and hydrology projections from the previous chapter, putting the results in the context of a West-wide hydroclimate summary and comparing the findings with those from other contemporary results and reports.

Chapter 5 presents a summary discussion of the uncertainties associated with the culminating hydrologic analysis. These uncertainties arise from the climate projection variability, from the downscaling technique, and from the hydrologic model and parameter estimates utilized to assess the natural hydrologic response to the climate projections.

This page intentionally left blank.

2. Background

2.1. Global Climate Projections

Projections of future climate conditions have been developed by the global climate modeling community using a wide range of global climate models (GCM) forced with emissions scenarios. The emission scenarios encapsulate possible future trajectories of global greenhouse gas emissions and the corresponding atmospheric composition. The World Climate Research Programme established the Coupled Model Intercomparison Project (CMIP) in 1995 to facilitate broader analysis and application of GCMs. The CMIP framework provides standards and guidelines for comparing GCM results developed by the global climate modeling community and which form the basis for periodic global and national climate impacts assessment. Examples of global climate model assessments include the ones conducted by the IPCC, specifically the Third, Fourth, and Fifth Assessment Reports (IPCC 2001, 2007, and 2014). An example of a national assessment is the National Climate Assessment conducted every 4 years by the U.S. Global Change Research Program. The current version is the Third National Climate Assessment, completed in 2014 (Melillo et al. 2014).

To date, the contemporary climate assessments mentioned above use GCM-based climate projections from two CMIP phases: (1) CMIP Phase 3 (CMIP3) multi-model dataset completed in 2007, and (2) CMIP Phase 5 (CMIP5) multi-model dataset completed in 2013. For this report, no variables from these or other future climate projections were used directly from GCMs at their native scales. Because the GCMs are run to simulate climate over the whole Earth for 100 years or more, their geospatial scales are large, on the order 100-200 km on a grid side. These native-scale outputs must be post-processed to make them useful at the finer spatial and temporal scales where assessment questions mostly arise.

In addition, comparing GCM-derived precipitation and temperature outputs from 20th century simulations, for example, with observations on a common scale nearly always reveals model biases. Therefore, the coarse GCM outputs must be downscaled to a finer spatial scale that is appropriate for impact assessment studies and to correct for inherent biases in GCM outputs. The downscaling process is a current area of active research, and there is a continuum of downscaling methods ranging from statistical approaches to physically oriented dynamic modeling methods. The climate projections used in the hydroclimate analysis for this report were derived from GCM projections that were downscaled using a statistical method referred to as BCSD (Bias-Correction and Spatial Disaggregation) (Wood et al. 2004). The same method was used for the 2011 WWCRA Bias-Corrected and Spatially Downscaled Surface Water Projections

report (Reclamation, 2011b), which supported the 2011 SECURE Water Act Report to Congress (Reclamation, 2011a).

The 2011 WWCRA hydroclimate projections report was based on the monthly BCSD CMIP3 climate projection dataset, whereas this report has been based on the monthly BCSD CMIP5 climate projections. A brief description follows of what has changed between the CMIP3 and CMIP5 climate projection datasets. Specifically, it focuses on the monthly climate projections that are provided through the Downscaled Climate and Hydrology Projections (DCHP) archive (Maurer et al. 2014). The DCHP archive has been the primary resource for Reclamation's WaterSMART studies.

The downscaled monthly CMIP3 climate projections available from the DCHP archive include results from 23 GCMs. Most of these were run using more than one initial condition, and all were forced with three emission scenarios representing high (A2), medium (A1B), and low (B1) emissions. In addition, some of the GCMs were used for additional simulations, reflecting different initial conditions of the coupled land-atmosphere-ocean system. The CMIP3 DCHP archive, therefore, includes 112 projections developed using 23 GCMs.

The downscaled monthly CMIP5 climate projections available from the DCHP archive include results from 36 GCMs. Each of these GCMs was used for a minimum of four simulations, reflecting forcing of the climate system with four emission scenarios. The emissions scenarios in the CMIP5 archive are the same ones defined in the IPCC Fifth Assessment (IPCC 2014), where they are referred to as representative concentration pathways (RCPs). These scenarios are designated as RCP2.6, the high-mitigation scenario, also considered as the low-emissions scenario; RCP4.5, a scenario that achieves medium emissions by 2040; RCP6.0, a scenario achieving medium emissions by 2080; and RCP8.5, or the high-emissions scenario. The numeric value for each RCP represents the possible range of radiative forcing values by the year 2100 relative to pre-industrial era (e.g., +2.6 W/m2, +4.5 W/m2, etc.).

Similar to the approach taken for the CMIP3 archive, most combinations of GCM and RCP scenarios were run with one or more initial atmospheric conditions, forming small model-RCP projected ensembles and resulting in an overall total of 231 monthly projections. In addition to using more GCMs in CMIP5 (36 versus 23 in CMIP3), the CMIP5 models were run as a set of two experiments, first as near-term projections of the next few decades through 2035, and second as the long-term projections through the end of the 21st century (Taylor et al. 2012) that were the focus of this report. Additional details on the development of the downscaled CMIP5 climate projection archive and information on other contemporary downscaled climate projection archives are presented in the following section.

2.2. Downscaled Climate Projections

The global climate models aim to simulate fundamental physical laws based on mass, energy, and momentum conservation in the coupled land-atmosphere-ocean system. Governing equations of these physical processes are solved numerically to provide a time evolution of state variables representing the earth's climate. The computing resources necessary to solve the governing equations numerically are finite, and process approximations or parameterizations are necessary to perform century-length simulations at the high temporal resolutions needed to resolve physical processes. Thus, in practice, GCM simulations are performed at horizontal computational grid resolutions (about 100 km) that are an order of magnitude greater than the spatial scale of interest for most regional climate impacts assessments (e.g., about 10 km). Among other factors, the simulation of physical processes at a coarse spatial resolution leads to systematic discrepancies in comparisons between simulation results and observations. These systematic discrepancies are commonly referred to as model bias. In order to obtain credible climate information for climate variables relevant to a climate impacts assessment, such as precipitation and temperature, among others, it is necessary to reduce or eliminate such model biases.

A continuum of methodologies is currently available to translate climate information from GCM-level spatial resolution to the resolutions needed for regional climate impacts assessments. The process of relating climate information from the coarse GCM scale to the finer climate impacts assessment scale is referred to as downscaling. The available methodologies are broadly classified under two categories: (a) statistical downscaling, and (b) dynamical downscaling. The climate projections presented in this report were based on the BCSD statistical method described above.

As mentioned in the previous section, a total of 231 downscaled monthly climate projections of precipitation and surface air temperature (average, minimum and maximum) from the CMIP5 climate models are available from the DCHP archive (Maurer et al. 2014). These data fields are available at a spatial resolution of one-eighth degree latitude by one-eighth degree longitude (approximately 12 km x 12 km) for the contiguous United States (CONUS) and transboundary watersheds for the time period of January 1950 through December 2099.

The monthly BCSD CMIP5 archive is a widely accepted and used climate resource. Gutmann et al (2014) showed that monthly datasets developed using the BCSD downscaling algorithm (Wood et al. 2004) and subsequent disaggregation to daily sequences performed nearest to observed datasets for a number of performance metrics (e.g., wet day fraction, wet [dry] spell length, or interannual variation), in addition to traditional measures such as monthly bias.

Thus, the assessment of hydroclimate and surface water hydrology projections here was based on the DCHP archive. Furthermore, archival choice is guided, to an extent, by the climate-impact questions that are being evaluated. The 2011 WWCRA hydroclimate projections report was also based on the DCHP archive, using the same archival resource provides methodological consistencies. The DCHP archive houses both CMIP3 and CMIP5 outputs and supporting information noting differences in the models, emissions drivers, and the downscaling techniques for CMIP5 and CMIP3. The information presented in this report is the downscaled CMIP5 climate projections, which have been updated from the CMIP3 set of projections.

Comparing climate impacts using multiple downscaling approaches and climate information at multiple spatial resolutions is an area of active research. In future assessments, it could be worthwhile to explore impact results using data from multiple archives and to compare and contrast such findings. Limitations notwithstanding, the next section describes the development of hydrologic projections using the monthly CMIP5 projections in the DCHP archive.

2.3. Developing Hydrologic Projections

The method used in the 2011 WWCRA hydroclimate projections report for developing hydrologic projections from climate projections was based on the macro-scale hydrologic model VIC (Variable Infiltration Capacity; Liang et al. 1994). The specific version of the VIC model used in the 2011 report was numbered 4.0.7. This current study is based on an updated version of the VIC model numbered 4.1.2. This section explains the rationale for choosing the VIC model and highlights the key differences between the VIC model versions 4.0.7 and 4.1.2.

The VIC model (Liang et al. 1994; Liang et al. 1996; Nijssen et al. 1997) is a gridded macro-scale (grid resolution greater than 1 km) hydrology model that is spatially distributed and solves the water balance at each model grid cell. The grid resolution for the VIC application is one-eighth degree latitude by one-eighth degree longitude (approximately 12 km x 12 km), which is the same grid resolution for the BCSD downscaled CMIP5 climate projections. The model was initially developed as a land-surface model for direct integration with GCMs, but it now is run almost exclusively as a standalone hydrology model using a daily simulation timestep. Some of the prominent features of the VIC model that make it suitable for climate studies are:

- Minimal meteorological data are input at a daily time step. VIC requires precipitation, minimum temperature, maximum temperature, and wind speed, the first three of which are the most commonly available surface meteorological parameters. The BCSD CMIP5 climate projections from the DCHP archive provide monthly data on precipitation and minimum

and maximum temperatures, and these data require disaggregation to daily values before they can be used in the VIC model. The disaggregation methodology is described in Section 4.3 of the 2011 WWCRA hydroclimate projections report.[4] The wind-speed data necessary to run the VIC model are also available from the DCHP archive; however, wind speed is not adjusted from historical values in developing the hydrology projections.

- VIC uses the meteorological inputs of daily precipitation, minimum and maximum temperature, and wind speed to internally compute (through established algorithms) other hydroclimate variables such as incoming shortwave radiation, incoming longwave radiation, humidity, vapor pressure, and vapor pressure deficit.
- An energy balance algorithm is applied to simulate snow dynamics, and evapotranspiration is computed internally via the Penman-Monteith formulation (Monteith, 1965).
- Runoff generated at individual grid cells from the water balance simulations subsequently can be routed via a channel network to form streamflow at locations of interest.

Chapter 4 of the 2011 WWCRA hydroclimate projections report and references therein provide additional details on the VIC model itself and describe the overall approach used to develop hydrologic projections (Reclamation, 2011b). All of the VIC applications used in this study remain available through the University of Washington VIC model repository.[5]

The following list summarizes the largest changes between VIC 4.0.7 and VIC 4.1.2.6 Some of the changes may be more relevant to hydrologic projection analysis under climate change; however, additional diagnostic simulations beyond the scope of this study would be required to make that determination.

- VIC 4.0.7 to 4.1.0:
    - Added an exponential grid transformation option for soil thermal nodes in the finite difference heat equation.

[4] For the daily disaggregation of temperature in the BCSD CMIP5 monthly projections, mean daily minimum and maximum temperatures were disaggregated individually. For the 2011 WWCRA hydroclimate projections report, which used BCSD CMIP3 projections, only a monthly projection of mean daily average temperature was available, so an additional assumption was necessary in the disaggregation step to account for consistent minimum and maximum temperature distributions (Reclamation, 2011b).

[5] Variable Infiltration Capacity (VIC) Macroscale Hydrologic Model, http://vic.readthedocs.org/en/master/

[6] To learn about model changes between these versions, readers may refer to the following links: (1) http://vic.readthedocs.org/en/master/ and (2) https://github.com/UW-Hydro/VIC/blob/master/src/ChangeLog

  - Added an implicit solution option for the finite difference frozen soils algorithm.
  - Added permafrost enhancements and the EXCESS_ICE option.
  - Added logic to use bare soil evaporation when the leaf area index equals zero.
  - Dropped the simulation of very thin snow dynamics from the canopy.
  - VIC 4.1.0 to 4.1.1:
  - Added the ability to control how aerodynamic resistances in the overstory are corrected for the presence of snow in the canopy.
  - Added the PLAPSE option to lapse air pressure by grid cell average elevation.
  - Improved temperature profile stability.
  - Added an option to select the aerodynamic resistance algorithm in the snow-filled canopy.
  - Improved the ground flux computation.
  - Added an option to select different snow density algorithms (Bras and SNTHRM).
  - Added the dynamic lake/wetland model.
  - Added soil temperature heterogeneity (Spatial Frost).
  - Added partial snow cover (Spatial Snow).
  - Added blowing-snow sublimation.
  - Improved canopy temperatures and energy balance in the presence of snow.

- VIC 4.1.1 to 4.1.2:
  - Updated VIC's internal version of the MTCLIM (mountain microclimate simulation model; Hungerford et al. 1989) forcing disaggregation functions from version 4.2 (Thornton and Running, 1999) to include elements of version 4.3 (Thornton et al., 2000).
  - Extended the computation of soil temperatures, ice contents, and ground fluxes to all modes of model operation.
  - Added the ability to simulate organic soil.
  - Added the computation of water table position.
  - Improved and added features to the lake model.

The VIC model version 4.1.2 was used in developing the hydrologic projections from the CMIP5 BCSD climate projections under 64-bit computing. Of the 231 monthly CMIP5 climate projections, a set of 97 projections representing 31 CMIP5 climate models and 4 representative concentration pathways were converted into hydrologic projections. The selection of only a subset of projections was constrained by hydrologic modeling practicalities to complete this effort. Furthermore, this set of projections is of comparable size to the number of hydrologic projections (a total of 112) used in the 2011 WWCRA hydroclimate projections report (Reclamation, 2011b).

As was done in 2011, routed streamflow was developed for the 43 selected locations given in Table 1. Analysis of the climate and streamflow data is presented in Chapter 3.

Table 1. Station Descriptions for the 43 WWCRA Reporting Locations

Basin(s)*	Site Name and Description	Latitude	Longitude	State(s)
Colorado	Colorado River at Lees Ferry	36.8647	–111.5875	AZ
	Colorado River above Imperial Dam	32.8834	–114.4685	CA-AZ
	Green River near Greendale	40.9086	–109.4224	UT
	Colorado River near Cameo	39.2392	–108.2656	CO
	Gunnison River near Grand Junction	38.9766	–108.4562	CO
	San Juan River near Bluff, UT	37.1469	–109.8642	UT
Columbia	Snake River at Brownlee Dam	44.8389	–116.8995	ID
	Columbia River at Grand Coulee	47.9656	–118.9817	WA
	Columbia River at The Dalles	45.6075	–121.1722	OR
	Yakima River at Parker	46.5061	–120.4519	WA
	Deschutes River near Madras	44.7261	–121.2465	OR
	Snake River near Heise	43.6128	–111.6600	ID
	Flathead River at Columbia Falls	48.3619	–114.1839	MT
Klamath	Williamson R. below the Sprague River	42.5577	–121.8442	OR
	Klamath River below Iron Gate Dam	41.9281	–122.4431	CA
	Klamath River near Seiad Valley	41.8529	–123.2311	CA
	Klamath River at Orleans	41.3036	–123.5336	CA
	Klamath River near Klamath	41.5111	–123.9783	CA
Missouri	Missouri River at Canyon Ferry Dam	46.6494	–111.7275	MT
	Milk River at Nashua	48.1297	–106.3639	MT
	South Platte River near Sterling	40.6192	–103.1886	CO
	Missouri River at Omaha	41.2589	–95.9222	NE
	Bighorn River at Yellowtail Dam	45.3079	–107.9567	MT
	North Platte River at Lake McConaughy	41.2145	–101.6434	NE
Rio Grande	Rio Grande near Lobatos	37.0786	–105.7564	CO
	Rio Chama near Abiquiu	36.3183	–106.5972	NM
	Rio Grande near Otowi	35.8762	–106.1433	NM
	Rio Grande at Elephant Butte Dam	33.1563	–107.1905	NM
	Pecos River at Damsite No. 3 near Carlsbad	32.5114	–104.3342	NM
	Sacramento River at Freeport	38.4561	–121.5003	CA

Basin(s)*	Site Name and Description	Latitude	Longitude	State(s)
Sacramento-San Joaquin	Sacramento River at Bend Bridge near Red Bluff	40.2642	–122.2219	CA
	Feather River at Oroville	39.5217	–121.5467	CA
	San Joaquin River near Vernalis	37.6761	–121.2653	CA
	Stanislaus River at New Melones Dam	37.9472	–120.5292	CA
	Sacramento-San Joaquin Rivers at Delta	38.0645	–121.8567	CA
	San Joaquin River at Millerton Lake (Friant Dam)	36.9981	–119.7066	CA
	American River at Fair Oaks	38.6366	–121.2284	CA
	Tulare-Buena Vista Lakes	36.0524	–119.7187	CA
Truckee	Little Truckee River below Boca Dam	39.3883	–120.0950	CA
	W.F. Carson River at Woodfords	38.7697	–119.8328	CA
	Truckee River at Farad Gage (just above CA stateline)	39.4540	–120.0063	CA
	Truckee River at Nixon Gage	39.7780	–119.3392	NV
	Carson River at Fort Churchill Gage	39.3272	–119.1508	NV

* Note – the Pecos, Tulare and Carson are not SWA Basins but are respectively included under the Rio Grande, Sacramento-San Joaquin and Truckee Basins, as these locations are of interest from a water operations standpoint.

3. Hydroclimate Projections for Major Reclamation River Basins

3.1. Evaluation Approach

This chapter presents hydroclimate projections for the major Reclamation river basins. The projections include distributions and changes in precipitation, mean temperature, snow-water equivalent, and runoff. The figures and analysis for each major Reclamation river basin are grouped under two sections. The first section is referred to as Hydroclimate Projections and provides an overview for each of the major Reclamation river basins. The second section presents climate change impacts on annual runoff and seasonal cycles for selected runoff locations within the major basins. Runoff impacts are reported at 43 locations (refer to Table 1) covering all the major Reclamation river basins.

Under the hydroclimate projections section, three sets of plots are presented for each major river basin. These include:

- Time-series plots of six hydroclimate variables;
- Spatial plots showing the spatial distribution of temperature, precipitation, and April 1st snow-water equivalent (SWE)[7]; and
- Plots depicting April 1st SWE distribution and change with elevation.

3.1.1. Hydroclimate Projections

3.1.1.1. Time Series Plots

Basin- and projection-specific annual time series plots are presented for six hydroclimate indicator variables covering the period 1950–2099.

- Annual Total Precipitation
- Annual Mean Temperature
- April 1st Snow-water equivalent
- Annual Runoff
- December-through-March Runoff
- April-through-July Runoff

Three variables—annual total precipitation, annual mean temperature, and April 1st snow-water equivalent—vary spatially (at one-eighth degree or 12-km grid resolution) across the basins. To estimate total annual precipitation for a given basin, basin-wide average precipitation (averaged across the grid cells in the

[7] All references to SWE (snow-water equivalent) in this report correspond to April 1st SWE values.

basin) was first calculated for each month of the years 1950-2099. These monthly precipitation values then were summed for each year (1950-2099) to obtain the annual total precipitation.

To estimate basin mean temperature, average temperature was calculated from all the grid cells in the basin for each month of the years 1950-2099. Next, these monthly temperatures for any given year were averaged to estimate the basin-wide annual mean temperature.

Snow-water equivalent (SWE) on April 1st of a given year is a widely used measure to assess snowpack and subsequent spring-summer runoff conditions in the snowmelt-dominated basins of the western United States. SWE is a state variable that is output from the VIC hydrology model, calculated by the internal VIC hourly timestep energy balance snow model. For each of the simulation years, 1950-2099, April 1st SWE was saved from the simulations for the model grid cells in a given basin. This gridded SWE on April 1st was averaged over all the grid cells for the given basin to calculate the basin-wide April 1st SWE in each of the simulation years, 1950-2099.

Runoff for each of the locations listed in Table 1 was calculated for the annual timescale and for two seasonal timescales, December-through-March total runoff conditions and April-through-July total runoff conditions. For the VIC model, the term *total runoff* signifies the sum of VIC's surface runoff and baseflow variables, which, when combined, represent stream channel input that can be routed to estimate streamflow at a particular location. For each of the simulation years 1950-2099, monthly total runoff was aggregated on a water-year8 basis to calculate water-year-specific total annual runoff, December-through-March runoff, and April-through-July runoff.

The annual time series plots for the six hydrologic indicator variables for all the projections were calculated, and the results are presented to reflect ensemble central tendency and ensemble spread. The central tendency is measured using the ensemble median and the 10th and 90th percentile bounds from the 97 projections provides the lower and upper uncertainty bounds in the envelope of hydroclimatic possibility through time.

3.1.1.2. Spatial Plots

The second sets of plots presented in this report include spatial plots of decade-mean precipitation, temperature, and April 1st SWE. These plots show the spatial distribution for the variables across the contributing basins in each of the eight

[8] Water year *t* is defined as the period from October 1 of year *t–1* to September 30 of year *t*. For example, water year 1951 spanned from October 1950 through September 1951. So there are 149 water years spanning the calendar years 1950–2099. For time series plotting of runoff, values from water year 1951 were repeated for 1950.

major Reclamation river basins (a total of seven locations[9]). The spatial plots are developed on a water-year basis (affecting calculations for only precipitation and temperature averaging) for the reference decade of the 1990s (water years 1990-1999).

The spatial distribution of temperature for the 1990s is presented as an ensemble median of the 97 projections. At each grid cell in a given basin and for each of the 97 selected projections, the mean annual temperature is first calculated from the 12 monthly values for each of the 10 water years 1990-1999. Next, for each grid cell, the ensemble median of the decade average mean temperature was calculated and used in developing the spatially varying temperature plots.

Temperature changes in each of the future decades were estimated as follows. At each grid cell in a given basin and for each of the 97 projections, the decade-mean temperature changes were calculated by averaging the mean annual temperature from the 10 water years in each of the respective future decades. Then, for a given projection and at a given grid cell, the difference (in °F) between a given future decade's mean annual temperature and the reference decade's mean annual temperature was calculated. The uncertainty in the distribution of the change in decade-mean temperature for the 2020s, 2050s, and 2070s is presented using the 25th and 75th percentile, and the median (50th percentile) represents the central tendency of change in decade-mean temperature distribution.

The calculations for decade-mean precipitation and April 1st SWE distribution follow steps similar to the ones used for deriving the temperature distributions. The spatial distribution of precipitation for the 1990s is presented as an ensemble median of the 97 projections. At each grid cell in a given basin and for each of the 97 projections, average total precipitation for the 1990s was calculated first. Next, for each grid cell, the ensemble median of the average total precipitation for each of the future decades was calculated and used in developing the spatially varying precipitation plots. A positive magnitude change implies wetter conditions and a negative change implies drier conditions, relative to the 1990s. The uncertainty in the distribution of the change in decade-mean precipitation for the future decades is presented using the 25th and 75th percentile, and the median (50th percentile) represents the central tendency of change in decade-mean precipitation distribution.

The spatial distribution of April 1st SWE for the reference decade is also presented as an ensemble median of the 97 projections. The VIC macro-scale hydrology model was used to simulate snow dynamics, when applicable, for grid cells in the basin. Typically, snow is present in only a subset of grid cells in a

[9] Seven locations result from the eight major Reclamation basins because the Sacramento–San Joaqulin Delta inflow location combines flows from two basins.

basin, and VIC simulated snow accumulation and melt dynamics only for these grid cells. At each of these grid cells in the basin and for each of the 97 projections, the average April 1st SWE for the 1990s was calculated first. Next, the ensemble median of the average April 1st SWE for each of the future decades was calculated and used in developing the spatially varying SWE plots.

SWE changes in each of the future decades were estimated as follows. For the relevant grid cells (i.e., grid cells with snow present) in a given basin and for each of the 97 projections, average April 1st SWE was calculated by averaging SWE values from the 10 water years in the decade. Then, for a given projection and at a given grid cell, the difference in average April 1st SWE between a given future decade and the reference decade was calculated. A positive magnitude change implies an increase in the SWE value, and a negative change implies a decrease in SWE, relative to the reference decade. The uncertainty in the distribution of the change in decade-mean SWE for the future decades is presented using the 25th and 75th percentile, and the median (50th percentile) represents the central tendency of change in decade-mean SWE distribution.

3.1.1.3. SWE Distribution and Change with Elevation

The distribution of SWE with elevation was estimated as follows. First, for a given basin, the elevation distribution was obtained for all the one-eighth-degree grid cells used in the VIC model. This list of elevation distribution was used to calculate the minimum and maximum elevation for the basin. A sequence of elevation bands was developed using a 100-foot interval starting with the minimum basin elevation. This step identifies the number of grid cells within a given 100-foot elevation band. From the grid cells identified within each such band, a subset of grid cells with at least 10 mm of April 1st SWE over the 1990s reference period was selected. Here, the reference period April 1st SWE for a grid cell is defined as the ensemble median of the reference decade April 1st SWE estimated from the 97 member VIC simulation for the basin.

Next, the April 1st SWE values for the grid cells with at least 10 mm (about 0.4 inch) of SWE in the reference decade were averaged to obtain the representative reference SWE. Similarly, the elevations for these same cells were averaged to obtain the representative elevation for the reference SWE. These two values—representative SWE and representative elevation—were plotted to obtain the reference SWE distribution with elevation for the 1990s decade.

To calculate change in April 1st SWE in each of the future decades, three percentile changes in SWE corresponding to the 25th, 50th, and 75th percentiles were obtained. As an example, to estimate the 50th percentile change for the 2050s, change in decade-mean SWE magnitude was first calculated for each projection as the difference in decade-mean April 1st SWE between the 2050s and the 1990s for a given grid cell. The 50th percentile change was then estimated by

taking the median (50th percentile) of the change values calculated for all the projections.

For a given future period, the changes in April 1st SWE were averaged for the same cells within each of the elevation bands identified as having SWE of at least 10 mm (about 0.4 inch) during the reference 1990s decade. Next, the percentage change in SWE for a given future period was calculated by dividing the relevant SWE change magnitude with the magnitude calculated for the reference 1990s decade. These points were plotted to show the distribution of percentage change in SWE from the 1990s with elevation. Finally, a locally weighted polynomial regression line using the LOWESS algorithm (Cleveland, 1981) in the R statistical language (R Core Team, 2015) was fitted (using R default parameters) to provide a smooth representation of the SWE distribution and change variation with elevation.

A set of four plots is presented for each basin (see Sections 3.2 through 3.8). The top left panel provides the distribution of April 1st SWE with elevation for the reference decade. The open gray circles in this plot correspond to the representative SWE, and elevation pair and the fitted regression line is shown in black color. The top right panel and the two bottom panels correspond to the percentage SWE change from the 1990s decade for the three future periods. In these decadal SWE change plots, the gray open circles correspond to the median change values. A regression line (shown in black) is next fitted to the median change values. Uncertainty in the estimated decadal April 1st SWE change is shown using the 25th and 75th percentiles. The point data corresponding to the 25th and 75th percentiles are not shown, but the regression lines for these two percentiles are presented in red and blue, respectively. Finally, these regression lines are used to estimate the percentage change in April 1st SWE in each of the three future decades and for each percentile for selected basin elevations. The basin elevations were selected using the approximate mid-points for four elevation bands spanning the SWE elevation range (see Table 4 in Section 4).

3.1.2. Impacts on Streamflow Annual and Seasonal Cycles

This section presents impacts on streamflow for selected sub-basin river locations within the major Reclamation basins. Streamflow is calculated by routing grid-cell runoff through the channel network to the selected location, and includes the time lags associated with channel routing. In contrast, basin-wide averages of runoff do not incudes routing time lag effects.

In the river basin sections that follow, the first set of plots for each basin demonstrates annual cycle variation and climate change impacts on the annual cycle at each of the selected locations for the three future periods. The second set of plots presents the uncertainty information in the flow projections using box-and-whisker plotting symbols (or boxplots for short). The box in the boxplot

corresponds to the inter-quartile range (i.e., the lower bound of the box corresponds to the 25th percentile, and the upper bound corresponds to the 75th percentile). The horizontal line within the box corresponds to the median value of the change estimated from the 97 flow simulations. The whiskers correspond to the 5th and 95th percentiles of the runoff magnitude change estimated from the 97 flow simulations. For each future decade, three boxplots are presented, corresponding to the annual runoff and the December-through-March and April-through-July seasonal runoff.

The third set of plots shows the shift in timing of the annual runoff volumes as boxplots. For each projection, the shift in runoff timing was estimated to be the difference in the centroid dates between the mean annual hydrographs of the future decade and the reference decade. A negative shift means that the future decade will have an earlier centroid date and that more of the annual runoff will occur earlier in the year. A positive shift indicates that more of the runoff will happen later in the year. Finally, these shifts in annual runoff timing are presented as separate boxplots for each of the three future decades. The boxplots show the uncertainty in the distribution of the shift in runoff timing estimated from the 97 projections.

The plots described here are presented in the subsequent Sections 3.2 through 3.8. The results for the eight river basins are presented in the following order:

- Colorado River Basin (Section 3.2)
- Columbia River Basin (Section 3.3)
- Klamath River Basin (Section 3.4)
- Missouri River Basin (Section 3.5)
- Rio Grande Basin (Section 3.6)
- Sacramento and San Joaquin River Basins (Section 3.7)
- Truckee and Carson River Basins (Section 3.8)

3.2. Colorado River Basin

The Colorado River Basin, located in the southwestern United States, occupies an area of approximately 250,000 square miles. The Colorado River is approximately 1,400 miles long; it originates along the Continental Divide in Rocky Mountain National Park, Colorado, and ends where it meets the Gulf of California in Mexico. The Colorado River is a critical resource in the West, because seven Basin States (Arizona, California, Colorado, Nevada, New Mexico, Utah and Wyoming) depend on it for water supply, hydropower production, recreation, fish and wildlife habitat, and other benefits. Although agricultural uses account for 70 percent of Colorado River water use, between 35 and 40

million people rely on the same water for some or all of their municipal needs. Moreover, the United States also has a delivery obligation to Mexico for some of the Colorado River waters pursuant to a 1944 treaty.

3.2.1. Hydroclimate Projections

Figure 1 shows six plots of hydroclimate indicators for the Colorado River above Imperial Dam: annual total precipitation (top left), annual mean temperature (top right), April 1st SWE (middle left), annual runoff (middle right), December-through-March runoff (bottom left), and April-through-July runoff (bottom right). The heavy black line is the annual time series of 50th percentile (i.e., median) values of the 97 projections. The shaded area is the annual time series of the 10th to 90th percentiles.

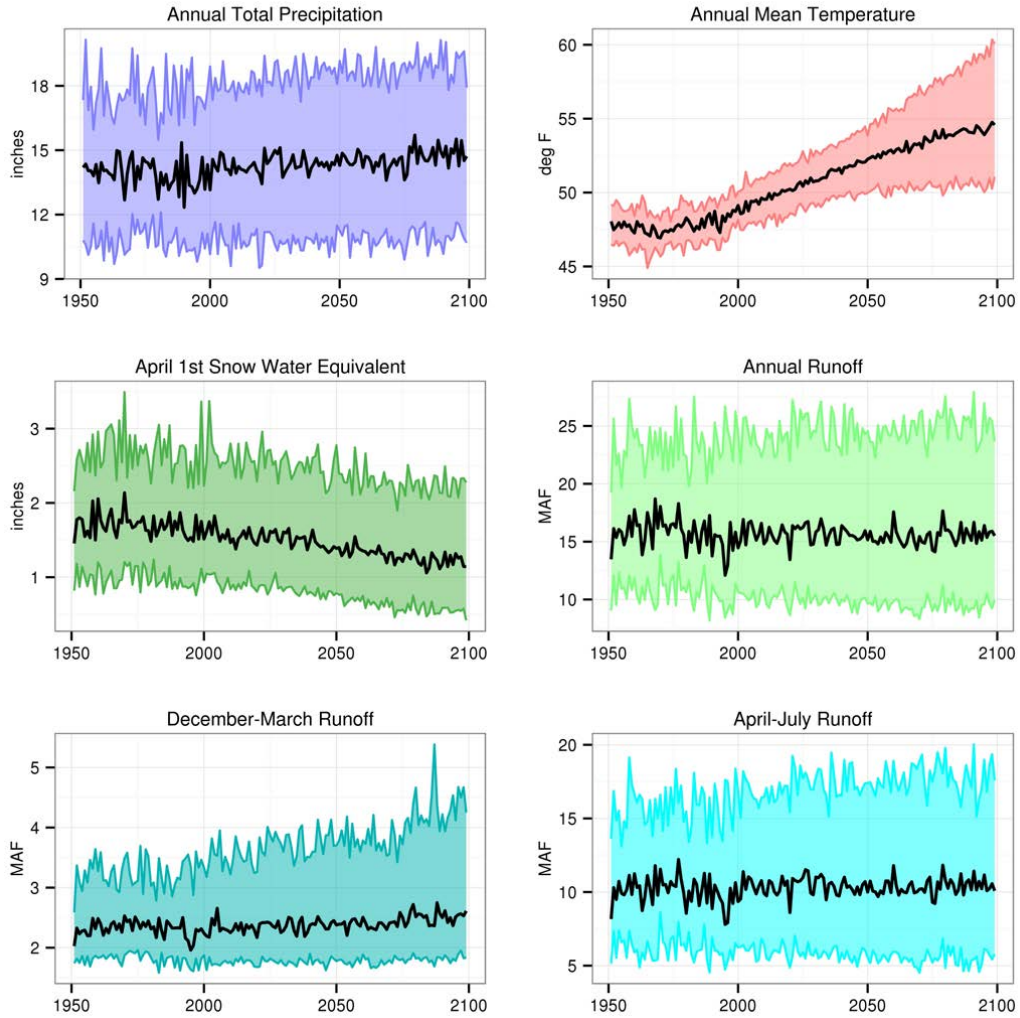

Figure 1. Colorado Basin – Time series plots for six projected hydroclimate indicators

The heavy black line is the annual time series median value (i.e., median). The shaded area is the annual time series of 10th to 90th percentiles.

Total annual precipitation throughout the basin has a slightly upward trajectory over the transient period going out to 2099. The uncertainty envelope appears to be largely constant over time, implying that there is no increase or decrease in the uncertainty envelope from the present for total annual precipitation magnitudes through time. The mean annual temperature throughout the basin shows an increasing trend and a widening uncertainty envelope, implying an increasing uncertainty over time. April 1st SWE shows a decreasing trend. The annual runoff shows no apparent trend. The December-through-March runoff volume also shows no apparent trend, but the upper limit of its uncertainty bound diverges over time. The April-through-July runoff also shows no apparent trend.

Figure 2, Figure 3, and Figure 4 show the spatial distribution of simulated decade mean temperatures, precipitation, and April 1st SWE, respectively, in the Colorado River Basin above Imperial Dam. In each figure, the simulated 1990s distribution of median decadal mean condition for the variable of interest is shown in the upper middle plot, and changes in the decadal mean condition are shown below for three future periods (2020s, 2050s, 2070s relative to the 1990s) at three change percentiles within the range of projections (25th, 50th, and 75th percentiles).

In Figure 2, the median change for the three future decades relative to the 1990s indicates increasing temperatures throughout the basin. In Figure 3, the median change in precipitation for the future decades indicates a wet pattern, particularly in the upper portion of the basin. Even at the 25th percentile level and for all the three future decades, the higher-elevation portions of the basin appear to be slightly wetter or unchanged. In Figure 4, the spatial plots indicate the nominally wet areas (April 1st SWE less than about 20 inches in the 1990s) generally having reduced snowpack. The wetter areas in higher elevations (April 1st SWE more than about 20 inches in the 1990s) show some increases in the future decades.

Figure 5 shows the distribution of April 1st SWE with elevation in the Colorado River Basin for the reference decade and the percentage change in this distribution for the three future decades. The 25th and 75th percentile estimates provide a way to quantify the uncertainty in the calculated changes.

The SWE elevation range for the Colorado River Basin (the elevation range of areas shown by the VIC model to have met the threshold April 1st SWE of at least 10 mm during the 1990s) was estimated to be approximately 6,000 to 12,000 feet. The 1990s SWE distribution is fairly linear, with greater snowpack at higher elevations. Furthermore, the dispersion of the points is minimal along the fitted regression line, indicating a largely uniform source in the development of the snowpack, specifically wintertime precipitation, in this case.

Overall, it appears from the analysis that there is substantial loss in SWE at lower elevations, but at higher elevations (around 11,000 feet) projections indicate that

the median SWE change increases in the future decades. Over time, however, even at higher elevations, the analysis indicates a net decline in the median SWE values from the 2020s to 2050s and from the 2050s to the 2070s.

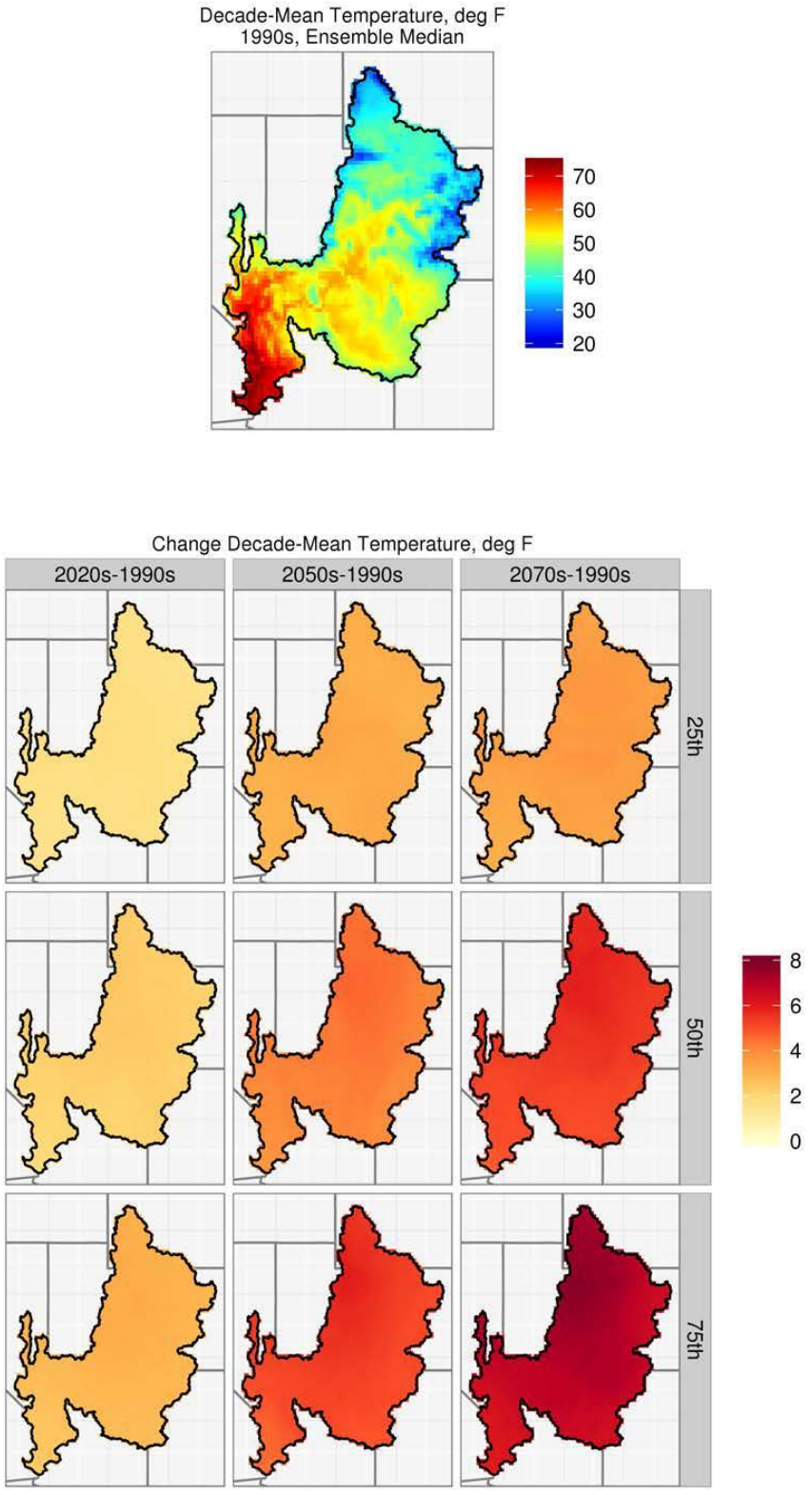

Figure 2. Colorado Basin – Spatial distribution of simulated decadal temperature

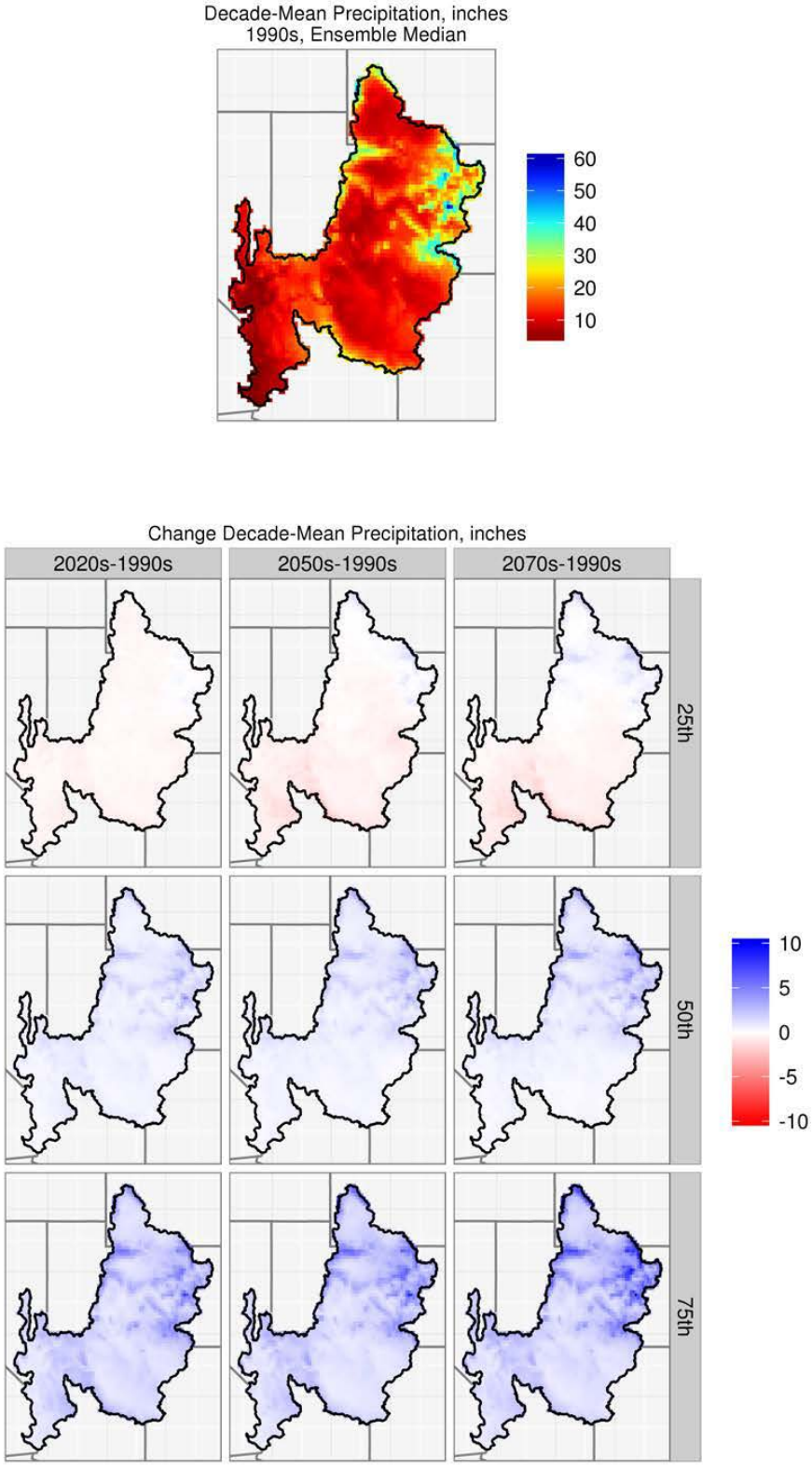

Figure 3. Colorado Basin – Spatial distribution of simulated precipitation

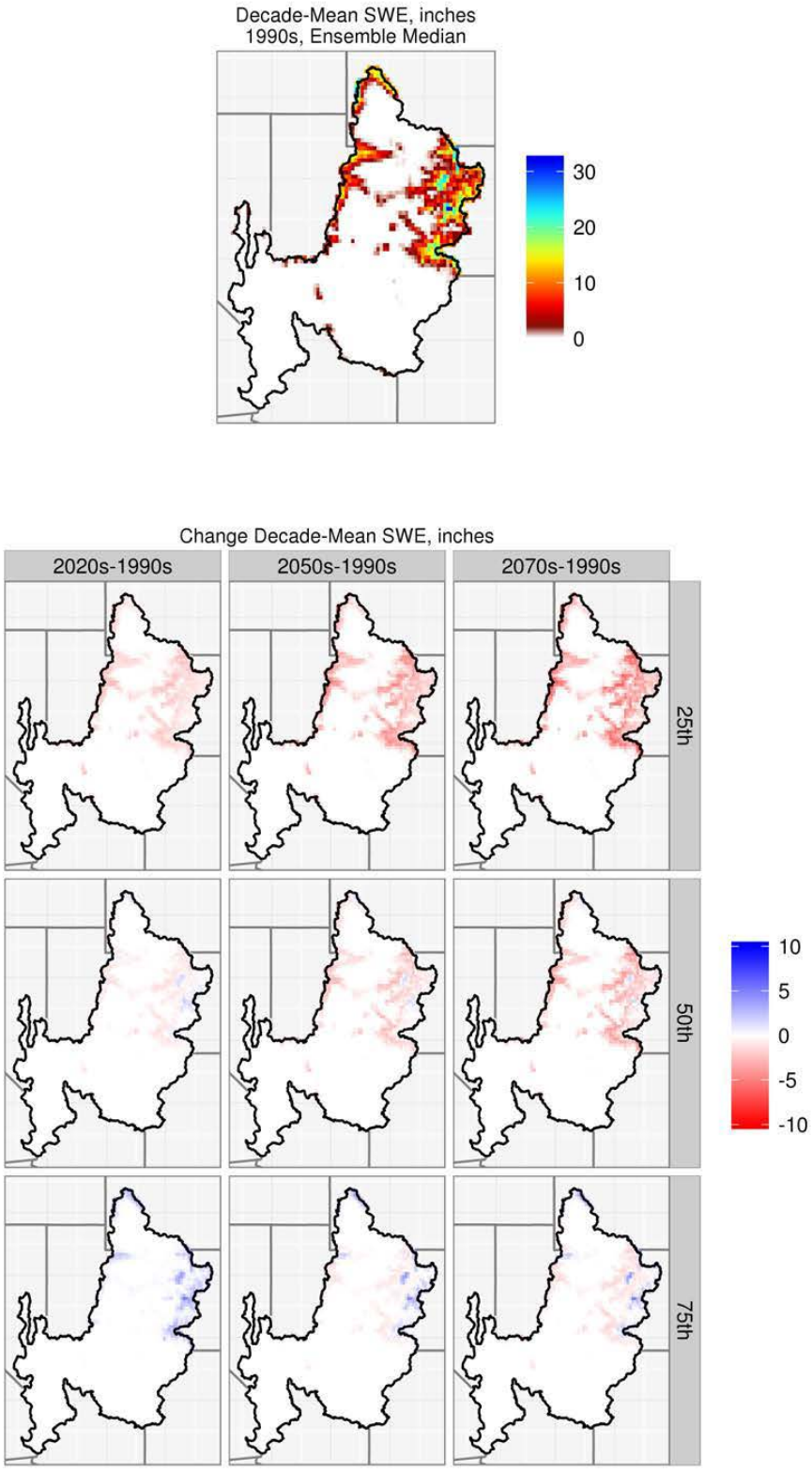

Figure 4. Colorado Basin – Spatial distribution of simulated decadal April 1st SWE

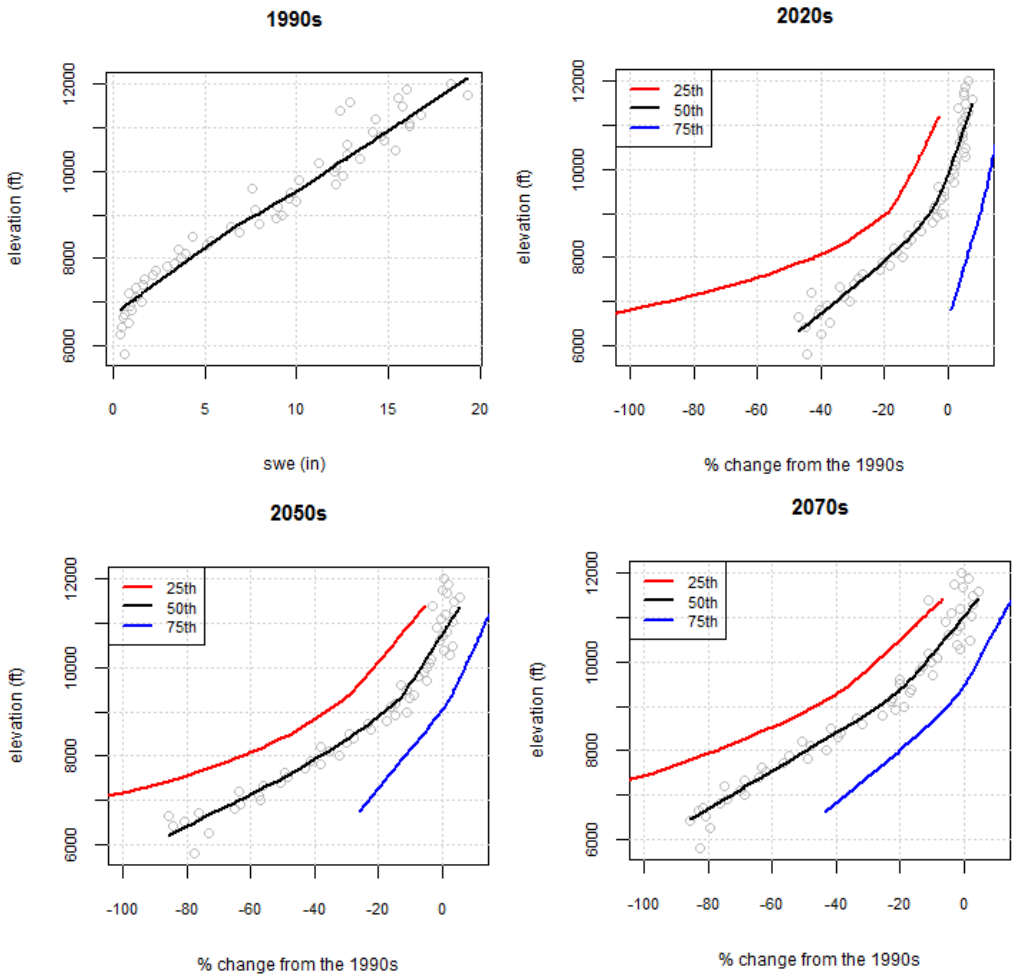

Figure 5. Colorado Basin – SWE distribution with elevation in the 1990s decade and future changes

The open light gray circles in this plot correspond to the median SWE values at each elevation with a fitted regression line is shown in black. The regression lines for the 25th and the 75th percentiles are presented in red and blue, respectively.

3.2.2. Impacts on Streamflow Annual and Seasonal Cycles

Figure 6 shows the mean monthly streamflow values for the 1990s, 2020s, 2050s, and 2070s in six Colorado River sub-basins. Overall, there is a shift to earlier runoff peaks, which is most prominent in the 2070s for the Colorado River at Lees Ferry and at Cameo, for the Gunnison River near Grand Junction, and for the San Juan River near Bluff.

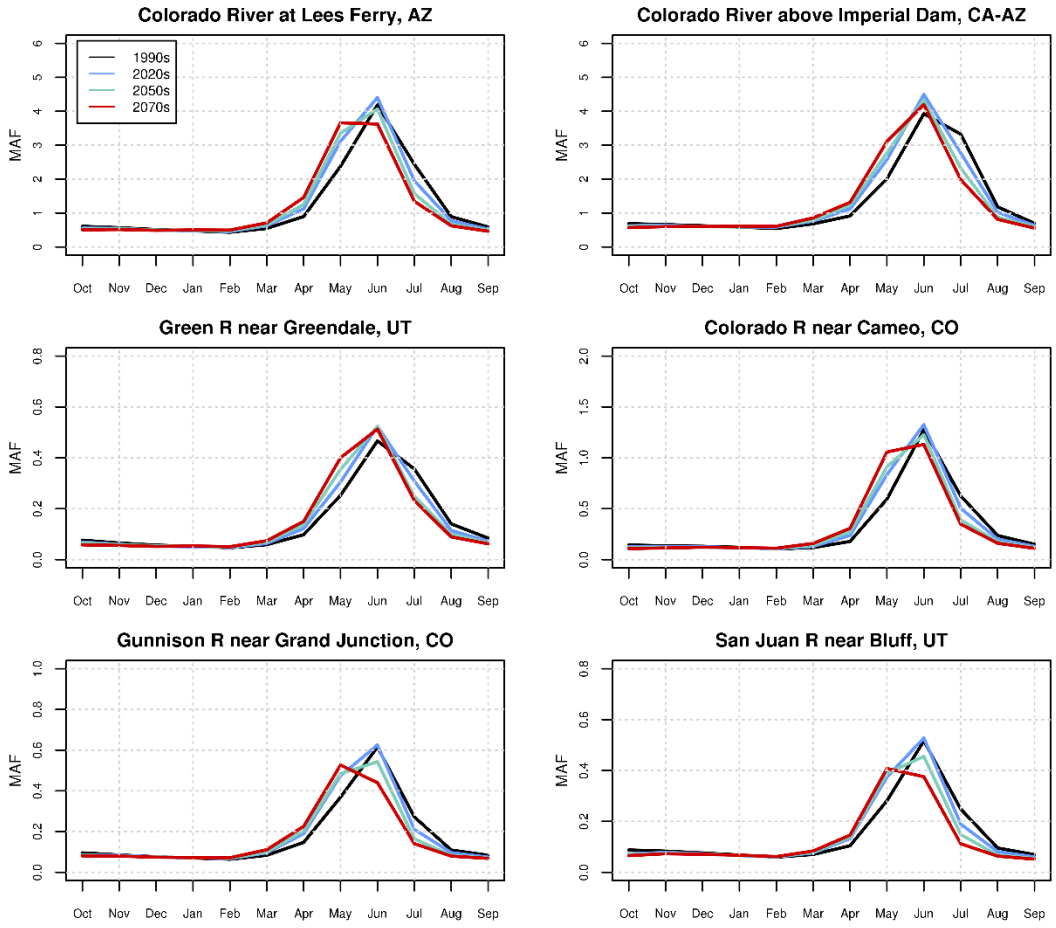

Figure 6. Colorado Basin – Simulated mean monthly streamflow for various sub-basins

Figure 7 shows boxplots of the distribution of simulated changes in runoff magnitude for annual, December-through-March, and April-through-July runoff in the six Colorado River sub-basins. The median change for the December-through-March period in all the three decades is positive, indicating an increase in runoff. The median annual streamflow change, both at Lees Ferry and at Imperial Dam, shows some increase for the 2020s, but no change for the 2050s and 2070s. Overall in the 2020s, the median annual flow change from the 1990s is positive for all the sub-basins. However, for the 2050s and 2070s, a decline in the median annual flows is indicated for the Gunnison (near Grand Junction, CO) and San Juan (near Bluff, UT) Rivers. Finally, in interpreting these change results, it is important to recognize the uncertainty in the change magnitude; here, the plots have been bounded to range from -40 to +60 percent.

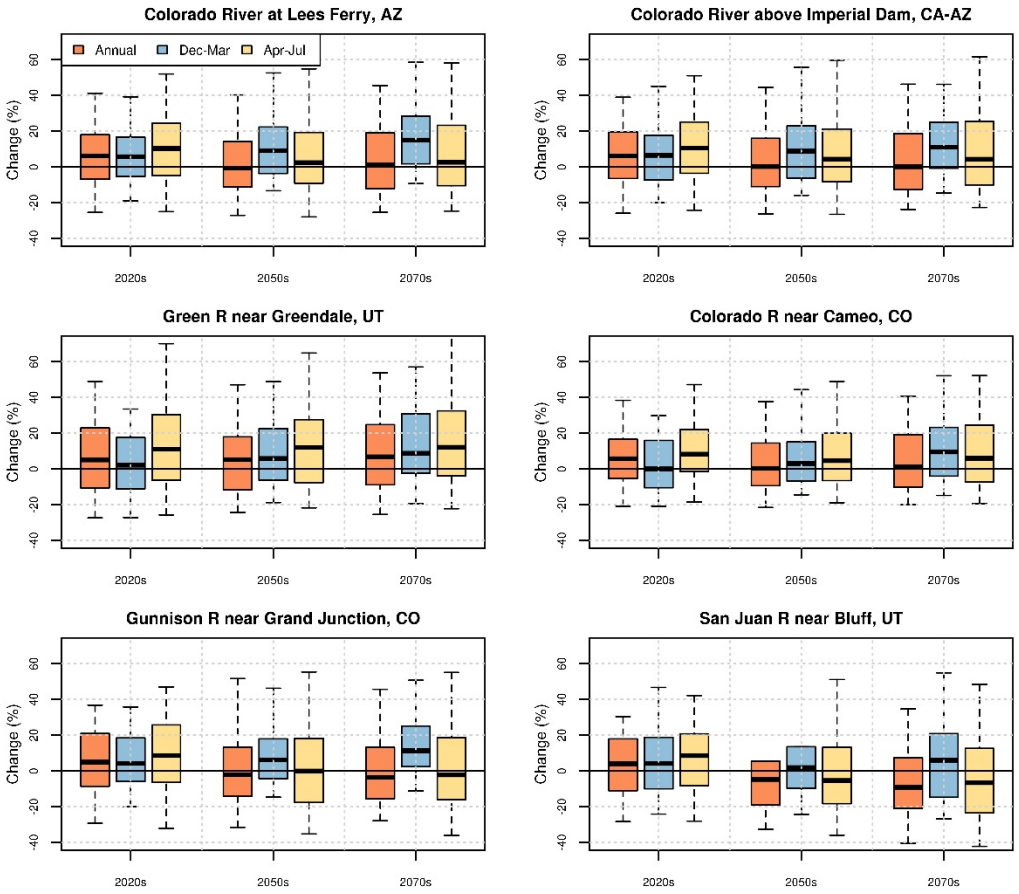

Figure 7. Colorado Basin – Simulated change in streamflow magnitude for various sub-basins

Figure 8 shows the simulated shift in runoff timing for the various sub-basins. Generally, it appears from the analysis that in the 2020s, nearly half of the projections (i.e., the median value in the boxplots) show that the mid-point of the annual streamflow volume (50 percent of annual streamflow volume) will occur about 5 to 7 days earlier than in the 1990s. By the 2050s, it is projected to be nearly 10 days, and by the 2070s, around 12 days earlier. Nearly all projections are pointing toward early runoff.

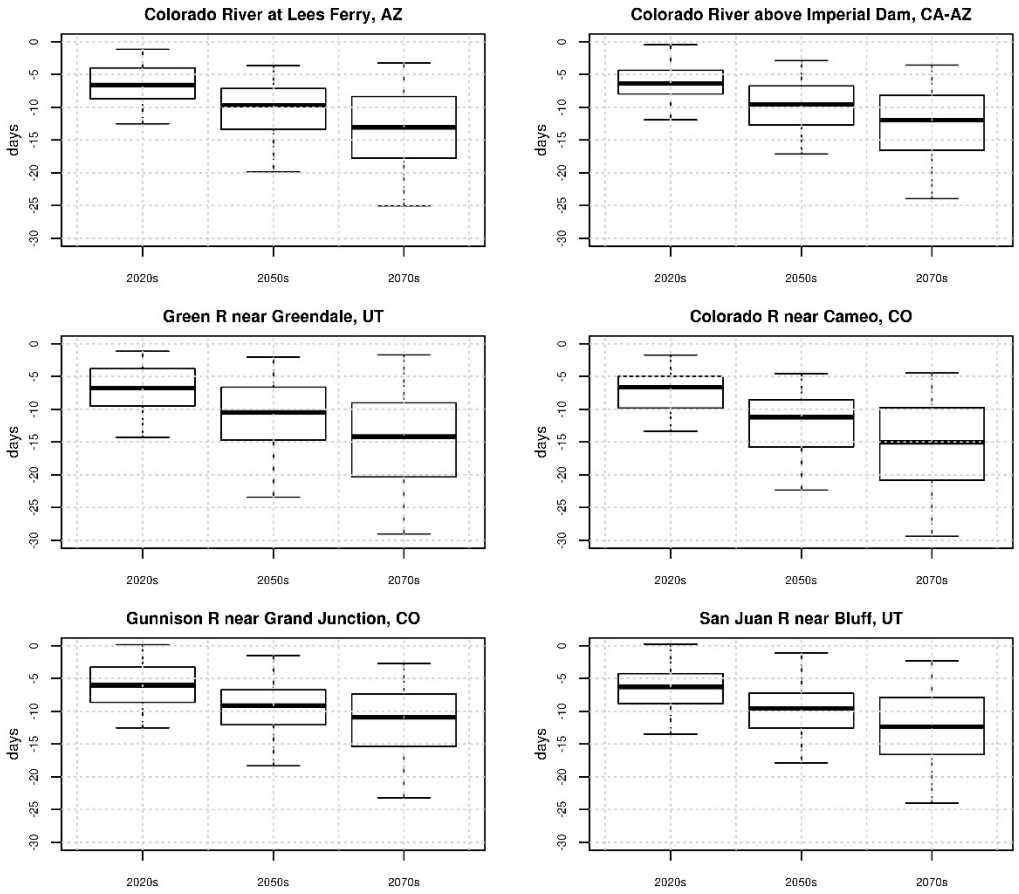

Figure 8. Colorado Basin – Simulated shift in streamflow timing for various sub-basins; negative values denote earlier runoff relative to the 1990s

3.3. Columbia River Basin

The Columbia River is the fourth largest river in North America, rising in the Rocky Mountains of British Columbia, Canada, and flowing 1,243 miles to the Pacific Ocean through Washington and Oregon. The river system has more than 400 dams, which provide hydroelectricity, irrigation, flood control, streamflow regulation, and storage and delivery of water. These projects provide up to 80 percent of the electrical needs in the Northwest, 39.7 million acre-feet of storage space for flood control, locks and other infrastructure for navigation of 17 million tons of cargo annually, and irrigation for 7.8 million acres of land and recreational opportunities for hundreds of thousands of Americans.

3.3.1. Hydroclimate Projections

Figure 9 shows six hydroclimate indicators for the Columbia River at The Dalles: annual total precipitation (top left), annual mean temperature (top right), April 1st SWE (middle left), annual runoff (middle right), December-through-March runoff (bottom left), and April-through-July runoff (bottom right). The heavy black line

is the annual time series of 50th percentile (i.e., median) values of the 97 projections. The shaded area is the annual time series of the 10th to 90th percentiles.

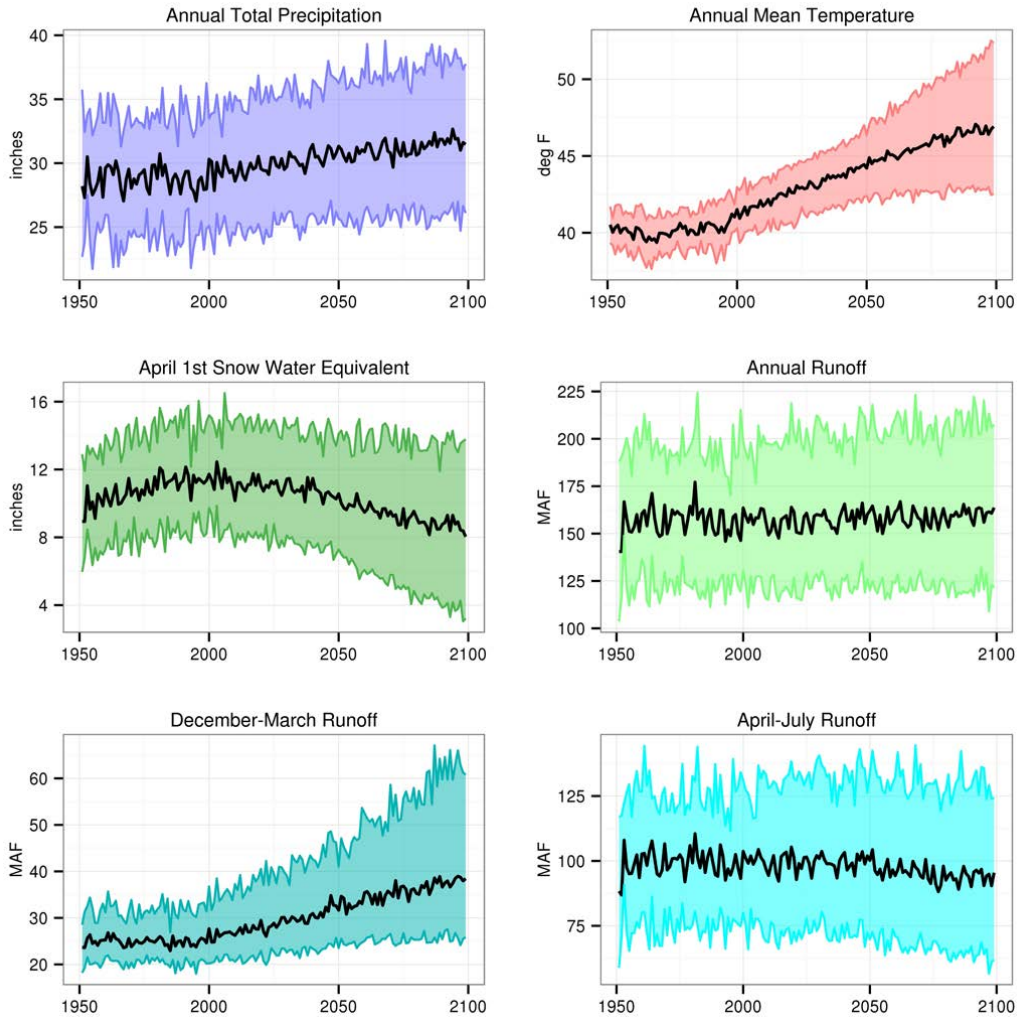

Figure 9. Columbia Basin – Projections for six hydroclimate indicators

The heavy black line is the annual time series median value (i.e., median). The shaded area is the annual time series of 10h to 90th percentiles.

There is an increasing trend of total annual precipitation across the basin through time. The uncertainty envelope for precipitation is also diverging. Mean annual temperature shows an increasing trend, with an expanding uncertainty envelope through time. The April 1st SWE appears to have a nonlinear trend. The SWE analysis indicates a decline in the post-2025 period. The annual runoff has no trend but has slightly expanding uncertainty bounds. The December-through-March runoff also shows an increasing trend, and the upper uncertainty bound shows divergence over time or increasing uncertainty. Meanwhile, the April-through-July runoff also appears to decrease slightly over time.

Figure 10, Figure 11, and Figure 12 show the spatial distribution of simulated decade mean temperatures, precipitation, and April 1st SWE, respectively, in the Columbia River above The Dalles. In each figure, the simulated 1990s distribution of median decadal mean condition for the variable of interest is shown in the upper middle plot, and changes in the decadal mean condition are shown below for the three future periods and at three change percentiles within the range of projections (25th, 50th, and 75th percentiles).

In Figure 10, the median change for the three future decades relative to the 1990s indicates increasing temperatures throughout the basin. Figure 11, the median change in precipitation for the future decades indicates a wet pattern, particularly in the higher-elevation portions of the basin. In Figure 12, the spatial plots indicate the basin is projected to have generally reduced snowpack. Analyses of results from Figures 9 through 12 indicate that warming is projected to lead to precipitation falling as rain instead of snow, leading to decreased snowpack in the basin.

Figure 13 shows the distribution of April 1st SWE with elevation in the Columbia River Basin for the reference decade and the percentage change in this distribution for the three future decades. The 25th and 75th percentile estimates provide a way to quantify the uncertainty in the calculated changes.

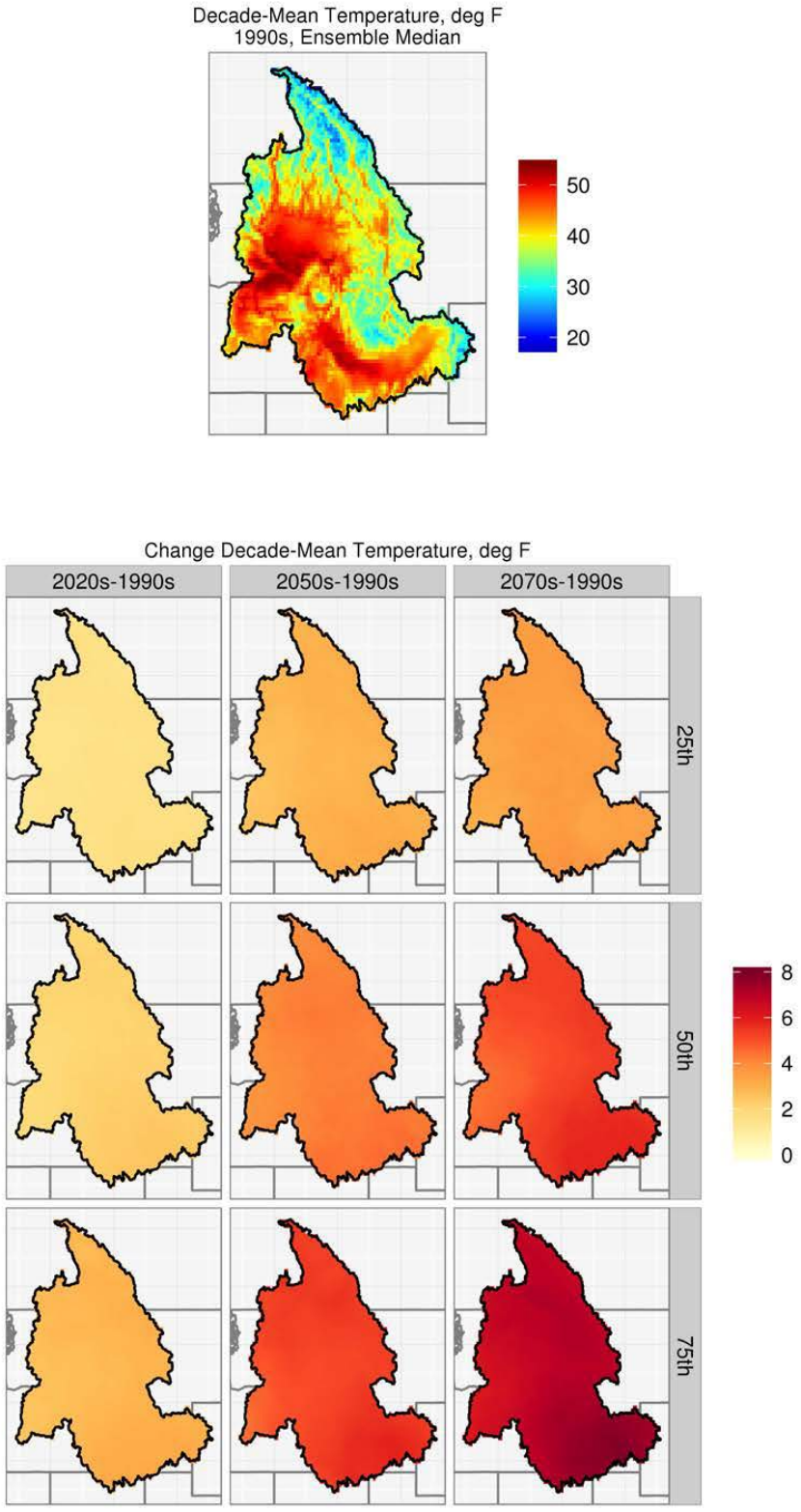

Figure 10. Columbia Basin – Spatial distribution of simulated decadal temperature

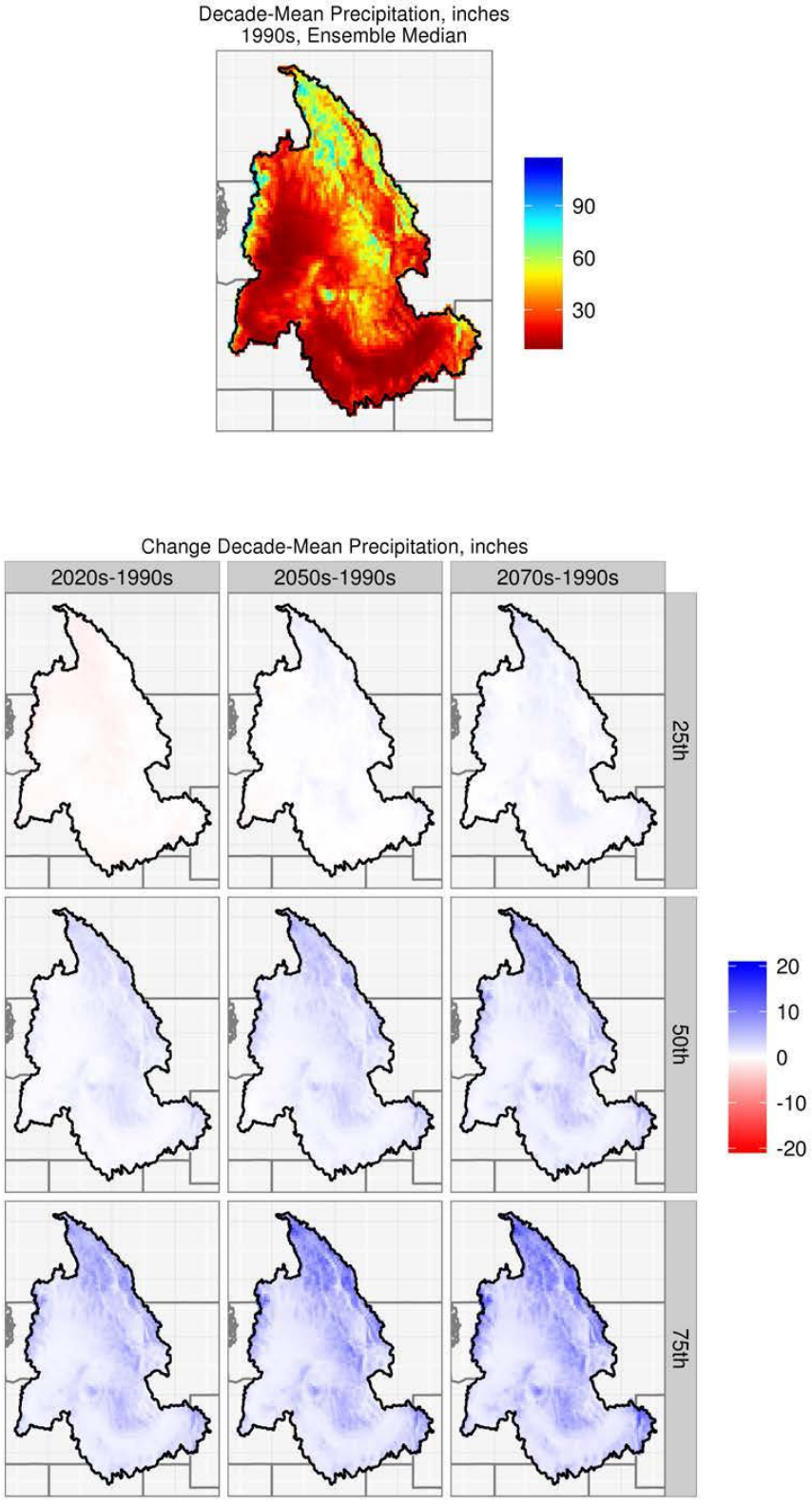

Figure 11. Columbia Basin – Spatial distribution of simulated decadal precipitation

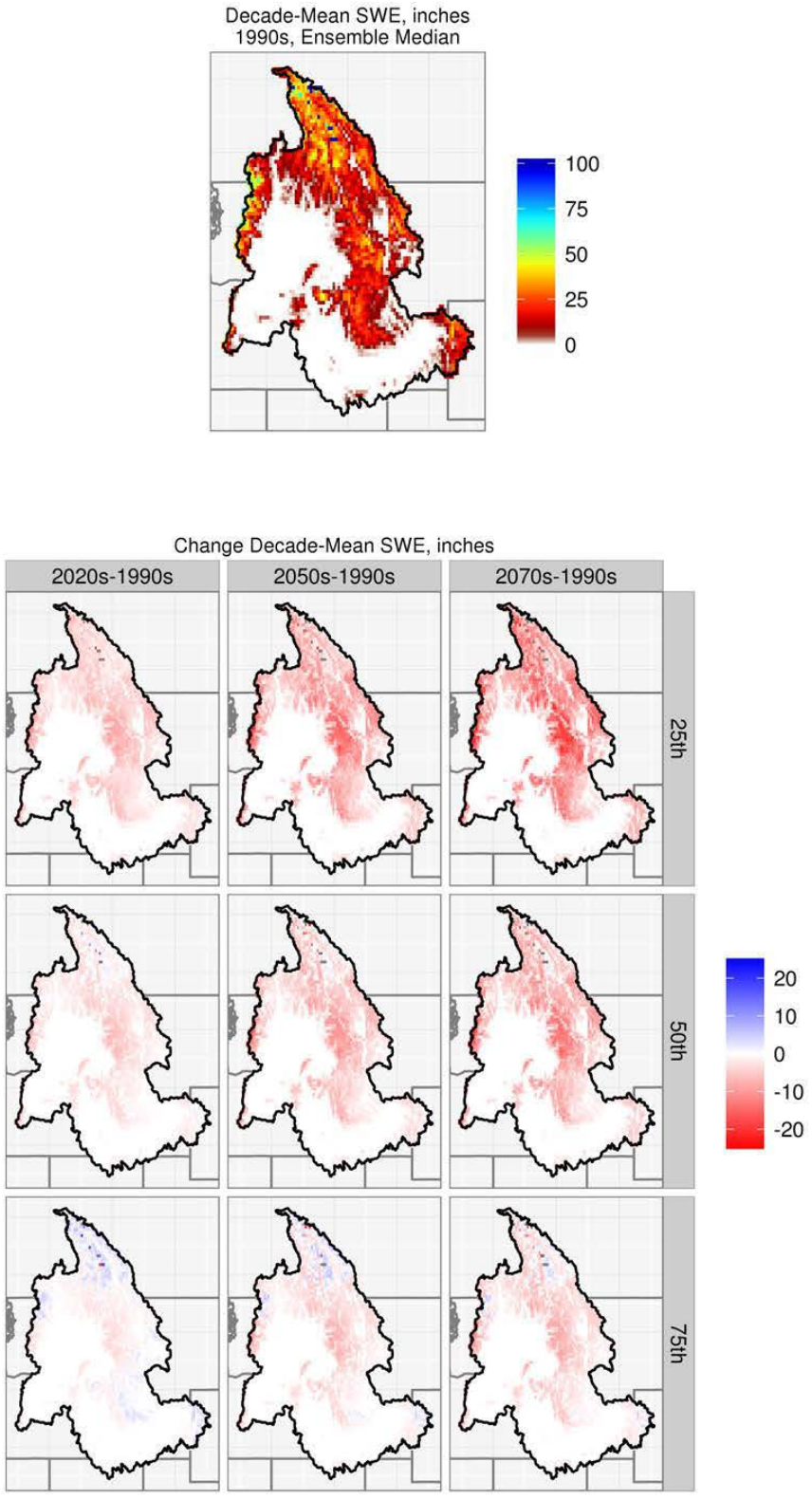

Figure 12. Columbia Basin – Spatial distribution of simulated decadal April 1st SWE

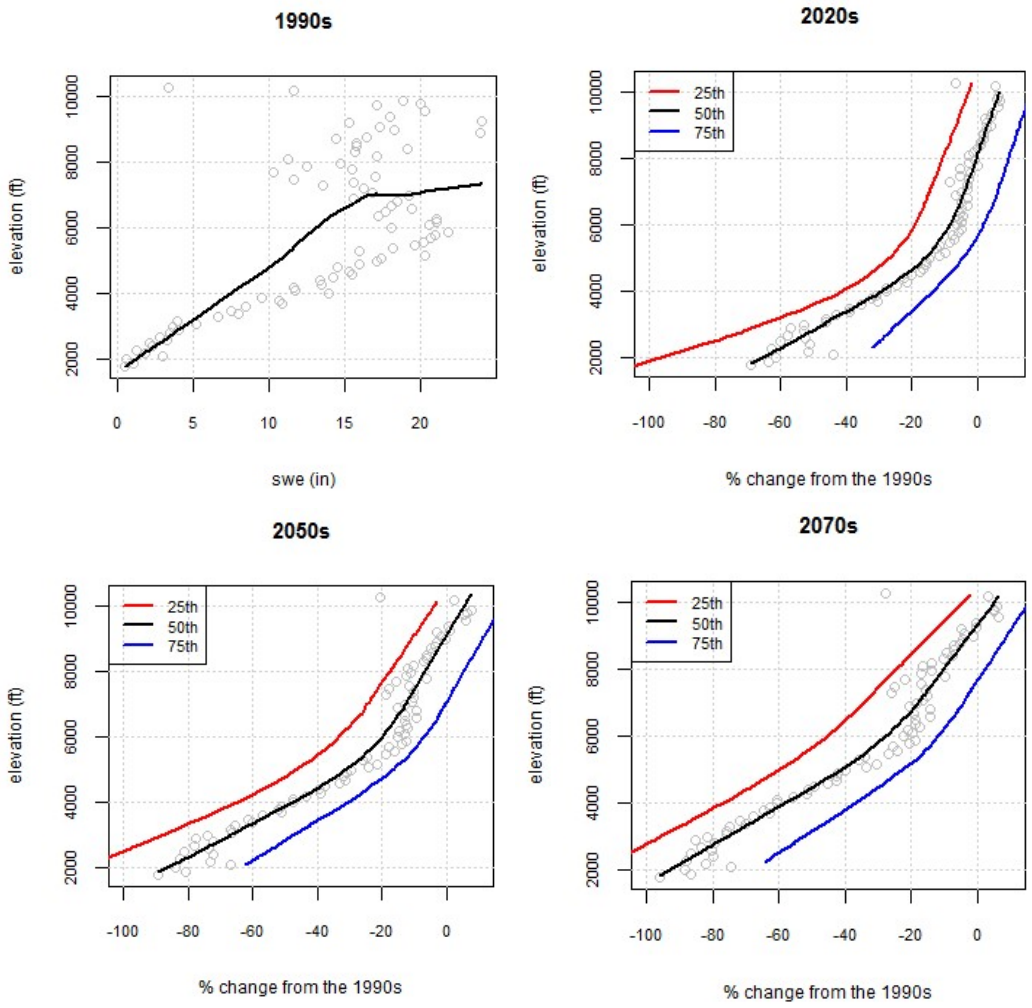

Figure 13. Columbia Basin – SWE distribution with elevation in the 1990s decade and future changes

The open light gray circles in this plot correspond to the median SWE values at each elevation with a fitted regression line is shown in black. The regression lines for the 25th and the 75th percentiles are presented in red and blue, respectively.

The SWE elevation range for the Columbia River Basin (the elevation range of areas shown by the VIC model to have met the threshold April 1st SWE of at least 10 mm during the 1990s) was estimated to be approximately 2,000 to 10,000 feet. The 1990s decade-mean SWE distribution (top left panel plot) shows multiple clusters with the regression line attempting to optimally fit the point scatter. Visually, there appear to be three clusters of points. First, the SWE distribution between the elevations of approximately 2,000 and 6,000 feet (lower elevation) appears to be fairly linear. A second set between about 6,000 and 8,000 feet (middle elevation) and a third set above about 8,000 feet (higher elevation) both appear to have a linear distribution of SWE. This distribution pattern of the points and the non-linearity of the fitted line suggest multiple systems of moisture sources, including a combination of high-elevation persistent snowpack (glacial)

and cyclical snowpack accumulation and ablation at middle to lower elevations driven by the annual hydrologic cycle.

Overall, the analysis seems to show a substantial loss in SWE at lower elevations in the 2020s. The higher elevations also appear to have a gradual net decline in the median SWE values from the 2020s to 2050s and from the 2050s to the 2070s. Generally, SWE declines throughout the basin, although the rate of decline is more pronounced at lower elevations than at higher elevations.

3.3.2. Impacts on Streamflow Annual and Seasonal Cycles

Figure 14 shows the mean monthly streamflow values for the 1990s, 2020s, 2050s, and 2070s in seven Columbia River sub-basins. Overall, there does not appears to be much of a shift in the peak runoff timing from the reference decade to the 2020s and 2050s. For the 2070s, though, all the sub-basins except for the Columbia River at Grand Coulee and at The Dalles show a noticeable shift.

Figure 15 shows boxplots of the distribution of simulated changes in streamflow magnitude for annual, December-through-March, and April-through-July runoff in the seven Columbia River sub-basins. For all the sub-basins in all three future decades, the median change for the December-through-March runoff is positive, indicating an increase in streamflow during this season. Coincidently, the April-through-July median streamflow shows declines in the 2050s and 2070s relative to the 1990s across some of the sub-basins (e.g., Deschutes River near Madras, Flathead River at Columbia Falls, and the Yakima River at Parker). The median annual runoff shows no change in any of the sub-basins in any of the three future periods.

Figure 16 shows the simulated shift in streamflow timing for the various sub-basins. For all the sub-basins in all three future decades, the median value of the change in runoff timing is negative. This implies that half of the annual flow occurs sooner than it did in the 1990s. For example, for the Columbia River at The Dalles, the earlier shift is about, 5, 8, and 11 days, respectively, in the 2020s, 2050s, and 2070s relative to the 1990s.

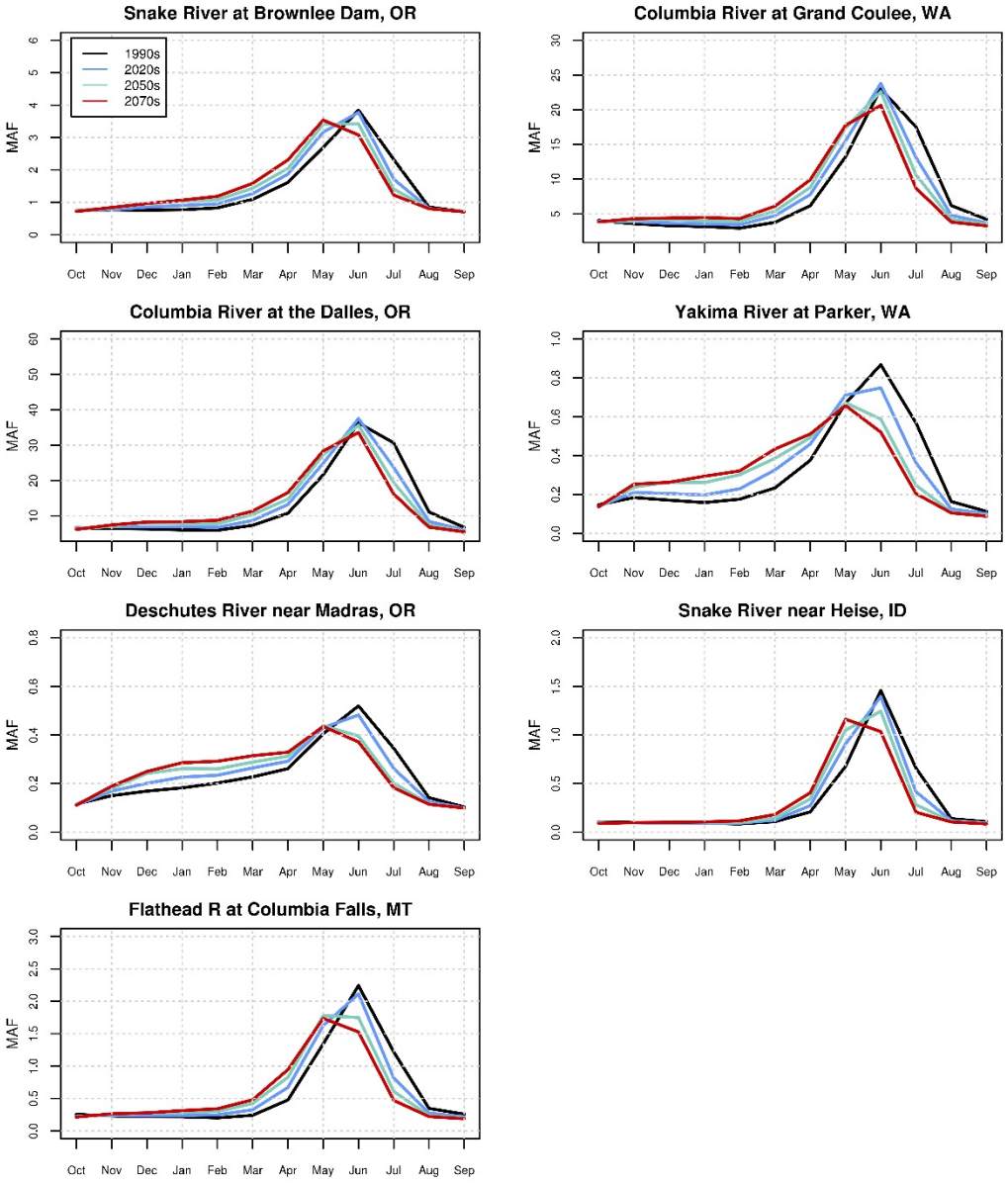

Figure 14. Columbia Basin – Simulated mean monthly streamflow for various sub-basins

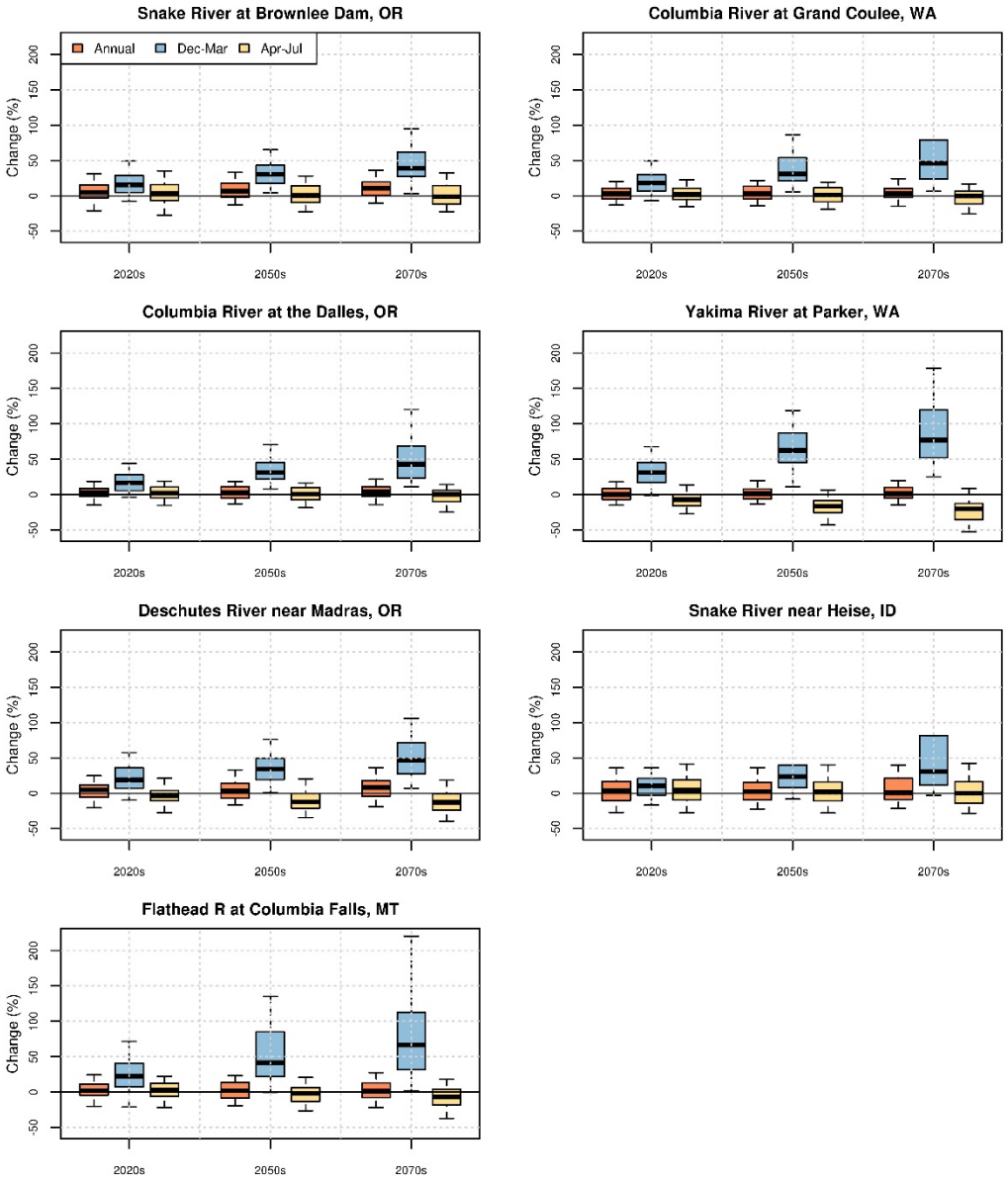

Figure 15. Columbia Basin – Simulated change in streamflow magnitude for various sub-basins

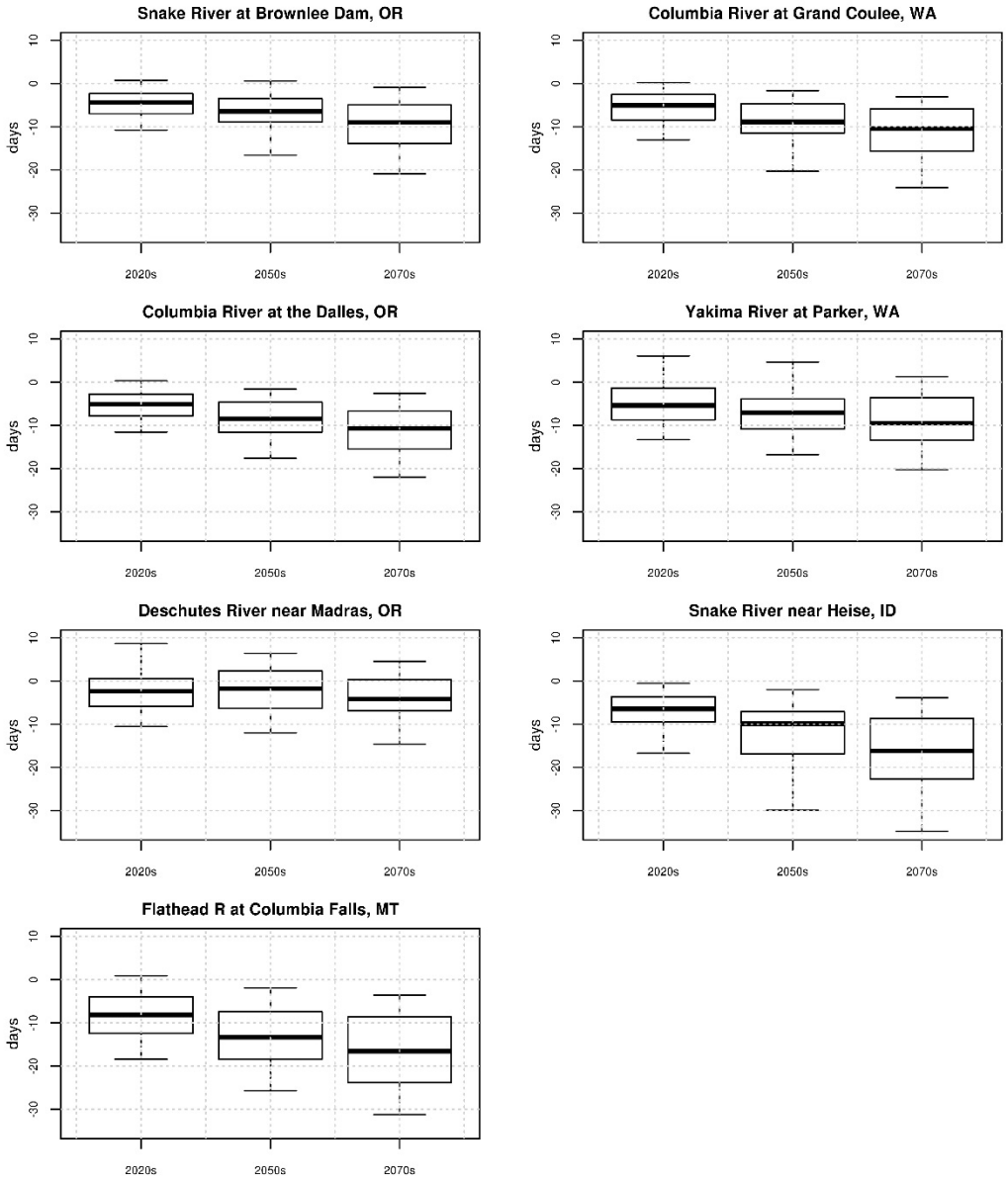

Figure 16. Columbia Basin – Simulated shift in streamflow timing for various sub-basins

3.4. Klamath River Basin

The Klamath River originates in headwater streams of south-central Oregon, eventually flowing southwest through the Cascade Range and picking up runoff from the Shasta, Scott, Salmon and Trinity Rivers in California, before flowing to the Pacific Ocean. Reclamation's Klamath Project provides irrigation water for approximately 210,000 acres of cropland and is an important recreation area for residents of northern California and southern Oregon, providing myriad boating, water skiing, fishing, hunting, camping and picnicking opportunities. Surplus water from the Trinity River is stored, regulated, and diverted through a system of

dams, reservoirs, tunnels, and powerplants into the Sacramento River, for use in water-deficient areas of California's Central Valley.

3.4.1. Hydroclimate Projections

Figure 17 shows six hydroclimate indicators for the basin above the Klamath River near Klamath gauging station: annual total precipitation (top left), annual mean temperature (top right), April 1st SWE (middle left), annual runoff (middle right), December-through-March runoff (bottom left), and April-through-July runoff (bottom right). The heavy black line is the annual time series of 50th percentile (i.e., median) values of the 97 projections. The shaded area is the annual time series of the 10th to 90th percentiles.

Total annual precipitation and the corresponding uncertainty envelope appear to be largely constant over time, implying that there is no increase or decrease in the uncertainty envelope from the present for total annual precipitation magnitudes. The mean annual temperature shows an increasing trend over time, and April 1st SWE shows a decreasing trend. Similar to precipitation, annual runoff shows no apparent trend. The December-through-March runoff volume shows a slightly increasing trend, while the April-through-July runoff shows a more apparent declining trend over time.

Figure 18, Figure 19, and Figure 20 show the spatial distribution of simulated decade mean temperatures, precipitation, and April 1st SWE, respectively, in the basin above the Klamath River near Klamath gauging station. In each figure, the simulated 1990s distribution of median decadal mean condition for the variable of interest is shown in the upper middle plot, and changes in the decadal mean condition are shown below for the three future periods and at three change percentiles within the range of projections (25th, 50th, and 75th percentiles).

In Figure 18, the median change for the three future decades relative to the 1990s indicates increasing temperatures throughout the basin. In Figure 19, the median change in precipitation for the future decades indicates a slightly wetter pattern in the lower basin. In Figure 20, the spatial plots indicate that a reduced snowpack is projected throughout the basin.

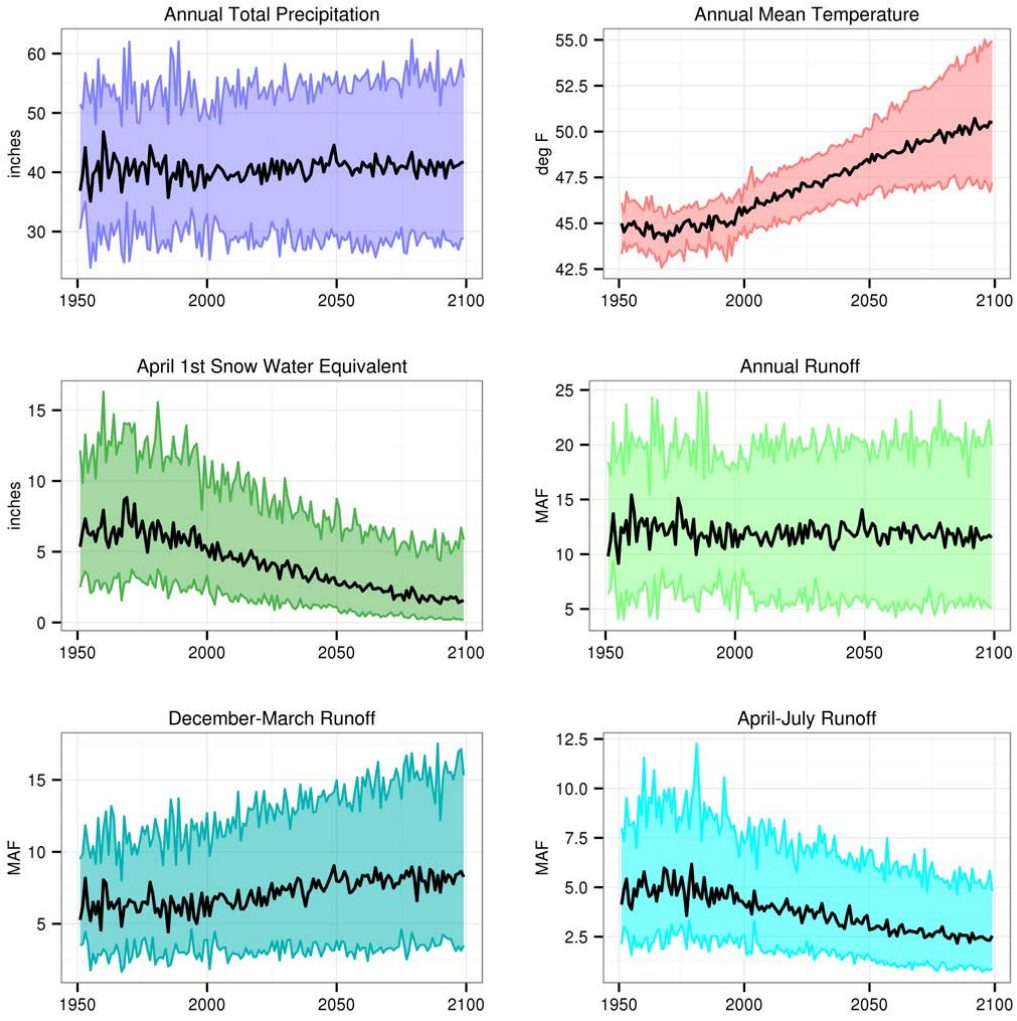

Figure 17. Klamath Basin – Projections for six hydroclimate indicators

The heavy black line is the annual time series median value (i.e., median). The shaded area is the annual time series of 10^{h} to 90th percentiles.

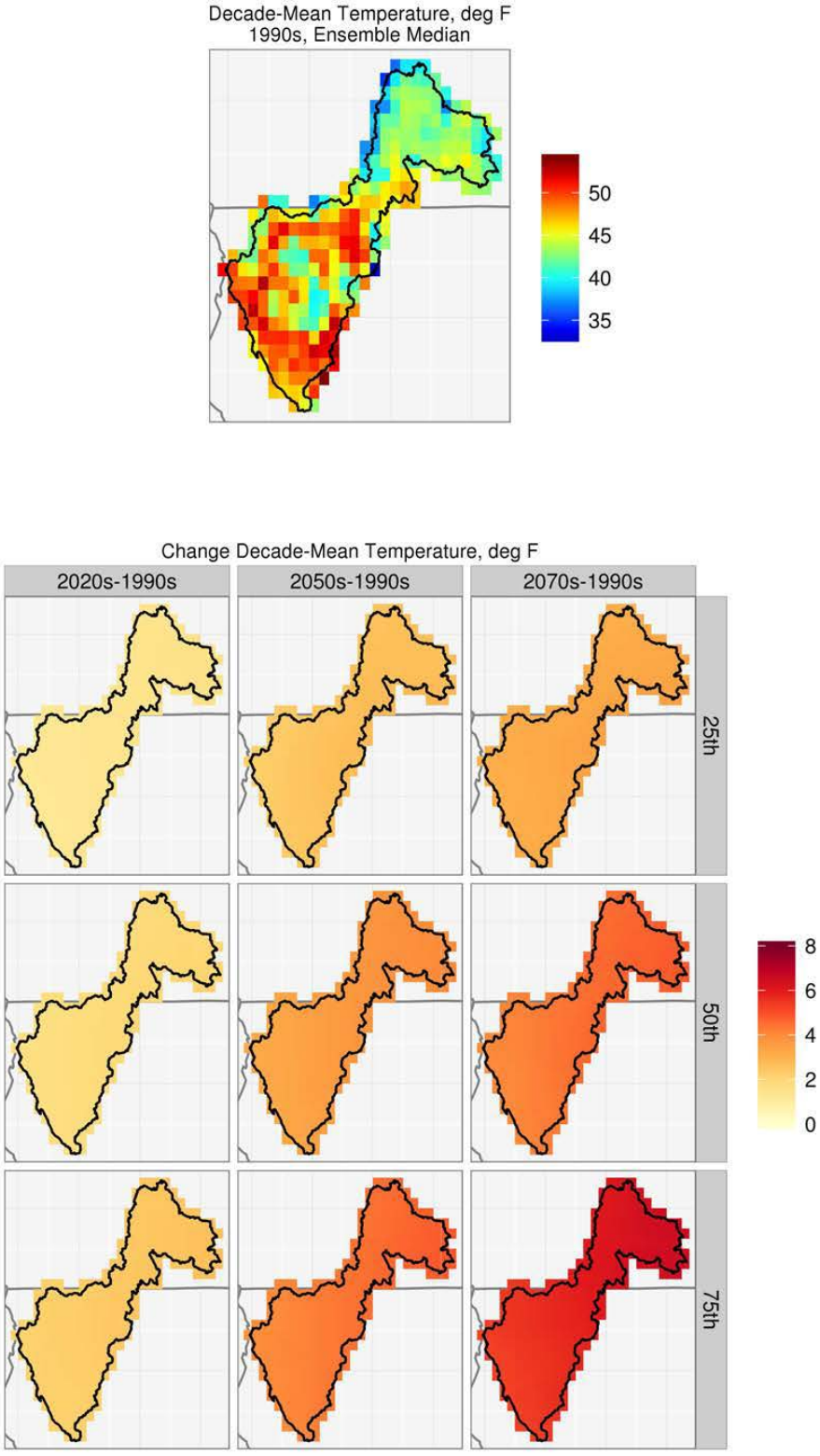

Figure 18. Klamath Basin – Spatial distribution of simulated decadal temperature

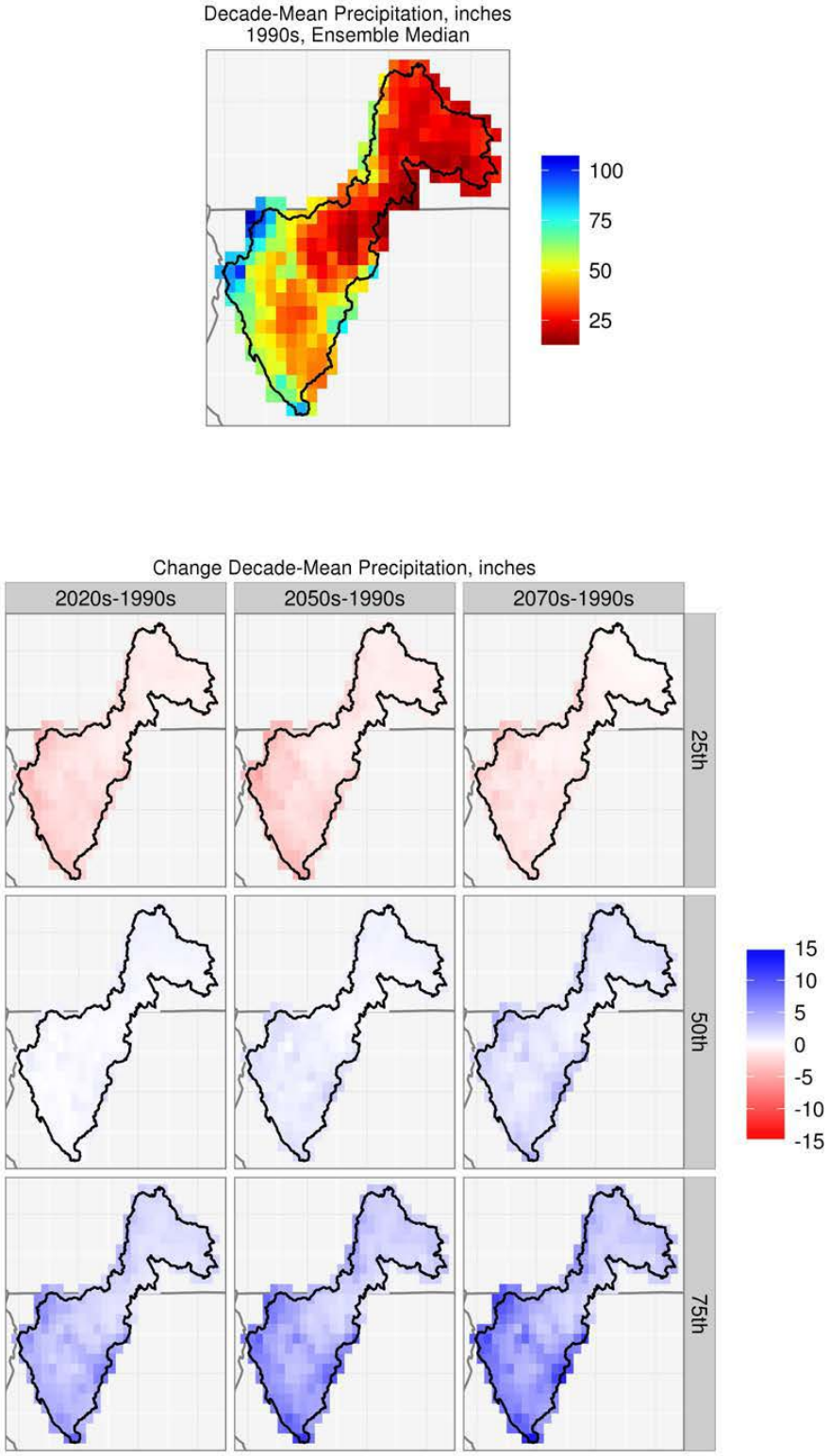

Figure 19. Klamath Basin – Spatial distribution of simulated decadal precipitation

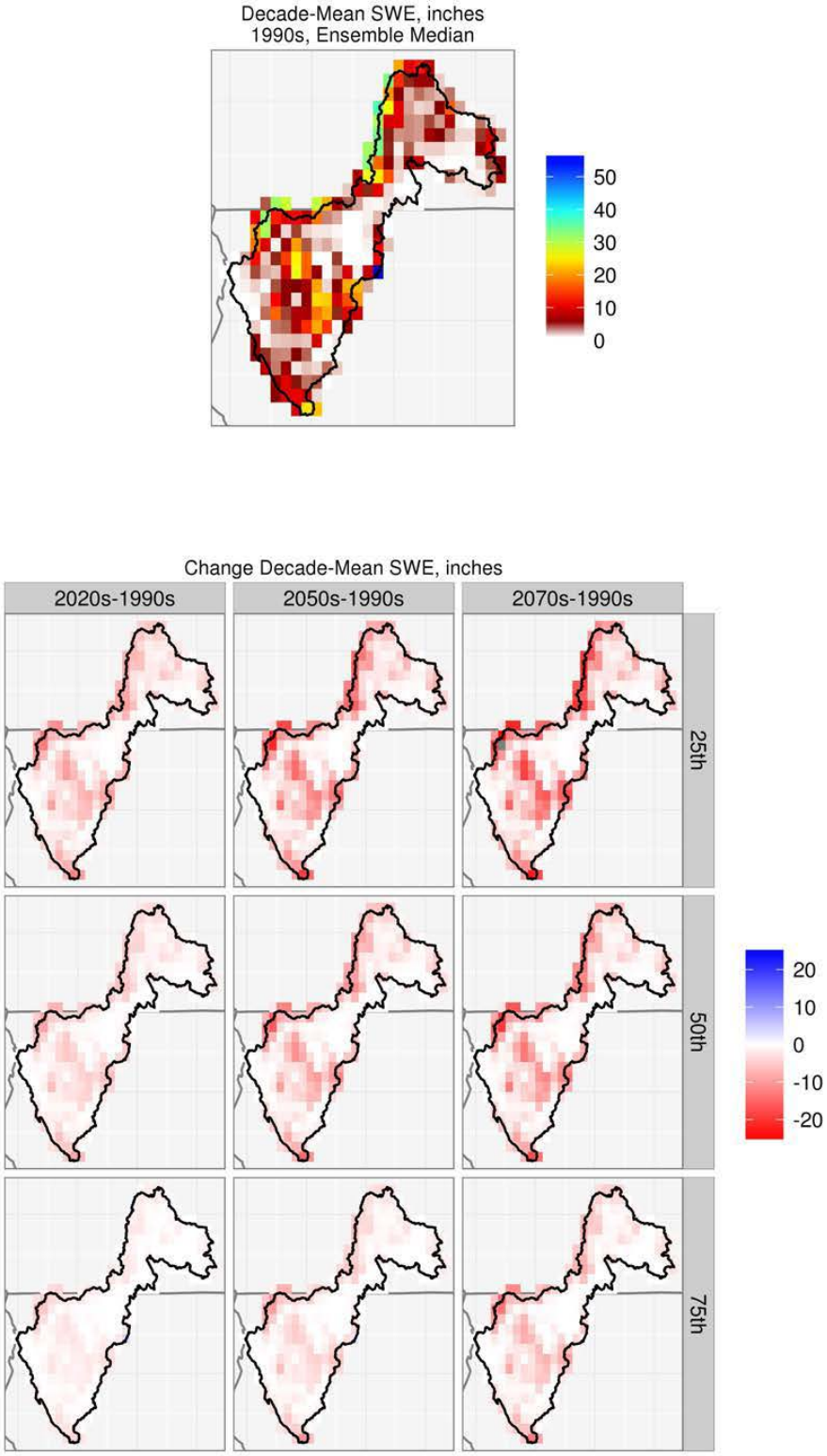

Figure 20. Klamath Basin – Spatial distribution of simulated decadal April 1st SWE

Figure 21 shows the distribution of April 1st SWE with elevation in the Klamath River Basin for the reference decade and the percentage change in this distribution for the three future decades. The 25th and 75th percentile estimates provide a way to quantify the uncertainty in the calculated changes.

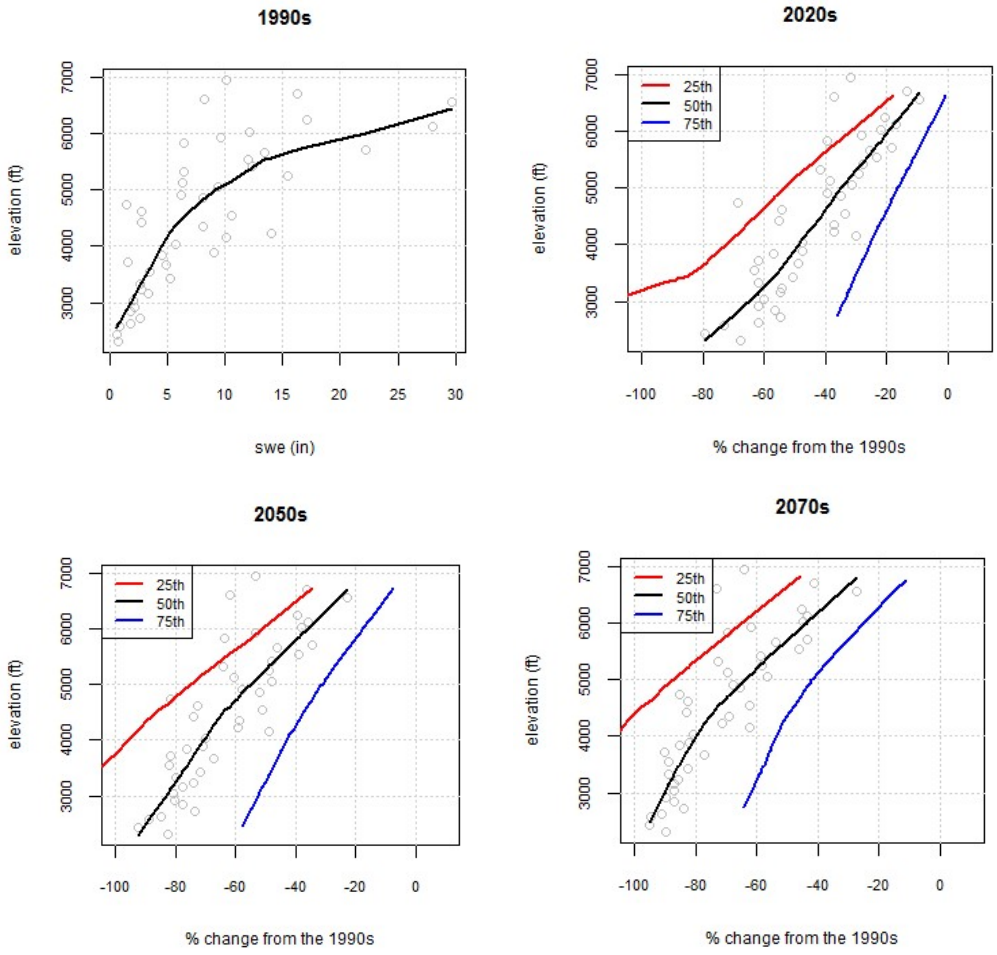

Figure 21. Klamath Basin – SWE distribution with elevation in the 1990s decade and future changes

The open light gray circles in this plot correspond to the median SWE values at each elevation with a fitted regression line is shown in black. The regression lines for the 25th and the 75th percentiles are presented in red and blue, respectively.

The SWE elevation range for the Klamath River Basin (the elevation range of areas shown by the VIC model to have met the threshold April 1st SWE of at least 10 mm during the 1990s) was estimated to be approximately 2,000 to 7,000 feet. The 1990s decade-mean SWE distribution (top left panel plot) shows a distributed pattern, with the regression line attempting to optimally fit the point scatter. Visually, it appears that points above 5,000 feet are more broadly distributed than those at lower elevations. This distribution pattern of the points and the non-linearity of the fitted line suggest multiple systems of moisture sources and

processes contributing to the annual snowpack development. Overall, there appears to be substantial loss in SWE at all elevations throughout the Basin from the 1990s, which becomes progressively greater in each of the future time periods.

3.4.2. Impacts on Streamflow Annual and Seasonal Cycles

Figure 22 shows mean monthly streamflow values for the 1990s, 2020s, 2050s, and 2070s in five Klamath River sub-basins. For all the five sites in this basin, the shift in peak runoff in all the future decades is clearly visible and fairly pronounced for the 2070s relative to the 1990s.

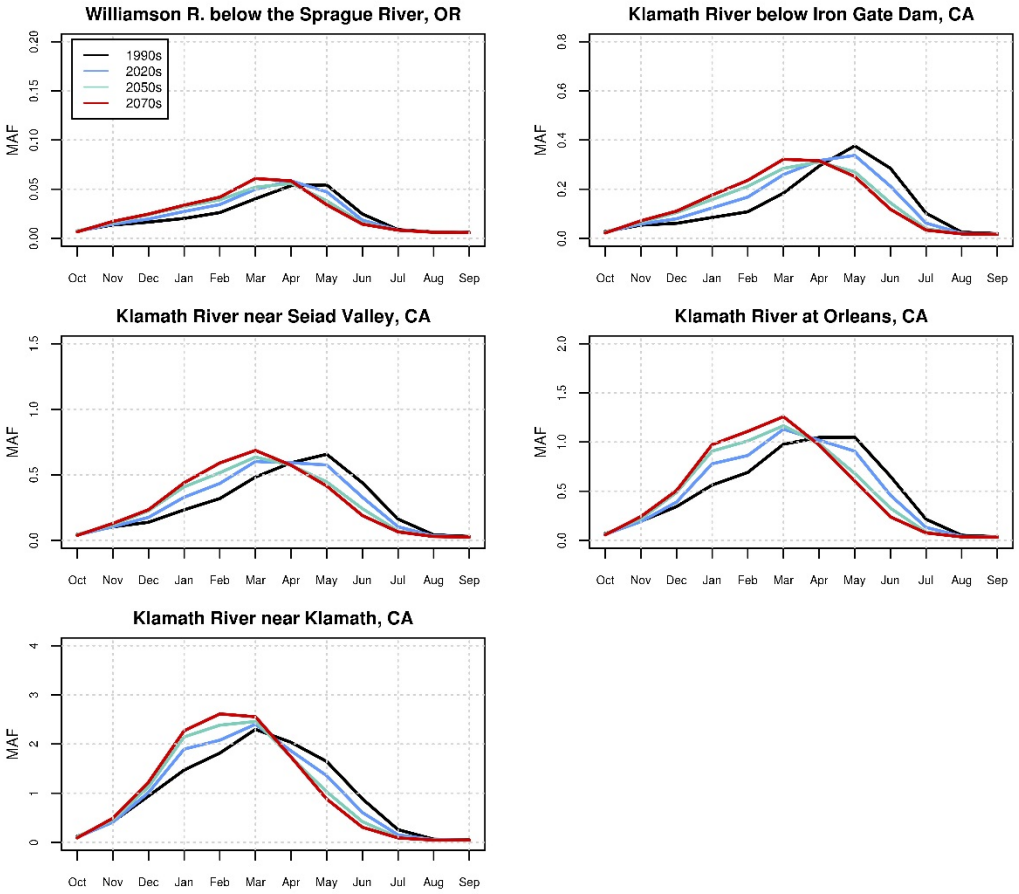

Figure 22. Klamath Basin – Simulated mean monthly runoff for various sub-basins

Figure 23 shows boxplots of the distribution of changes in runoff magnitude for annual, December-through-March and April-through-July runoff in the five Klamath River sub-basins. For all the sub-basins in all the three future decades, the median change for the December-through-March runoff is positive, indicating an increase in runoff during this season. However, the April-through-July median runoff shows declines in the 2020s, 2050s, and 2070s relative to the 1990s across all of the sub-basins. The median annual runoff shows no change in any of the sub-basins in any of the three future periods.

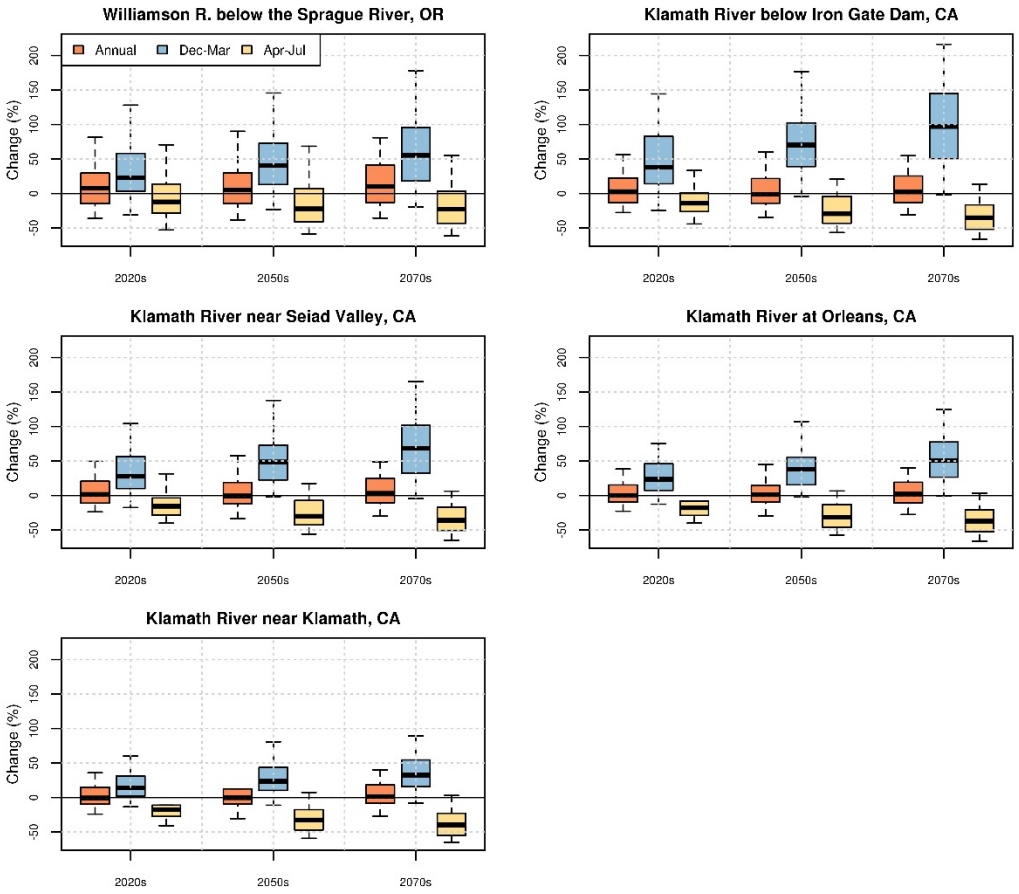

Figure 23. Klamath Basin – Simulated change in runoff magnitude for various sub-basins

Figure 24 shows the simulated shift in runoff timing for the various sub-basins. For all the sub-basins in all three future decades, the median value of the change in runoff timing is negative. This implies that half of the annual flow occurs earlier than it did in the 1990s. However, there is generally not much difference between the timing shifts shown for the three future decades. As an example, for the location Klamath River near Klamath, the median shift for all three future decades is about 4 days earlier than in the 1990s.

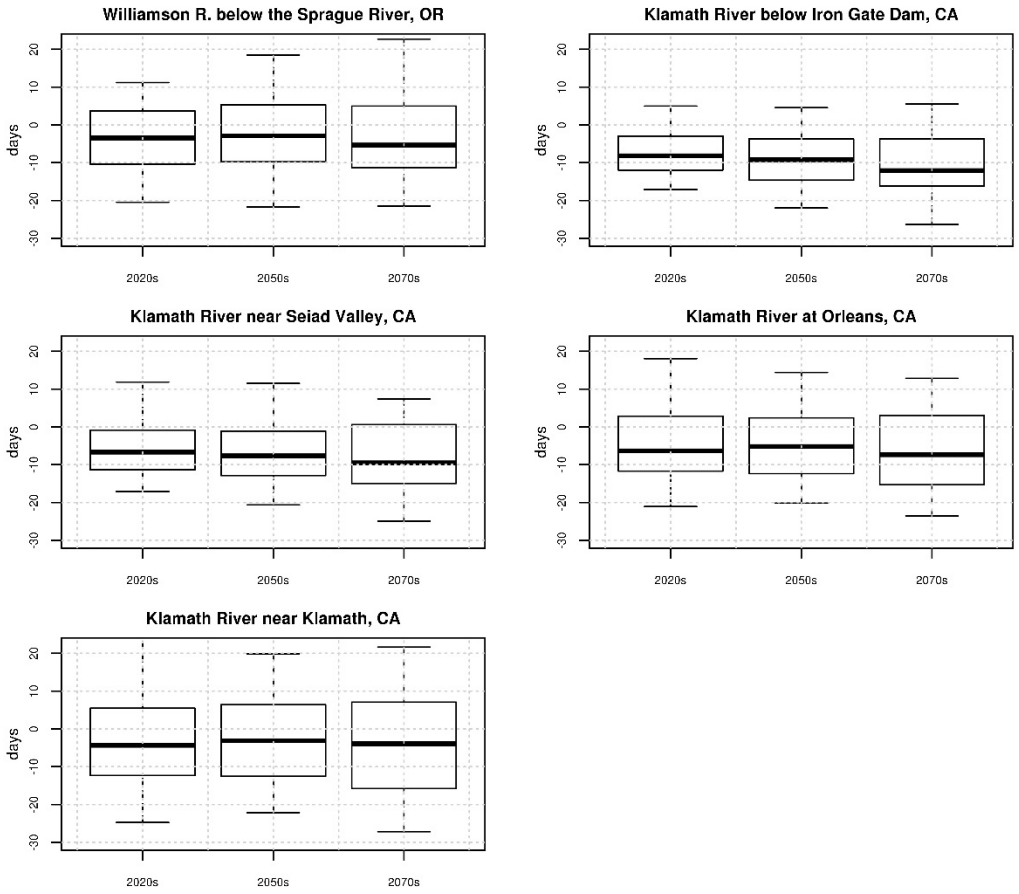

Figure 24. Klamath Basin – Simulated shift in runoff timing for various sub-basins

3.5. Missouri River Basin

The Missouri is the longest river in the United States. It has a watershed of more than 500,000 square miles, which includes portions of 10 states and one Canadian province and encompasses approximately one-sixth of the United States. The Missouri drains the largest watershed within the United States and produces annual yields of 40 million acre-feet. Reclamation has constructed more than 40 dams on Missouri River tributaries that have helped with agricultural development in the basin. The facilities in the basin also provide significant benefits, including flood control, navigation, irrigation, power, water supply, recreation, fish and wildlife, and water quality. Navigation is important in the lower Basin States. Reliable water delivery for agriculture and for municipal, rural, and industrial use is important in the upper Basin States.

3.5.1. Hydroclimate Projections

Figure 25 shows six hydroclimate indicators for the Missouri River Basin above Omaha: annual total precipitation (top left), annual mean temperature (top right), April 1st SWE (middle left), annual runoff (middle right), December-through-

March runoff (bottom left), and April-through-July runoff (bottom right). The heavy black line is the annual time series of 50th percentile (i.e., median) values of the 97 projections. The shaded area is the annual time series of the 10th to 90th percentiles.

There is an increasing trend of total annual precipitation and mean annual temperature across the basin through time. April 1st SWE shows a decreasing trend, while annual runoff shows an increasing trend. Both December-through-March and April-through-July runoff show increasing trends, and the upper uncertainty bound shows divergence over time or increasing uncertainty. The fact that annual total precipitation has an increasing trend contributes to the increased April-through-July runoff.

Figure 26, Figure 27, and Figure 28 show the spatial distribution of simulated decade mean temperatures, precipitation, and April 1st SWE, respectively, in the Missouri River Basin. In each figure, the simulated 1990s distribution of median decadal mean condition for the variable of interest is shown in the upper middle plot, and changes in the decadal mean condition are shown below for the three future periods and at three change percentiles within the range of projections (25th, 50th, and 75th percentiles).

In Figure 26, the median change for the three future decades relative to the 1990s indicates increasing temperatures throughout the basin. In Figure 27, the median change in precipitation for the future decades indicates a wetter pattern. In Figure 28, the spatial plots indicate the basin is projected to have generally reduced snowpack. Analyses of the results from Figures 25 through 28 indicate that warming is projected to lead to precipitation falling as rain instead of snow and, consequently, to decreased snowpack in the basin. However, due to projected increases in precipitation, runoff is expected to increase.

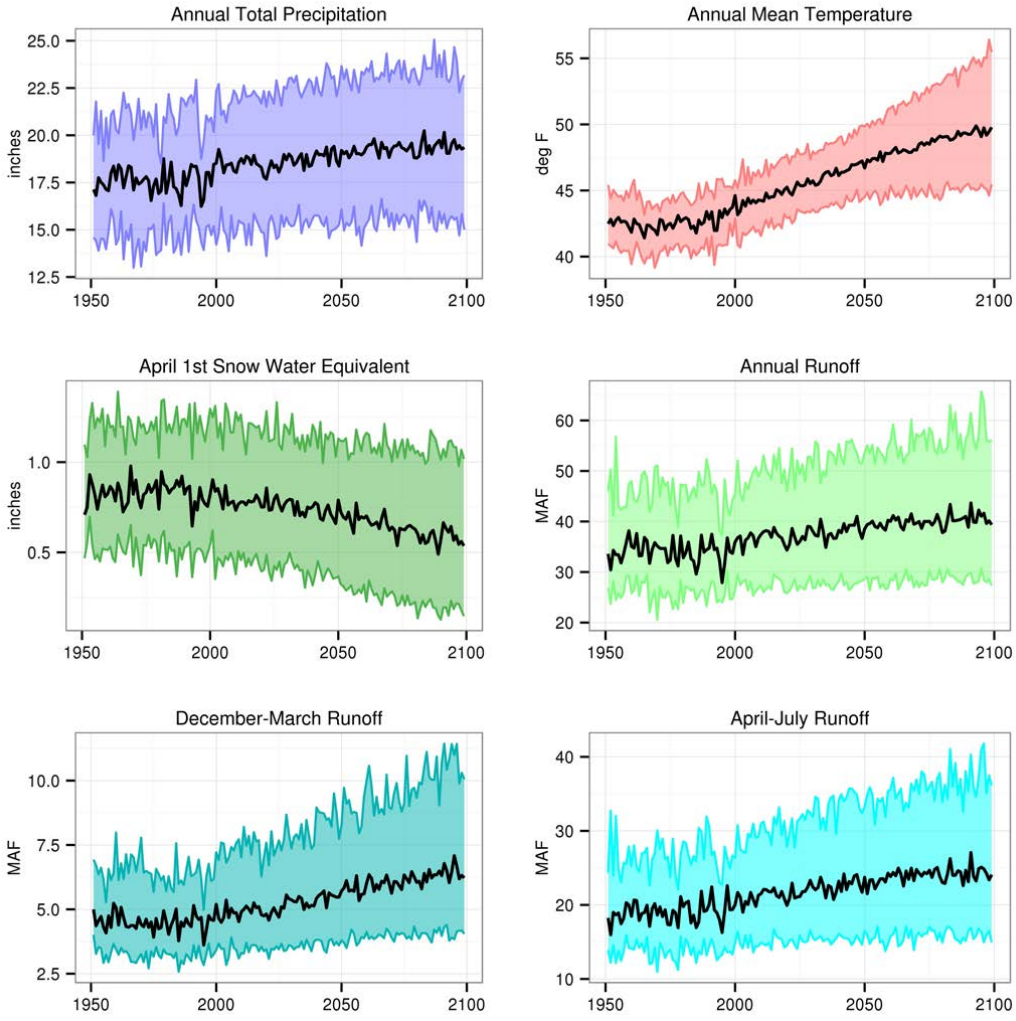

Figure 25. Missouri Basin – Projections for six hydroclimate indicators

The heavy black line is the annual time series median value (i.e., median). The shaded area is the annual time series of 10^{h} to 90th percentiles.

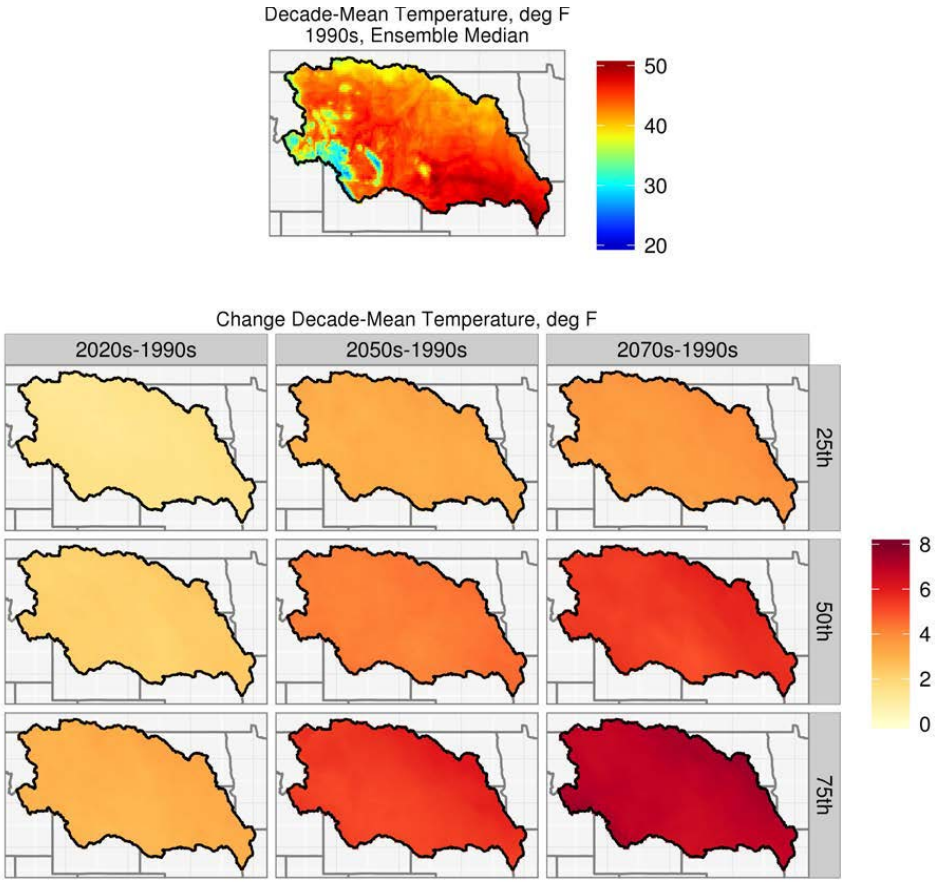

Figure 26. Missouri Basin – Spatial distribution of simulated decadal temperature

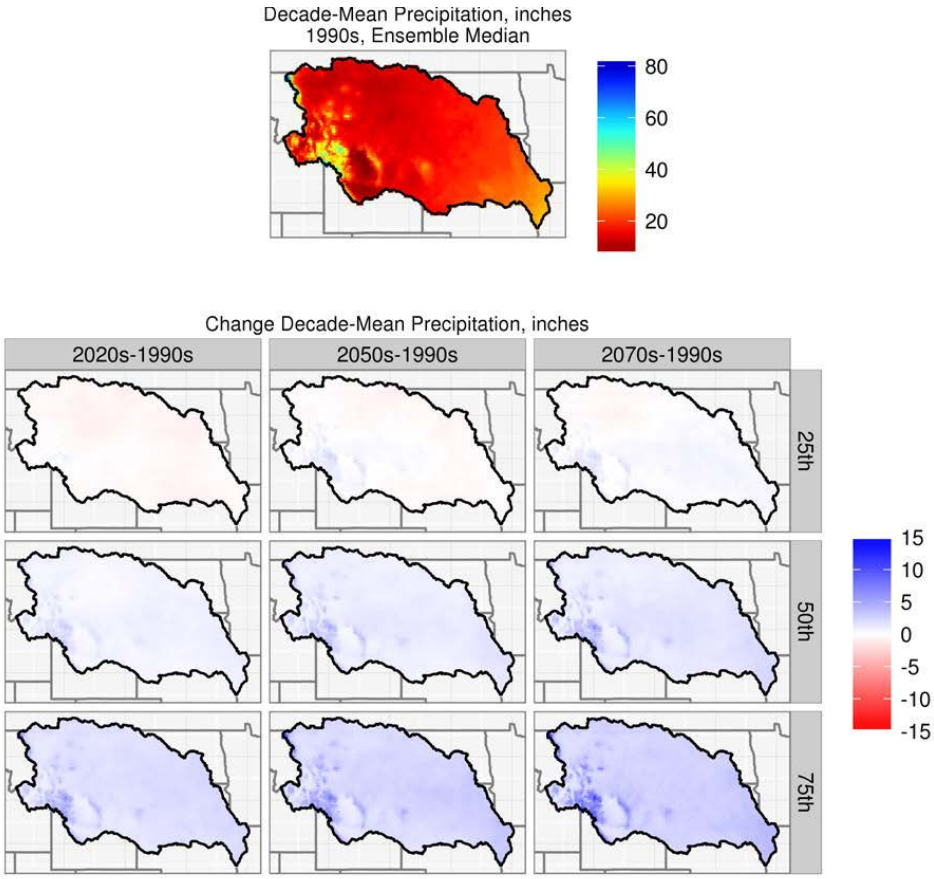

Figure 27. Missouri Basin – Spatial distribution of simulated decadal precipitation

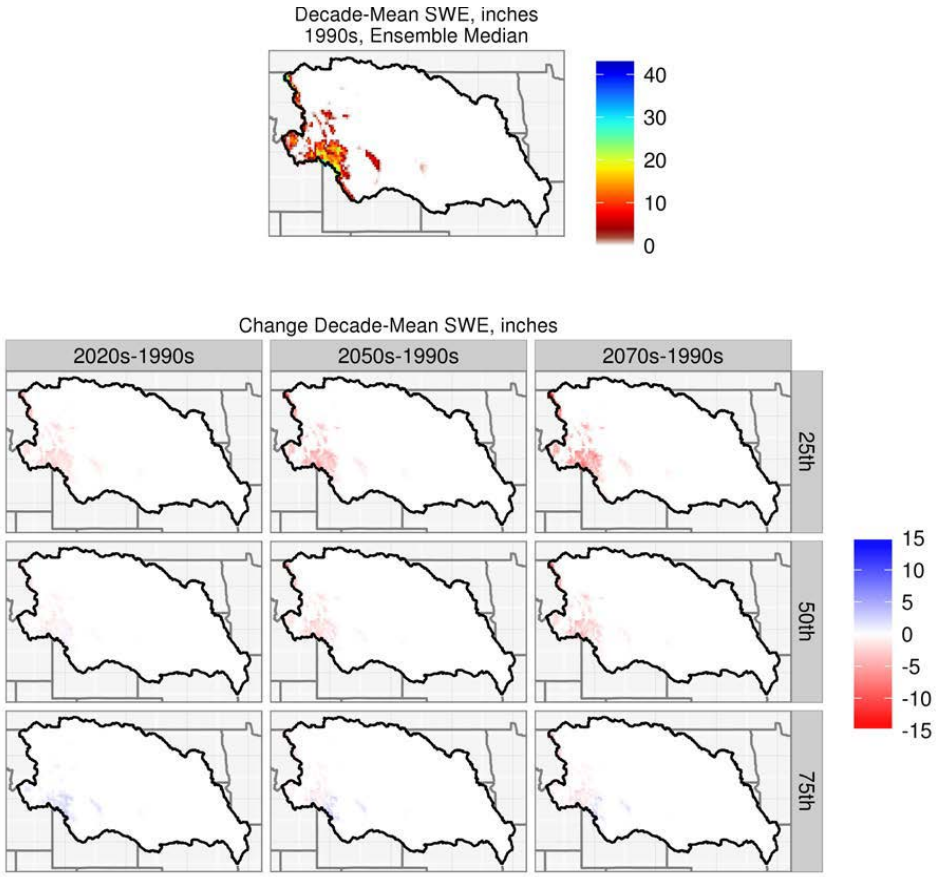

Figure 28. Missouri Basin – Spatial distribution of simulated decadal April 1st SWE

Figure 29 shows the distribution of April 1st SWE with elevation in the Missouri River Basin for the reference decade and the percentage change in this distribution for the three future decades. The 25th and 75th percentile estimates provide a way to quantify the uncertainty in the calculated changes.

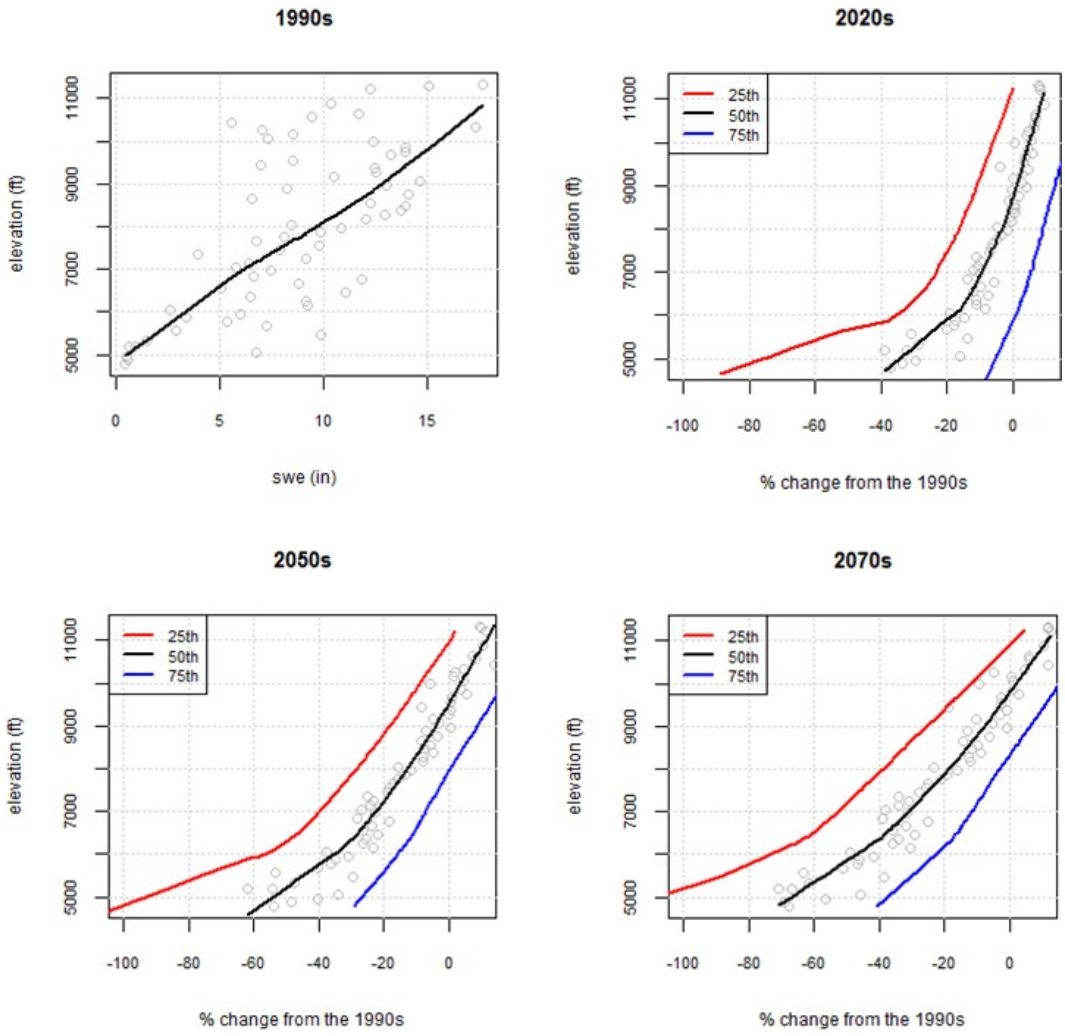

Figure 29. Missouri Basin – SWE distribution with elevation in the 1990s decade and future changes

The open light gray circles in this plot correspond to the median SWE values at each elevation with a fitted regression line is shown in black. The regression lines for the 25th and the 75th percentiles are presented in red and blue, respectively.

The SWE elevation range for the Missouri River Basin (the elevation range of areas shown by the VIC model to have met the threshold April 1st SWE of at least 10 mm during the 1990s) was estimated to be approximately 4,500 to 11,500 feet. The 1990s decade-mean SWE distribution (top left panel plot) shows highly distributed SWE values at various elevations and the regression line attempting to optimally fit the entire point scatter. Although significant scatter exists, the fitted regression line is linear, potentially indicating a single moisture source, specifically wintertime precipitation in the Basin, distributed across the broad latitude bands of the basin. The distribution may indicate north-south distribution of SWE in the basin across a broad latitude band.

Overall, it appears from the analysis that there is substantial loss in SWE at lower elevations, but at higher elevations (around 10,500 feet), the median SWE change does show some increase in the future decades from the reference decade. Also, at these higher elevations, there is very little change in the median SWE values from the 2020s to 2050s and from the 2050s to the 2070s.

3.5.2. Impacts on Runoff Annual and Seasonal Cycles

Figure 30 shows the mean monthly streamflow values for the 1990s, 2020s, 2050s, and 2070s in six Missouri River sub-basins. For several sub-basins (e.g., Bighorn River at Yellowtail Dam, Missouri River at Omaha, and North Platte River at Lake McConaughy) the hydrograph peak is higher in all the future decades from the 1990s reference. Also, there is an earlier shift in peak runoff timing from the 1990s decade that is apparent over the 2070s (e.g., Missouri River at Canyon Ferry Dam).

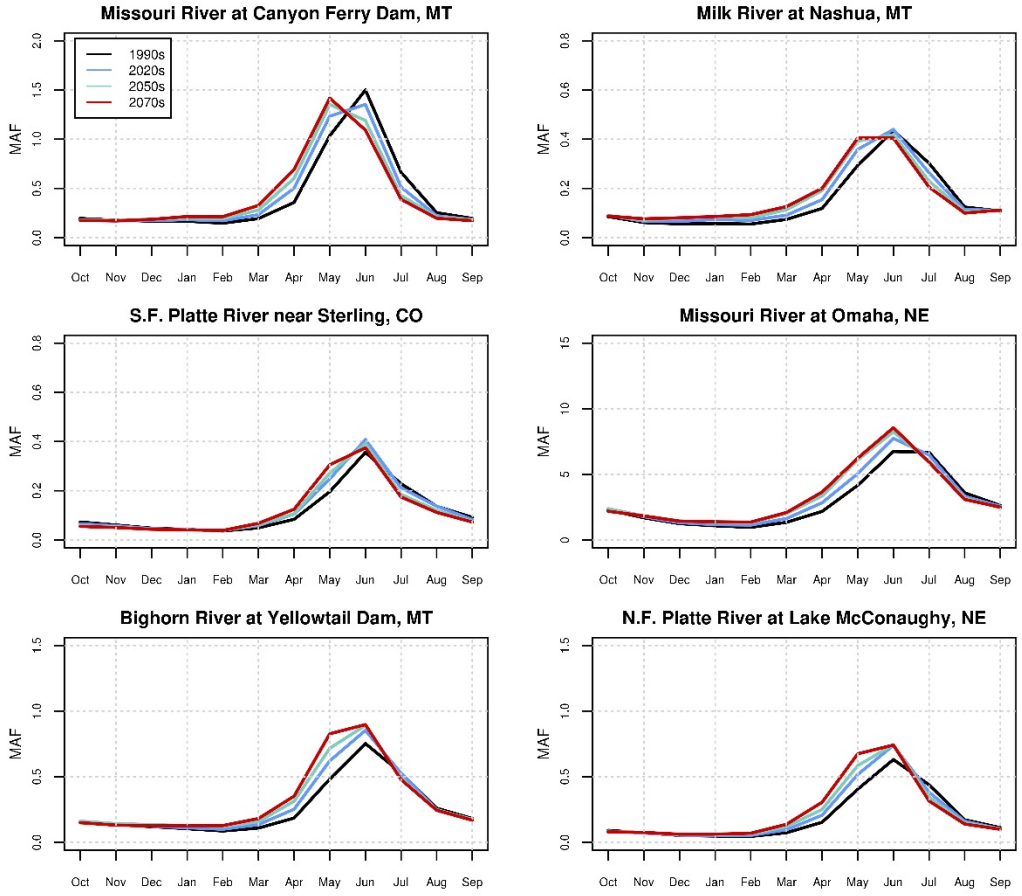

Figure 30. Missouri Basin – Simulated mean monthly runoff for various sub-basins

Figure 31 shows boxplots of the distribution of changes in runoff magnitude for annual, December-through-March, and April-through-July runoff in the six Missouri River sub-basins. Overall for all the sub-basins, the median change for the annual runoff, December-through-March and April-through-July runoff show

a positive change, indicating increased runoff at both annual and the two seasonal timescales.

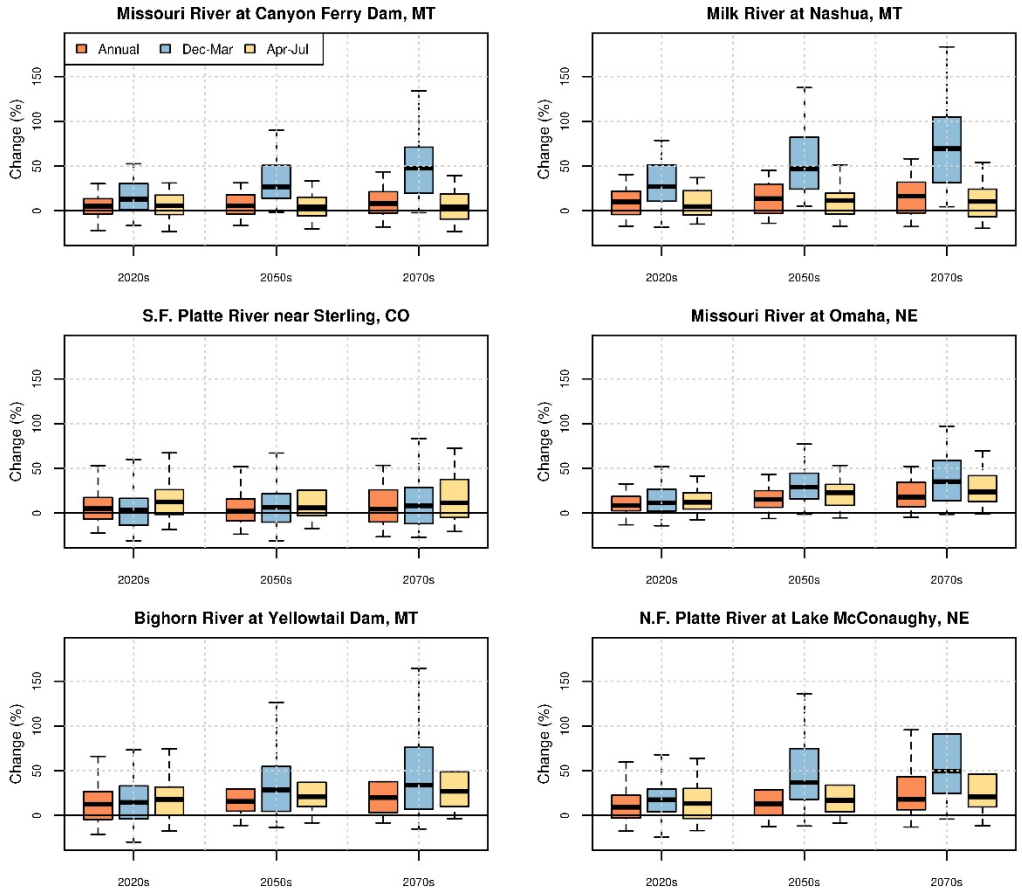

Figure 31. Missouri Basin – Simulated change in runoff magnitude for various sub-basins

Figure 32 shows the simulated shift in runoff timing for the various sub-basins. In all the sub-basins, the analysis shows that for each future decade, the median value of the change in runoff timing is negative. This implies that half of the annual flow occurs earlier relative to the 1990s reference. Also, relative to the 1990s decade, half of the annual flow is occurring earlier as the analysis through the three future decades (2020s, 2050s, and 2070s) shows. As an example, for the location Missouri River at Omaha, the earlier shift is about 6, 9, and 12 days, respectively, for the 2020s, 2050s, and 2070s decade, as compared to the 1990s decade.

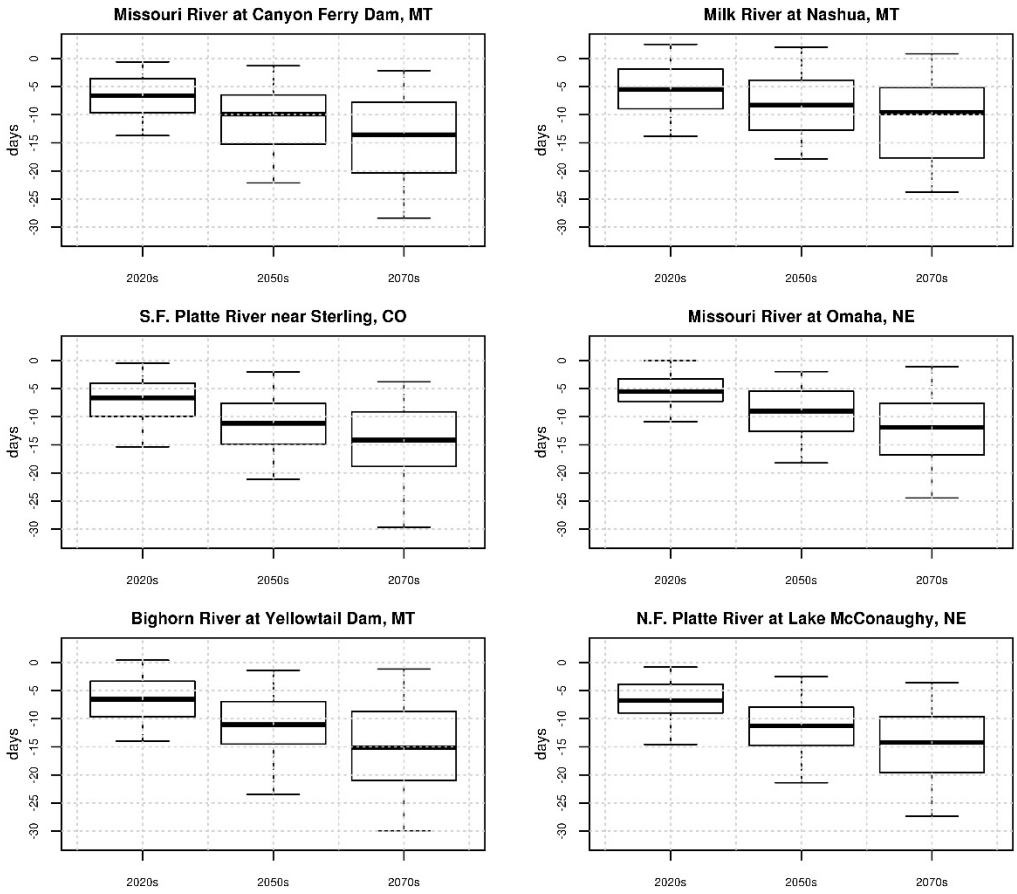

Figure 32. Missouri Basin – Simulated shift in runoff timing for various sub-basins

3.6. Rio Grande Basin

The Rio Grande Basin, located in the southwestern United States, provides water for irrigation, households, environmental, and recreational uses in Colorado, New Mexico, and Texas, as well as Mexico. Reclamation projects within the basin include the Closed Basin Project, Colorado; the San Juan-Chama trans-mountain diversion project, between Colorado and New Mexico; the Middle Rio Grande Project, New Mexico; and the Rio Grande Project, in New Mexico and Texas. These projects support approximately 200,000 acres of irrigated agriculture, which produces alfalfa, cotton, vegetables, pecans, and grain, for municipalities, tribes, and industry. Reclamation's facilities provide critical water and power for industry and communities, including Albuquerque and Las Cruces, New Mexico; El Paso, Texas; and Ciudad Juarez, Mexico. This analysis presents results for the upper portion of the basin above the Rio Grande at Elephant Butte Dam.

3.6.1. Hydroclimate Projections

Figure 33 shows six hydroclimate indicators for upper portion of the basin above the Rio Grande at Elephant Butte Dam: annual total precipitation (top left),

annual mean temperature (top right), April 1st SWE (middle left), annual runoff (middle right), December-through-March runoff (bottom left), and April-through-July runoff (bottom right). The heavy black line is the annual time series of 50 percentile (i.e., median) values of the 97 projections The shaded area is the annual time series of the 10th to 90th percentiles.

For the upper basin, total annual precipitation and the corresponding uncertainty envelope appear to be largely constant over time, implying that there is no increase or decrease in the uncertainty envelope from the present for total annual precipitation magnitudes. The mean annual temperature shows a consistently increasing trend over time and April 1st SWE shows a declining trend. December-through-March runoff is fairly constant over time; however, annual runoff and April-through-July runoff show a slightly decreasing trend over time.

Figure 34, Figure 35, and Figure 36 show the spatial distribution of simulated decade mean temperatures, precipitation, and April 1st SWE, respectively in the Rio Grande Basin above Elephant Butte Dam. In each figure, the simulated 1990s distribution of median decadal mean condition for the variable of interest is shown in the upper middle plot, and changes in the decadal mean condition are shown below for the three future periods and at three change percentiles within the range of projections (25th, 50th, and 75th percentiles).

In Figure 34, the median change for the three future decades relative to the 1990s indicates increasing temperatures throughout the basin. In Figure 35, the median change in precipitation for the future decades indicates a slightly wet pattern in the highest elevations of the basin. In Figure 36, the spatial plots indicate the median basin snowpack is projected to decrease.

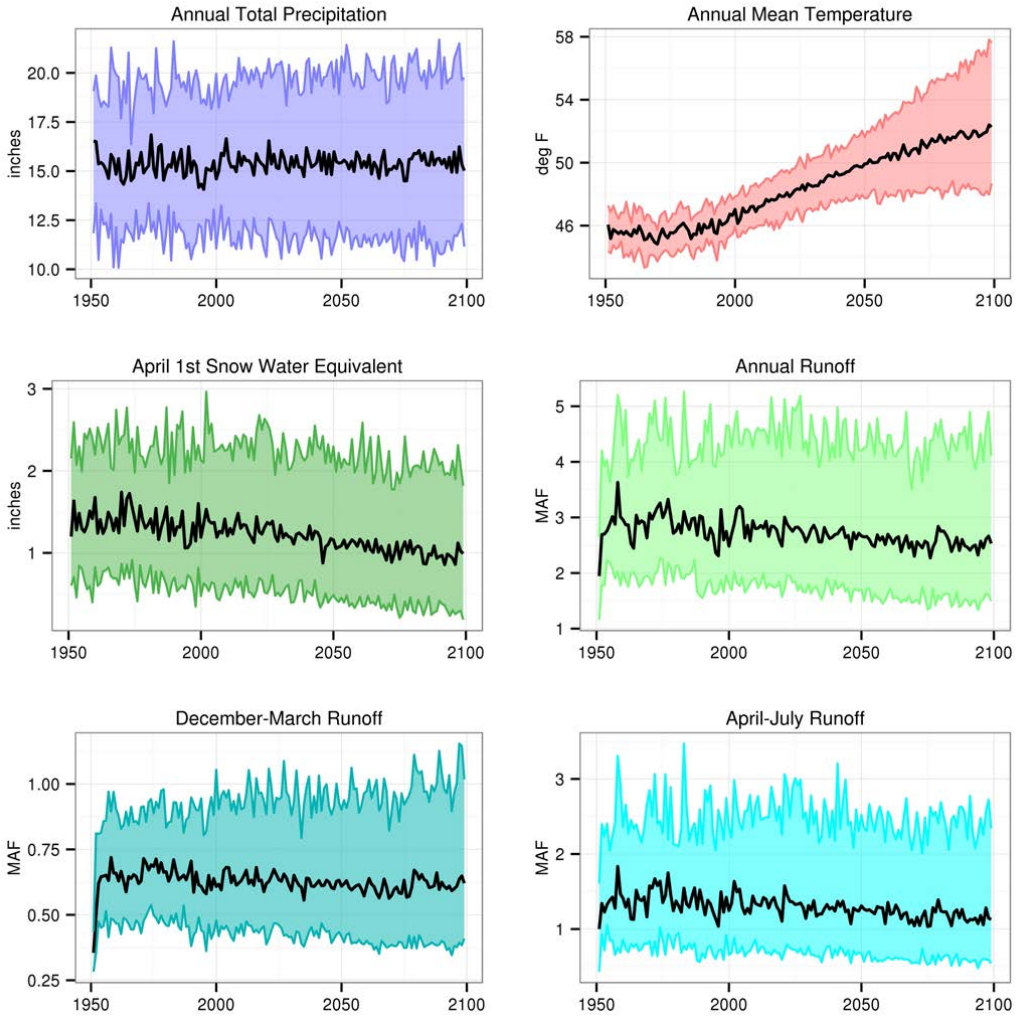

Figure 33. Rio Grande Basin – Projections for six hydroclimate indicators

The heavy black line is the annual time series median value (i.e., median). The shaded area is the annual time series of 10^{h} to 90th percentiles.

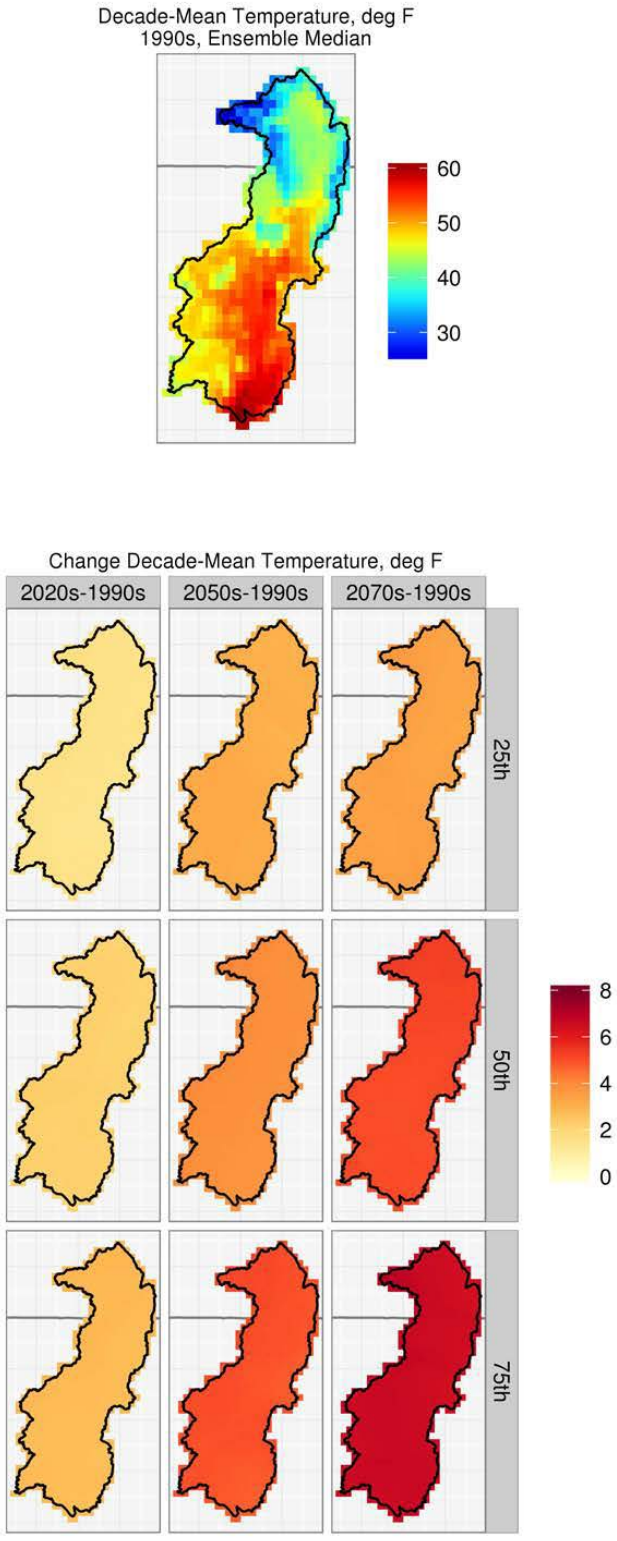

Figure 34. Rio Grande Basin – Spatial distribution of simulated decadal temperature

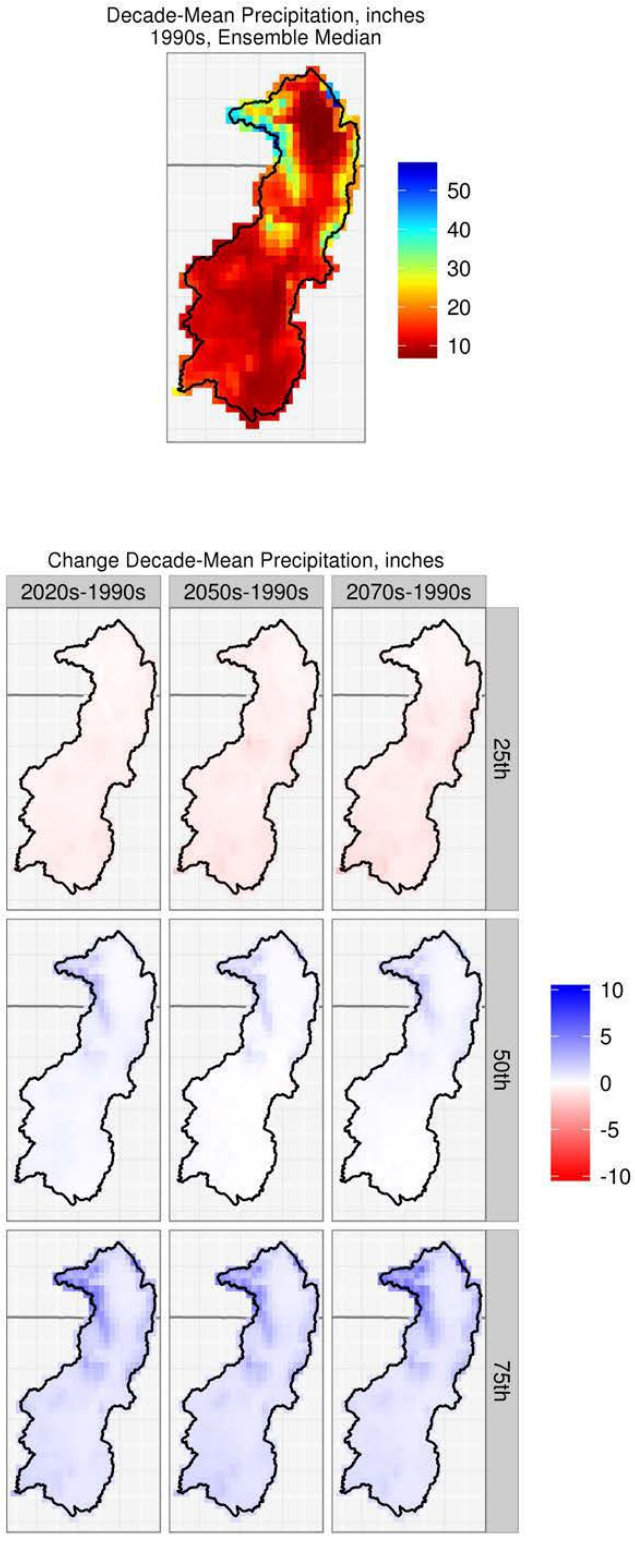

Figure 35. Rio Grande Basin – Spatial distribution of simulated decadal precipitation

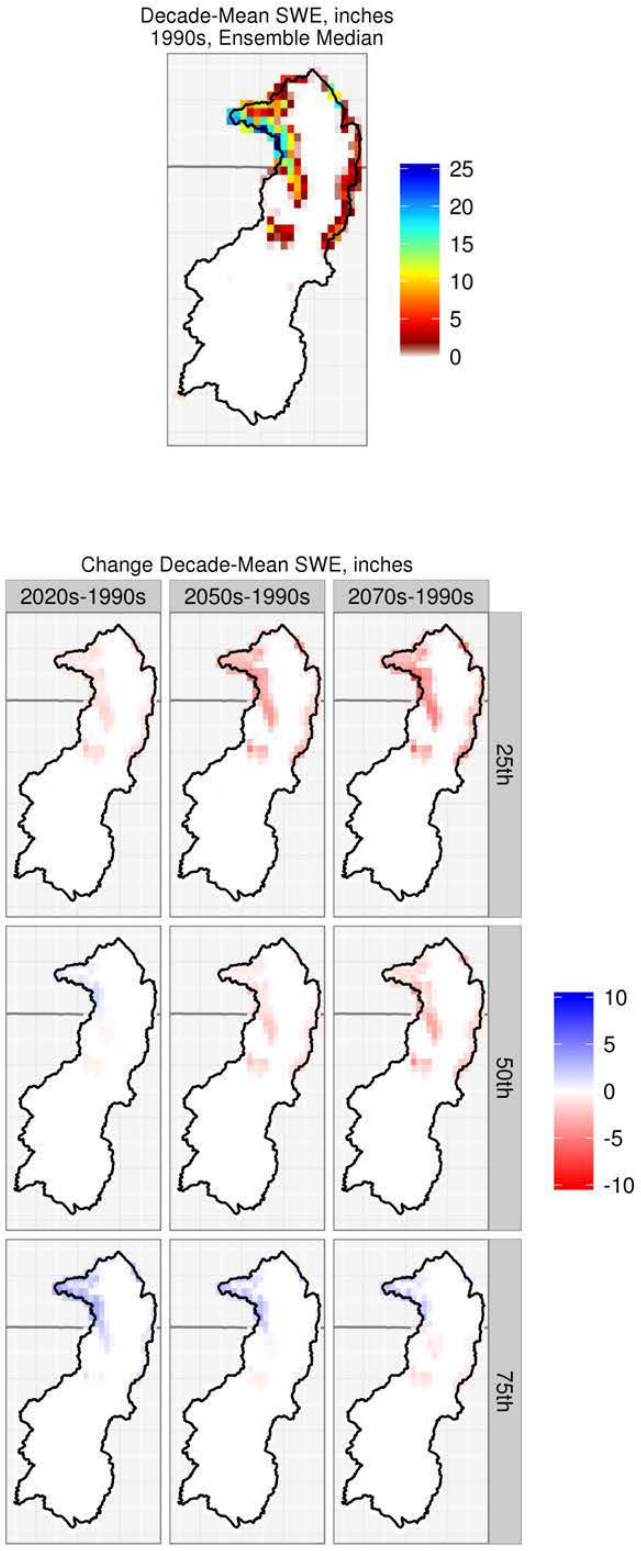

Figure 36. Rio Grande Basin – spatial distribution of simulated decadal April 1st SWE

Figure 37 shows the distribution of April 1st SWE with elevation in the Rio Grande Basin for the reference decade and the percentage change in this distribution for the three future decades. The 25th and 75th percentile estimates provide a way to quantify the uncertainty in the calculated changes.

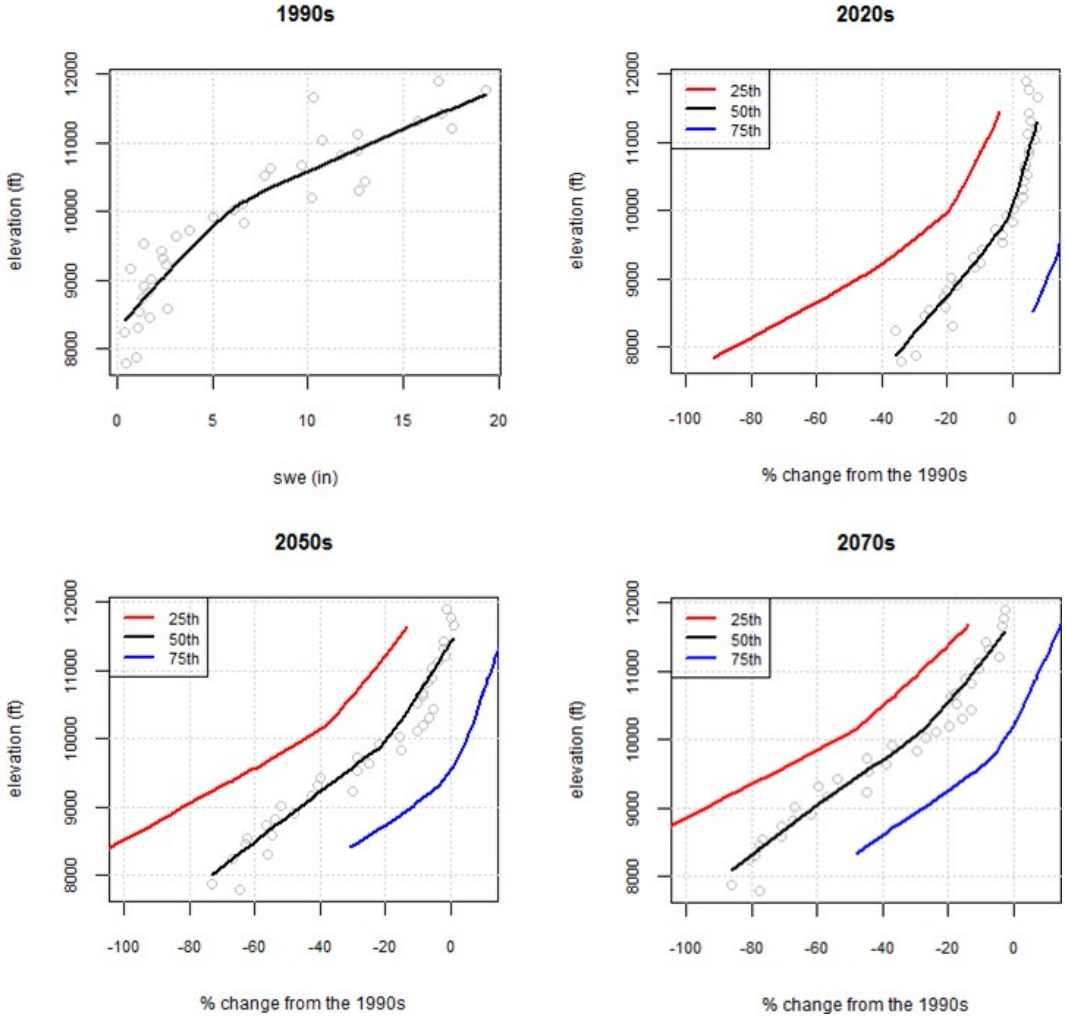

Figure 37. Rio Grande Basin – SWE distribution with elevation in the 1990s decade and future changes

The open light gray circles in this plot correspond to the median SWE values at each elevation with a fitted regression line is shown in black. The regression lines for the 25th and the 75th percentiles are presented in red and blue, respectively.

The SWE elevation range for the upper Rio Grande Basin (the elevation range of areas shown by the VIC model to have met the threshold April 1st SWE of at least 10 mm during the 1990s) was estimated to be approximately 8,000 to 12,000 feet. The 1990s decade-mean SWE distribution (top left panel plot) shows a clustered behavior with the regression line attempting to optimally fit through the entire point scatter. There are two clusters of points: one, the SWE distribution below about 10,000 feet, and a second cluster above about 10,000 feet. The fitted regression line appears to be piecewise linear with an inflexion point around

10,000 feet. Based on this distribution pattern, the primary moisture source contributing to snowpack development for the Basin is the wintertime precipitation.

Overall, the analysis shows that a decline in median SWE from the reference decade occurs throughout the elevation range of approximately 8,000 to 12,000 feet. There is some increase in the median SWE in the 2020s decade relative to the 1990s reference decade for elevations greater than about 10,000 feet. However, there is decline in the median SWE values even at high elevations from the 2020s to 2050s, and from the 2050s to the 2070s decade. Furthermore, the rate of decline in all the three future decades appears to be higher at elevations above about 10,000 feet relative to elevations below 10,000 feet. The 25th and 75th percentile estimates provide a way to quantify the uncertainty in the calculated changes.

3.6.2. Impacts on Runoff Annual and Seasonal Cycles

Figure 38 shows the mean monthly streamflow values for the 1990s, 2020s, 2050s, and 2070s in five upper Rio Grande sub-basins. For most locations in this basin, the runoff peaks appear to be occurring earlier in the spring during the later decade (2070) than the earlier decade (2020). The exception of this trend is the Pecos River near Carlsbad, NM where the hydrograph peak is attributed to summer monsoon runoff events.

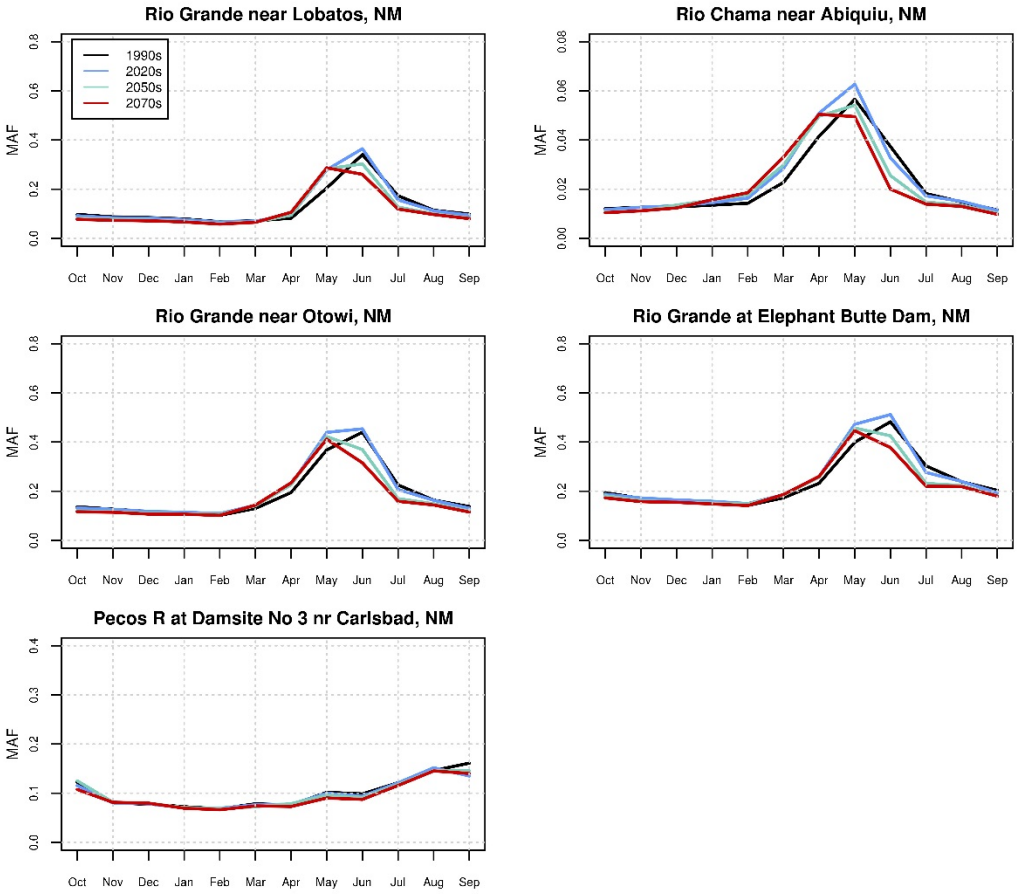

Figure 38. Rio Grande Basin – Simulated mean monthly runoff for various sub-basins

Figure 39 shows boxplots of the distribution of simulated changes in runoff magnitude for annual, December-through-March, and April-through-July runoff in the five upper Rio Grande sub-basins. In the 2020s decade, relative to the 1990s, there is an increase in median April-through-July runoff in all locations except the Pecos River site. For the Rio Chama location, there is also an increase in the ensemble-median December-through-March runoff in the 2020s, 2050s and 2070s from the reference decade, but a decline in the median April-through-July runoff in the 2050s and 2070s from the reference decade.

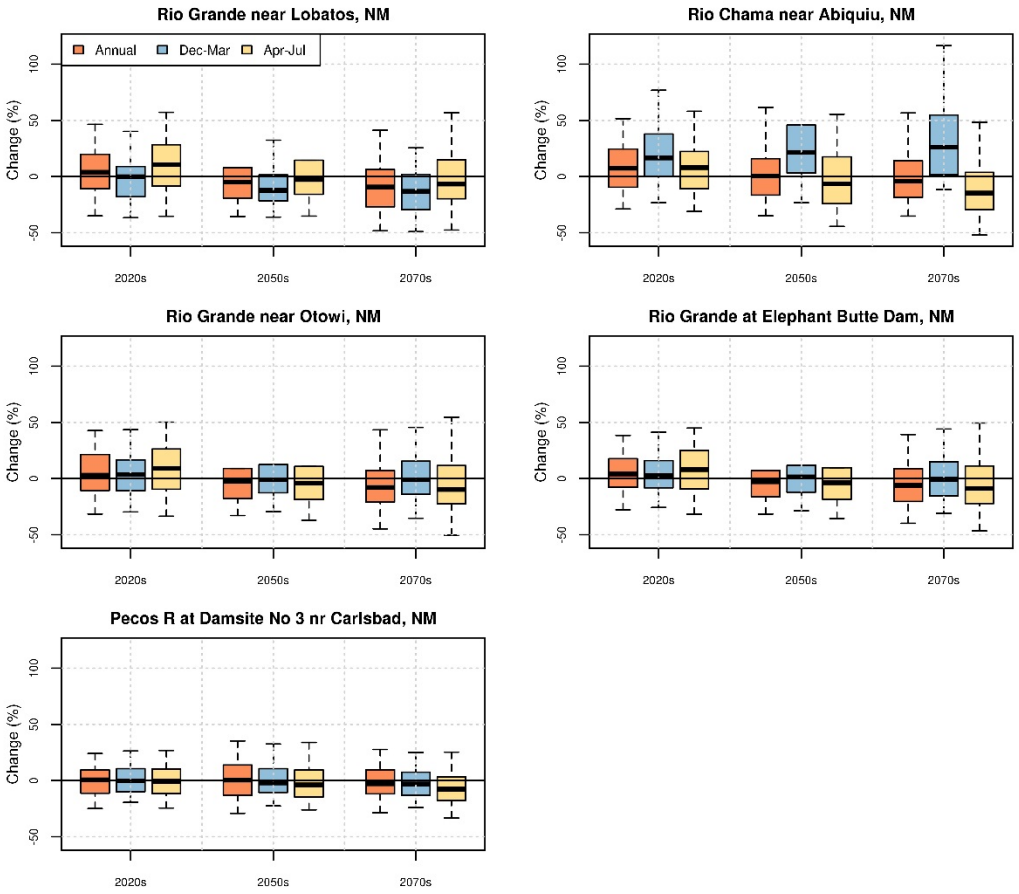

Figure 39. Rio Grande Basin –Simulated change in runoff magnitude for various sub-basins

Figure 40 shows the simulated shift in runoff timing for the various sub-basins. The Pecos River location shows a minimal (about 2 days) positive value (i.e., late) of the median change in runoff timing in all of the three future decades 2020s, 2050s and 2070s relative to the 1990s. For all the other upper Rio Grande locations, the analysis shows that for each future decade, the median value of the change in runoff timing is negative. This implies that half of the annual flow occurs sooner than it did in the 1990s. For example, for the Rio Grande at the Elephant Butte Dam, the earlier shift is approximately 3, 4, and 5 days, respectively, in the 2020s, 2050s and 2070s relative to the 1990s.

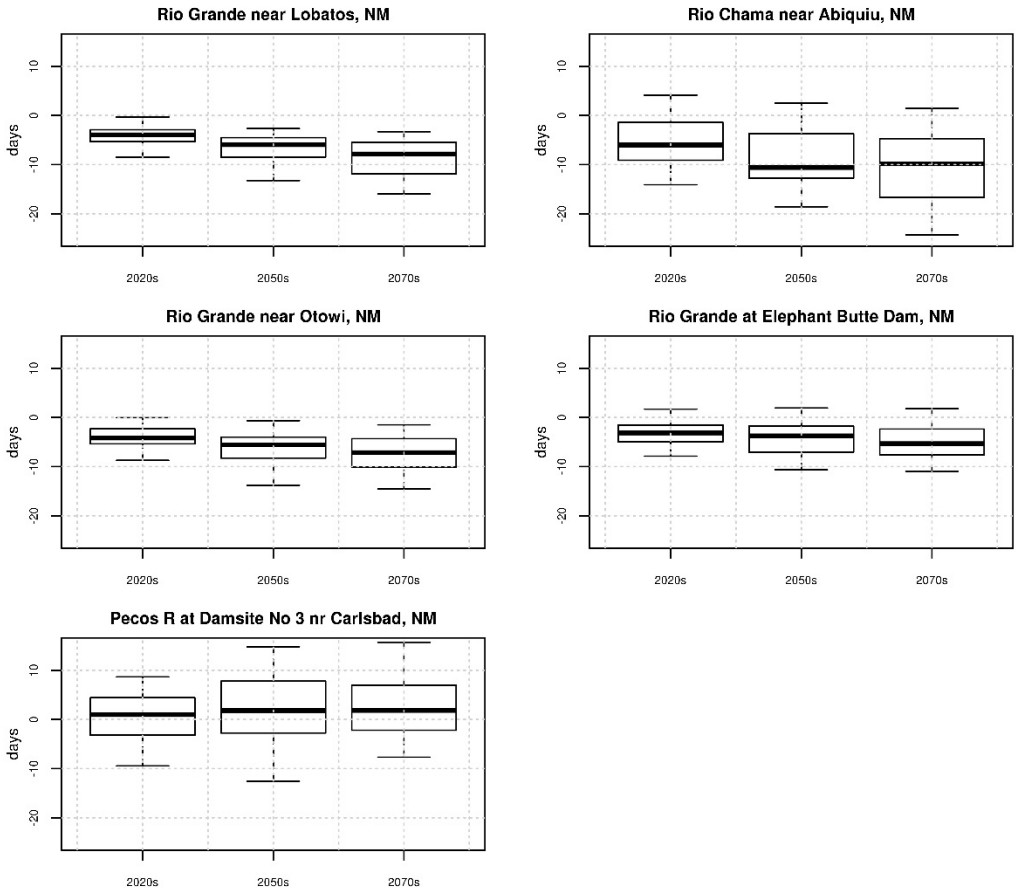

Figure 40. Rio Grande Basin – Simulated shift in runoff timing for various sub-basins

3.7. Sacramento and San Joaquin River Basins

The Sacramento and San Joaquin Basins include three major Central Valley watersheds – the Sacramento River in the north, and the San Joaquin River and Tulare Lake Basins in the south. The combined watersheds extend nearly 500 miles from northwest to southeast and range from 60 to 100 miles wide. The rivers – the two largest in California – meet in the Sacramento-San Joaquin Delta, the largest estuary on the West Coast and the hub of California's complex water supply system. The rivers play a key role in supporting California`s powerful economy, providing water for six of the top 10 agricultural counties in the nation's leading farm state. In addition to water for farms, homes, and industry in California`s Central Valley and major urban centers in the San Francisco Bay and Central Coast areas, the rivers sustain aquatic and terrestrial habitats, along with numerous managed waterfowl refuges.

3.7.1. Hydroclimate Projections

Figure 41 shows six hydroclimate indicators for the basin above the Sacramento and San Joaquin Rivers at the Delta: annual total precipitation (top left), annual

mean temperature (top right), April 1st SWE (middle left), annual runoff (middle right), December-through-March runoff (bottom left), and April-through-July runoff (bottom right). The heavy black line is the annual time series of 50 percentile (i.e., median) values of the 97 projections. The shaded area is the annual time series of the 10th to 90th percentiles.

Total annual precipitation and the corresponding uncertainty envelope appear to be largely constant over time, implying that there is no increase or decrease in the total annual precipitation magnitudes over time. The mean annual temperature shows an increasing trend over time, and April 1st SWE shows a decreasing trend. Similar to precipitation, annual runoff shows no apparent trend. The December-through-March runoff volume show a slightly increasing trend, while the April-through-July runoff shows a more apparent declining trend over time.

Figure 42, Figure 43, and Figure 44 show the spatial distribution of simulated decade mean temperatures, precipitation, and April 1st SWE, respectively, in the Sacramento and San Joaquin Basin above the Delta. In each figure, the simulated 1990s distribution of median decadal mean condition for the variable of interest is shown in the upper middle plot, and changes in the decadal mean condition are shown below for the three future periods and at three change percentiles within the range of projections (25th, 50th, and 75th percentiles).

In Figure 42, the median change for the three future decades relative to the 1990s indicates increasing temperatures throughout the basin. In Figure 43, the median change in precipitation for the future decades indicates a slightly wet pattern in the higher elevations of the basin. In Figure 44, the spatial plots indicate the median basin snowpack is projected to decrease.

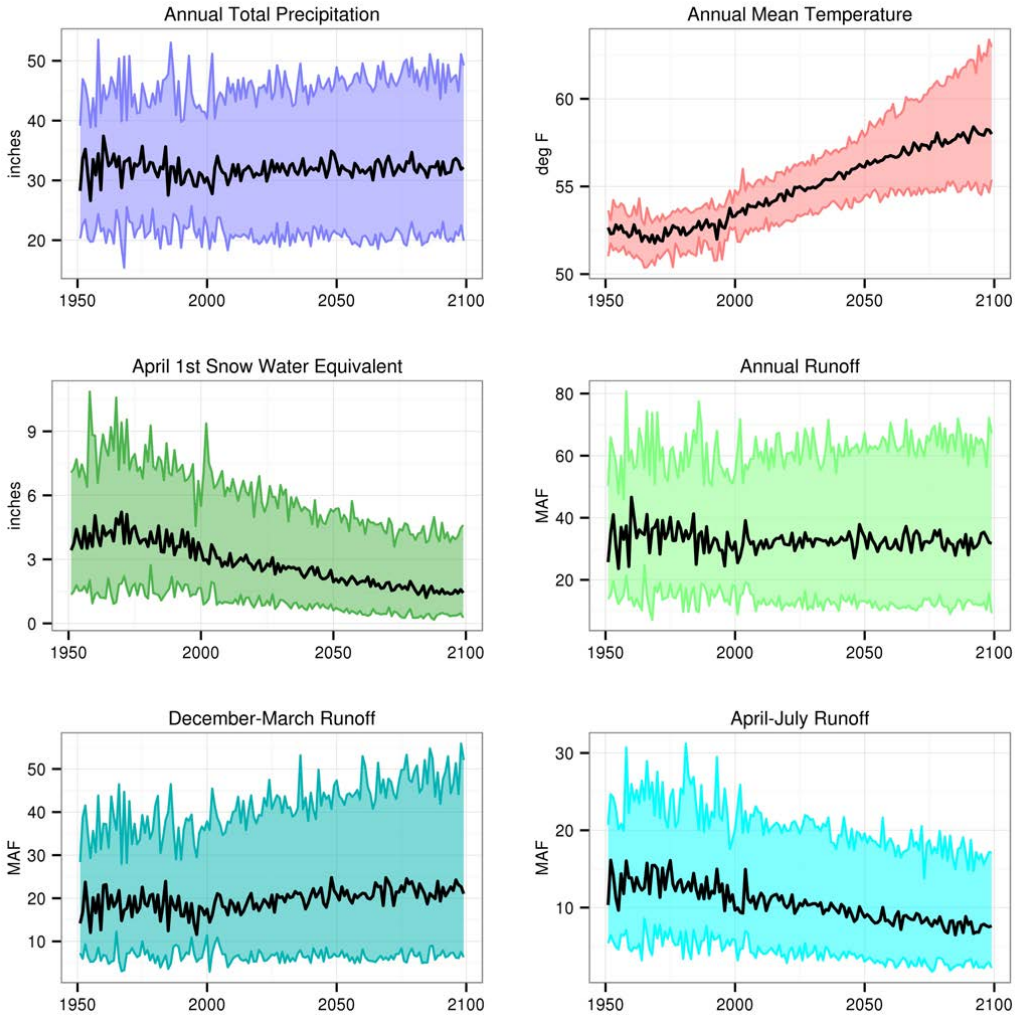

Figure 41. Sacramento and San Joaquin Basins – Projections for six hydroclimate indicators

The heavy black line is the annual time series median value (i.e., median). The shaded area is the annual time series of 10^{h} to 90th percentiles.

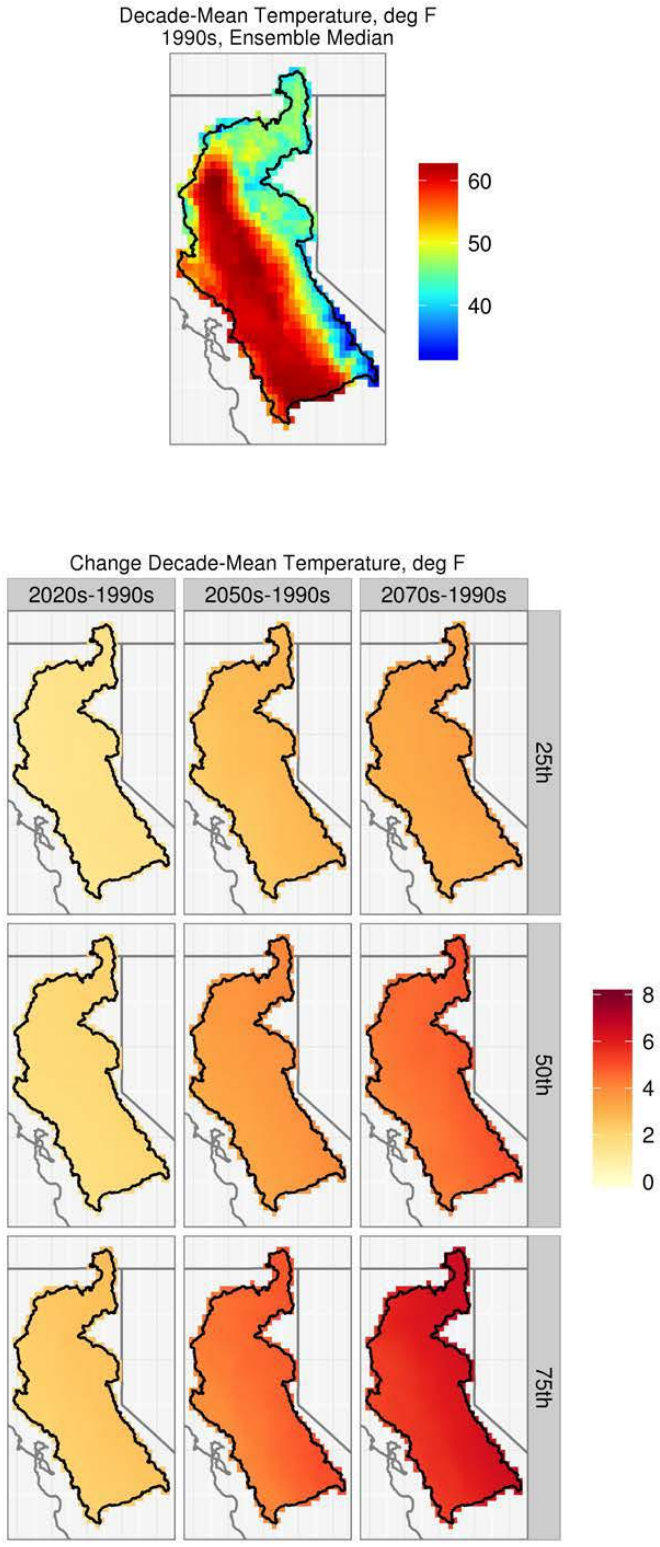

Figure 42. Sacramento and San Joaquin Basins – Spatial distribution of simulated decadal temperature

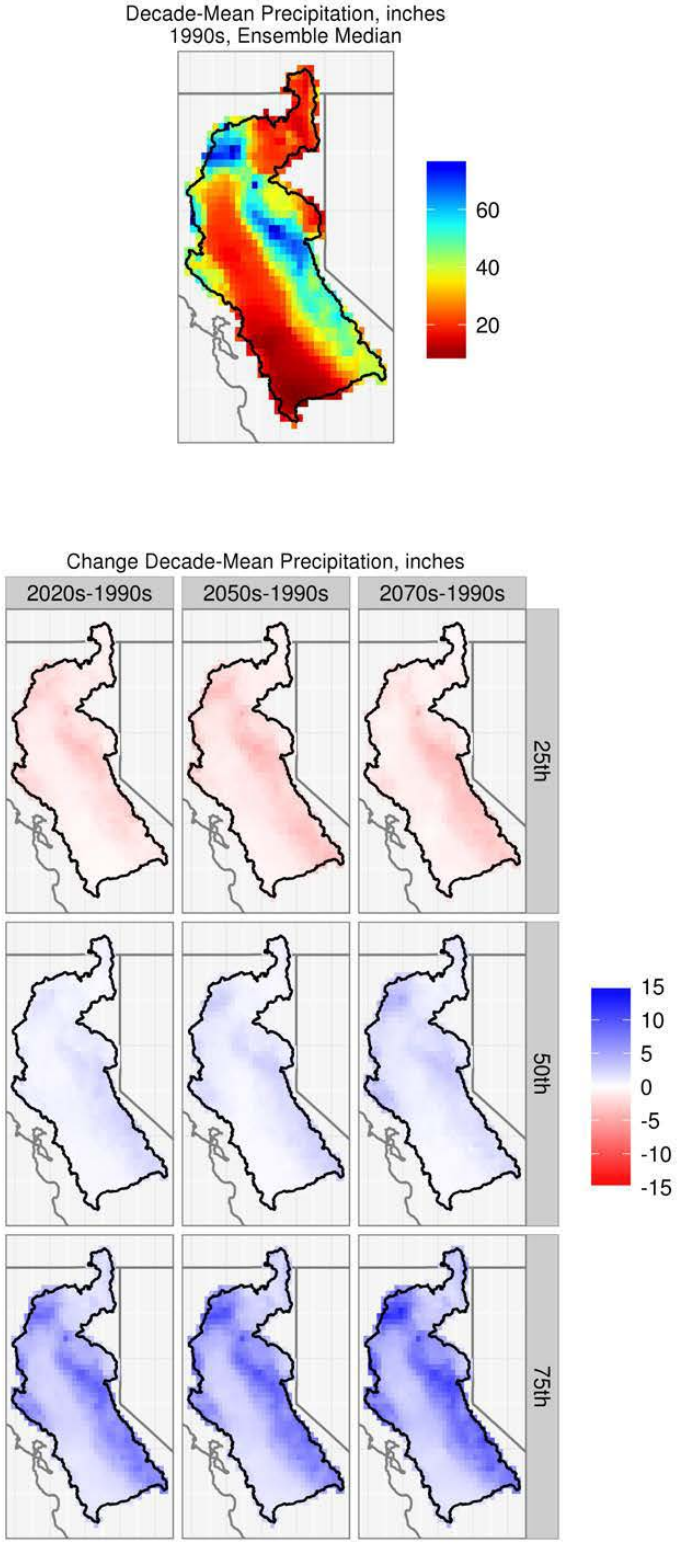

Figure 43. Sacramento and San Joaquin Basins – Spatial distribution of simulated decadal precipitation

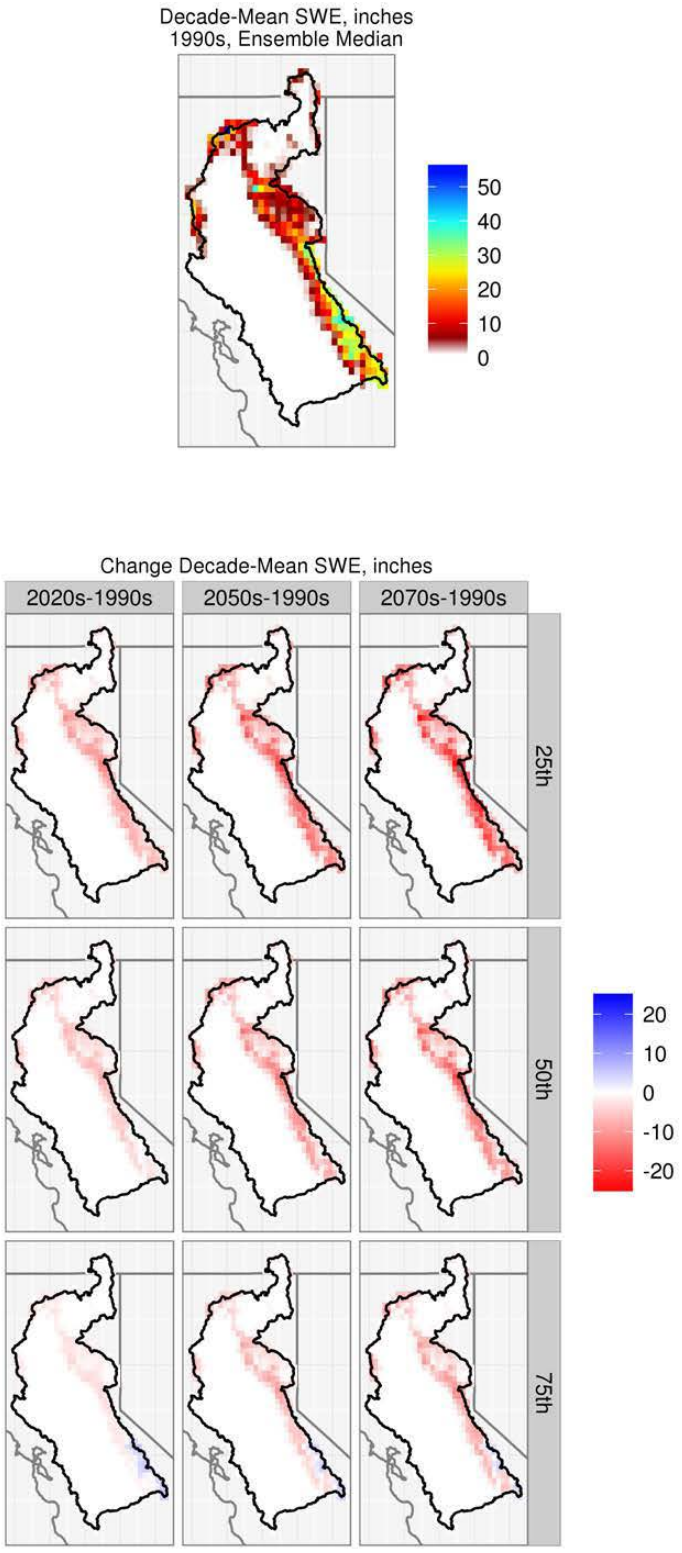

Figure 44. Sacramento and San Joaquin Basins – Spatial distribution of simulated decadal April 1st SWE

Figure 45 shows the distribution of April 1st SWE with elevation in the Sacramento and San Joaquin River Basins for the reference decade and the percentage change in this distribution for the three future decades. The 25th and 75th percentile estimates provide a way to quantify the uncertainty in the calculated changes.

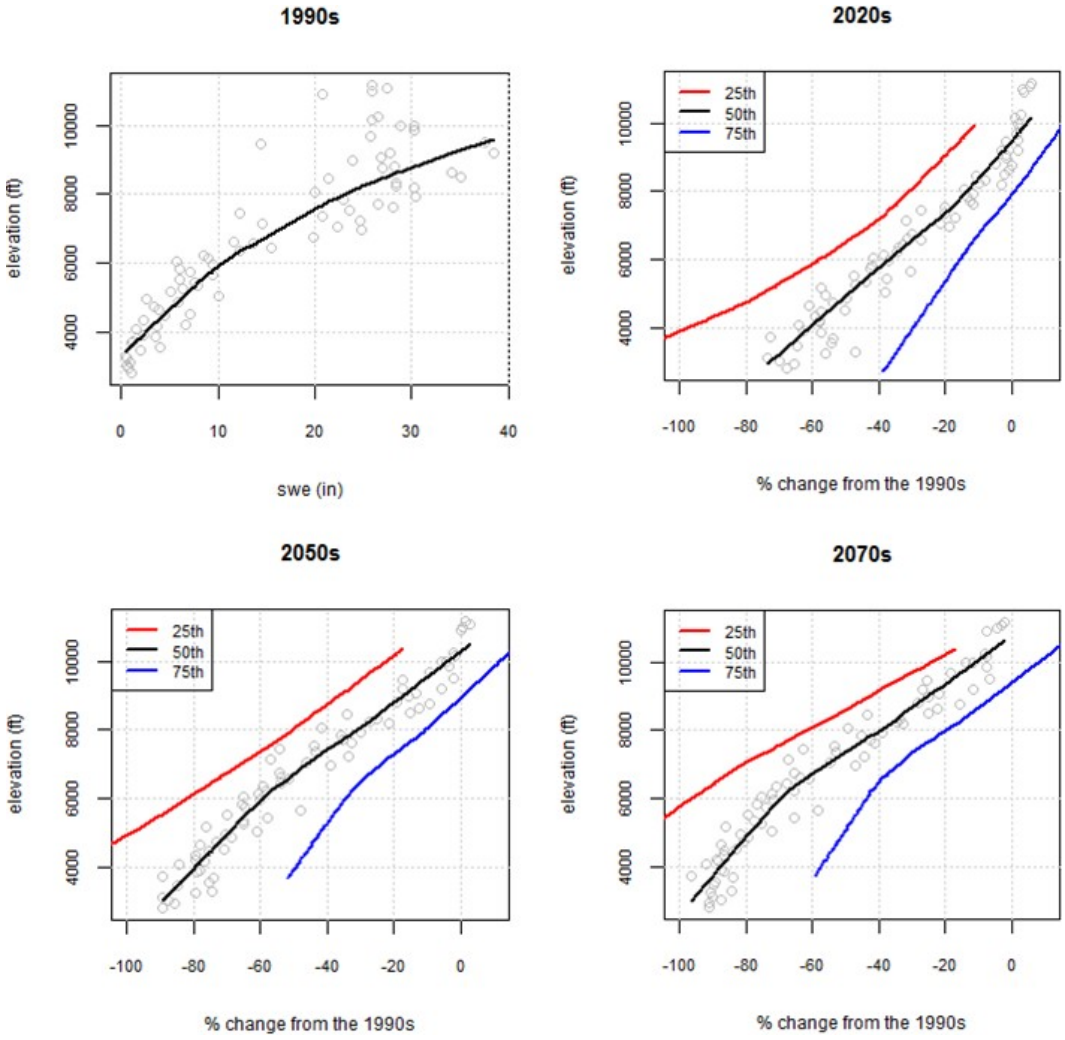

Figure 45. Sacramento and San Joaquin Basins – SWE distribution with elevation in the 1990s decade and future changes

The open light gray circles in this plot correspond to the median SWE values at each elevation with a fitted regression line is shown in black. The regression lines for the 25th and the 75th percentiles are presented in red and blue, respectively.

The SWE elevation range for the Sacramento and San Joaquin Basins (the elevation range of areas shown by the VIC model to have met the threshold April 1st SWE of at least 10 mm during the 1990s) was estimated to be approximately 3,000 to 11,000 feet. The 1990s decade-mean SWE distribution (top left panel plot) shows increasing point scatter at higher elevations. There are two sets of distributed points: one, the SWE distribution below about 7,000 feet, and a second

cluster above about 7,000 feet. The fitted regression line appears to be non-linear and may be contributing to the combined presentation of data from the relatively lower Sacramento Basin with the higher-elevation San Joaquin Basin. This distribution could be representative of the clustering of the SWE distribution observed in the plot (top left panel). The primary moisture sources in these two basins are distinct, with the lower-elevation Sacramento Basin, which is primarily rain-dominated, and the San Joaquin, which is driven by rain and snow. Overall, it appears from the analysis that a decline in median SWE relative to the 1990s occurs through all the elevation ranges. Generally, the trend is for declining SWE values from the 2020s to 2050s and from the 2050s to the 2070s decade.

3.7.2. Impacts on Runoff Annual and Seasonal Cycles

Figure 46 shows the mean monthly streamflow values for the 1990s, 2020s, 2050s, and 2070s in eight Sacramento and San Joaquin River sub-basins and the Tulare Basin. For all the locations, there appears to be an earlier shift in runoff peak.

Figure 47 shows boxplots of the distribution of simulated changes in runoff magnitude for annual, December-through-March, and April-through-July runoff in the eight Sacramento and San Joaquin River sub-basins and the Tulare Basin. Overall, the analysis shows that there is an increase in the median December-through-March runoff and decrease in the April-through-July runoff in all the three future decades, with nominal changes in the ensemble-median annual runoff magnitudes.

Figure 48 shows the simulated shift in runoff timing for the various sub-basins. For all the sub-basins, the shift represented by the ensemble median shows that half of the annual flow volume will occur earlier in the future decades relative to the 1990s decade. Also, it appears from the analysis that this earlier shift grows in the three future decades relative to the 1990s decade. For example, for the Delta inflow, the earlier shift is about, 4, 6, and 7 days respectively in the 2020s, 2050s and 2070s relative to the 1990s.

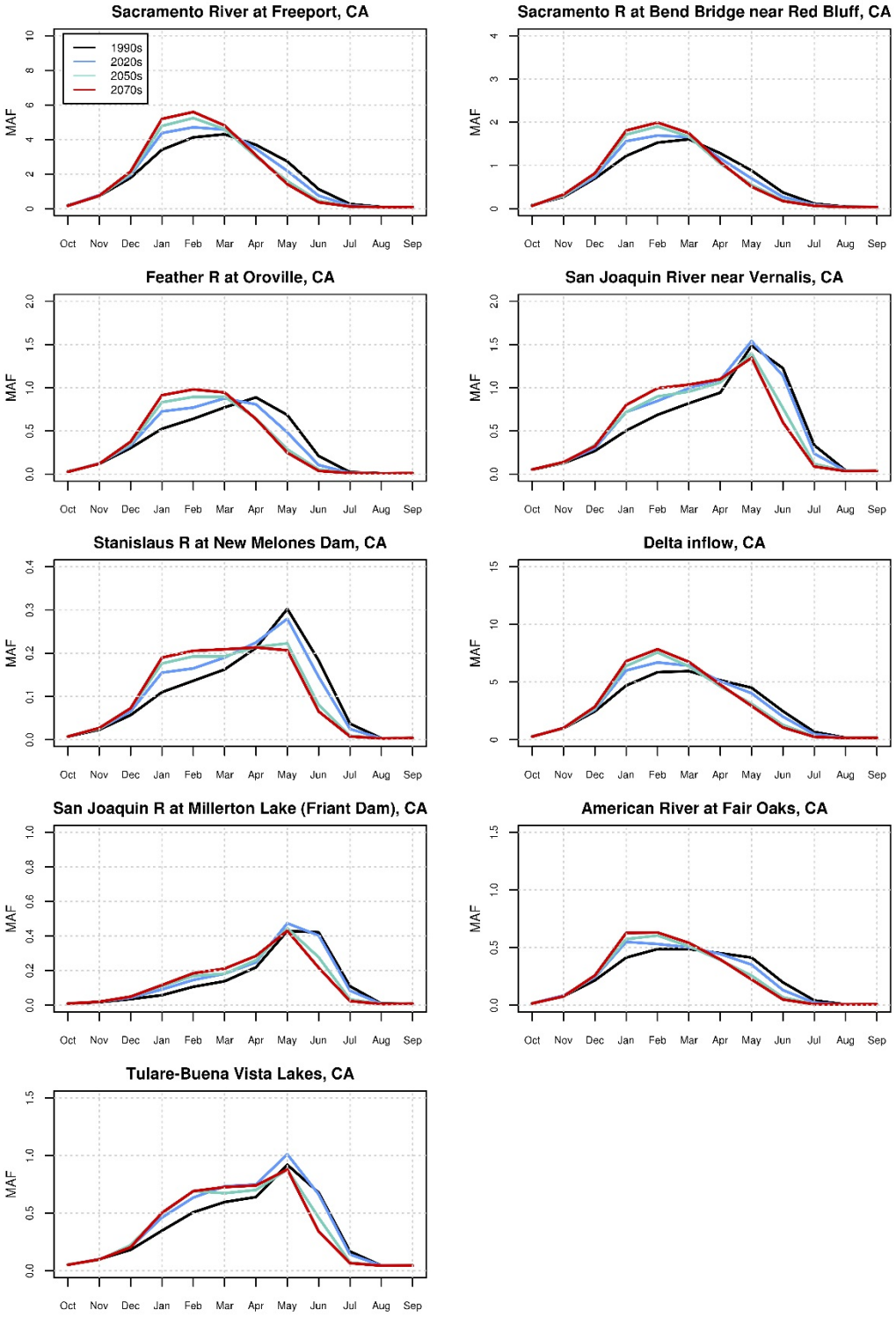

Figure 46. Sacramento and San Joaquin Basins – Simulated mean monthly runoff for various sub-basins

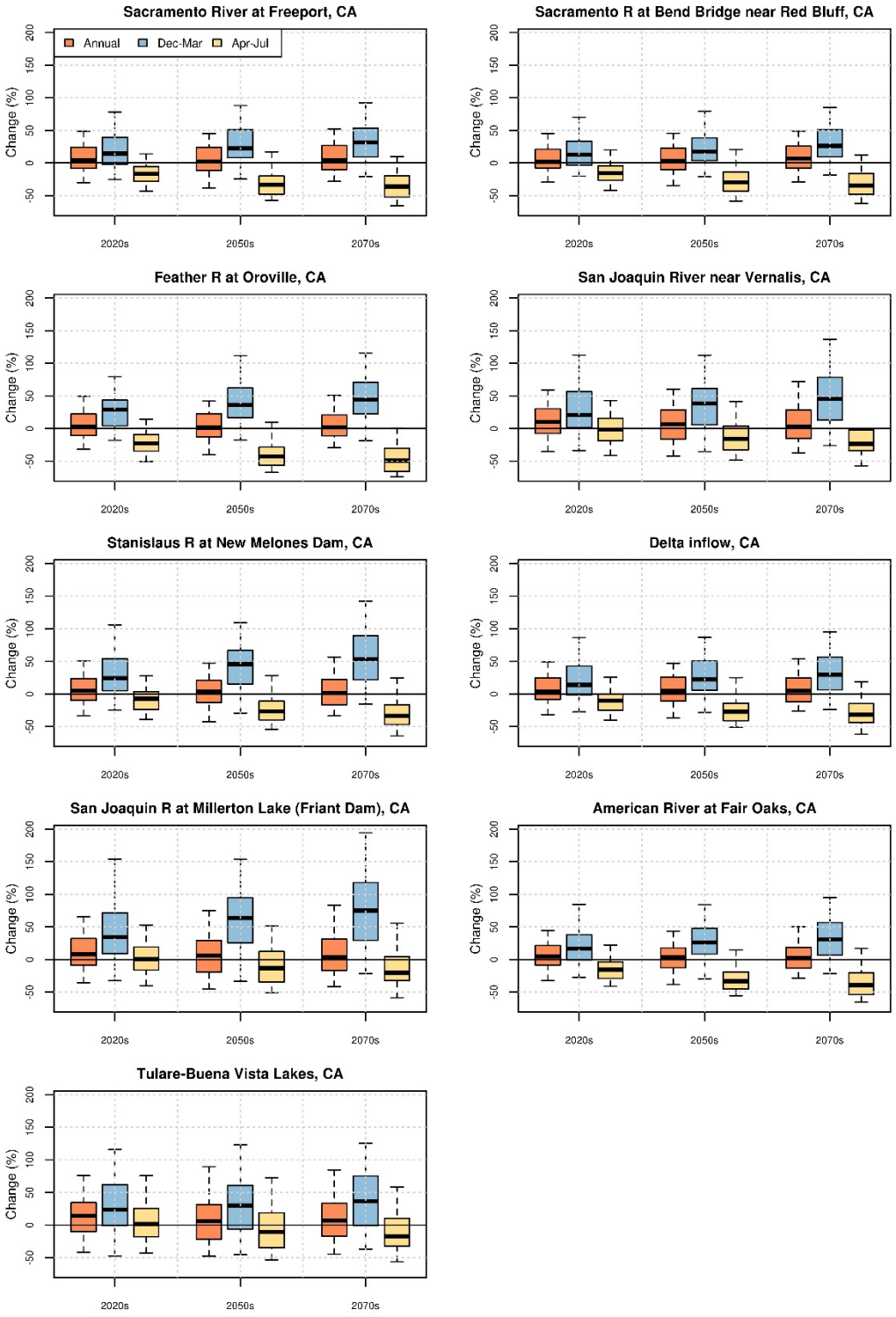

Figure 47. Sacramento and San Joaquin Basins – Simulated change in runoff magnitude for various sub-basins

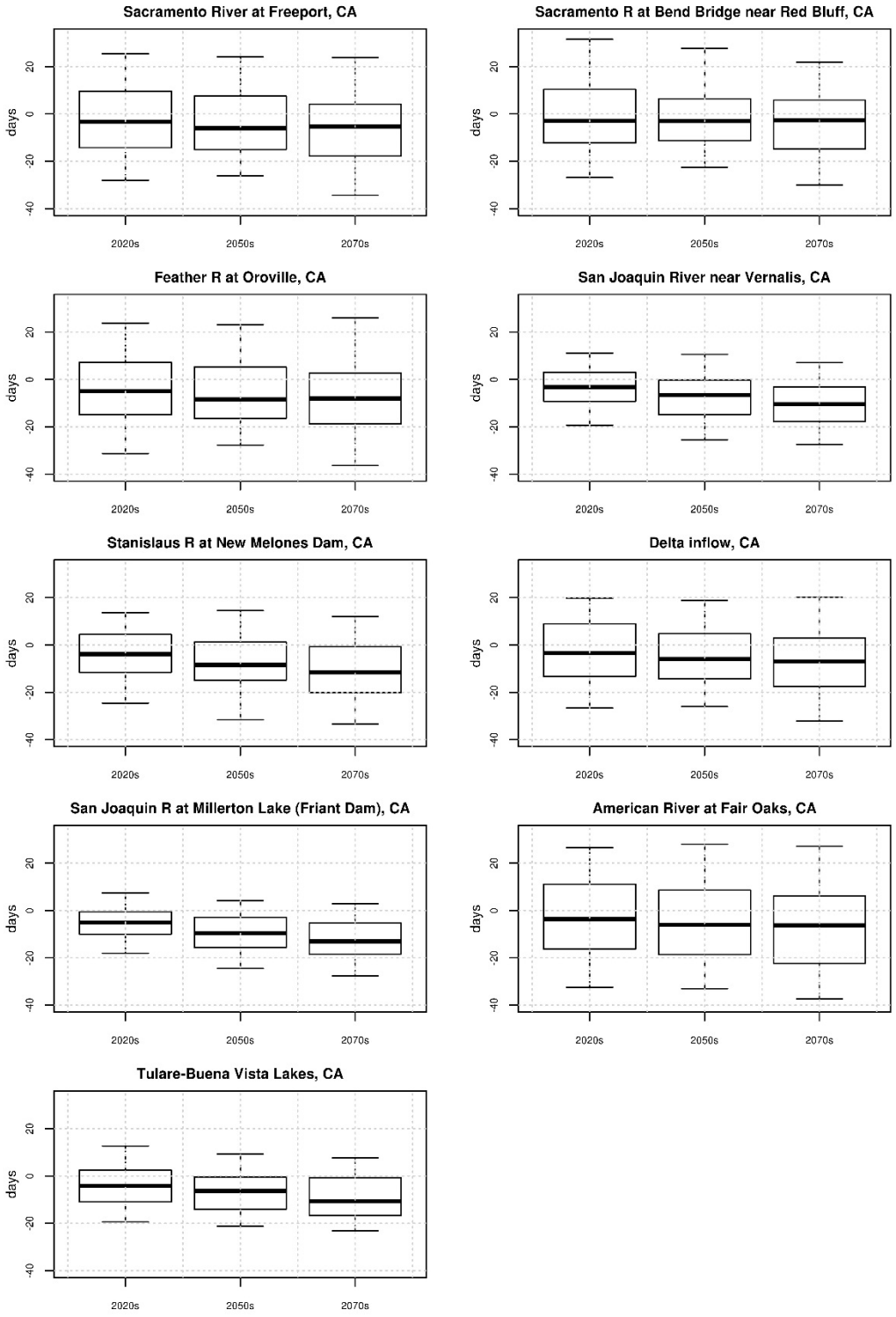

Figure 48. Sacramento and San Joaquin Basins –Simulated shift in runoff timing for various sub-basins

3.8. Truckee and Carson River Basins

The Truckee River originates at Lake Tahoe in California and flows over 105 miles north and east into Nevada, where it terminates in Pyramid Lake. The Truckee River is a major source of water for western Nevada, including the cities of Reno and Sparks. Along with the Carson River, the Truckee River supplies irrigation water to Reclamation's Newlands Project for approximately 57,000 acres of cropland. The Truckee River is also an important recreation resource for residents in California and Nevada, providing boating, rafting, kayaking, fishing, hunting, and camping opportunities. All water in the Truckee River is fully appropriated, with a Federal Water Master managing storage in the upper 6 feet of Lake Tahoe and the other five Truckee basin reservoirs in California.

3.8.1. Hydroclimate Projections

Figure 49 shows six hydroclimate indicators for the basin above the Truckee River at Nixon gage: annual total precipitation (top left), annual mean temperature (top right), April 1st SWE (middle left), annual runoff (middle right), December-through-March runoff (bottom left), and April-through-July runoff (bottom right). The heavy black line is the annual time series of 50 percentile (i.e., median) values of the 97 projections. The shaded area is the annual time series of the 10th to 90th percentiles.

Total annual precipitation and the corresponding uncertainty envelope appear to be largely constant over time, implying that there is no increase or decrease in the total annual precipitation magnitudes over time. The mean annual temperature shows an increasing trend over time, and April 1st SWE shows a decreasing trend. Similar to precipitation, annual runoff shows no apparent trend. The December-through-March runoff volume show a slightly increasing trend, with growing uncertainty in the projected envelop of conditions, while the April-through-July runoff declines over time.

Figure 50, Figure 51, and Figure 52 show the spatial distribution of simulated decade mean temperatures, precipitation, and April 1st SWE, respectively, in the basin above the Truckee River at Nixon gage. In each figure, the simulated 1990s distribution of median decadal mean condition for the variable of interest is shown in the upper middle plot, and changes in the decadal mean condition are shown below for the three future periods and at three change percentiles within the projections (25th, 50th, and 75th percentiles).

In Figure 50, the median change for the three future decades relative to the 1990s indicates increasing temperatures throughout the basin. In Figure 51, the median change in precipitation for the future decades indicates a slightly wet pattern in the higher elevations of the basin. In Figure 52, the spatial plots indicate the median basin snowpack is projected to decrease.

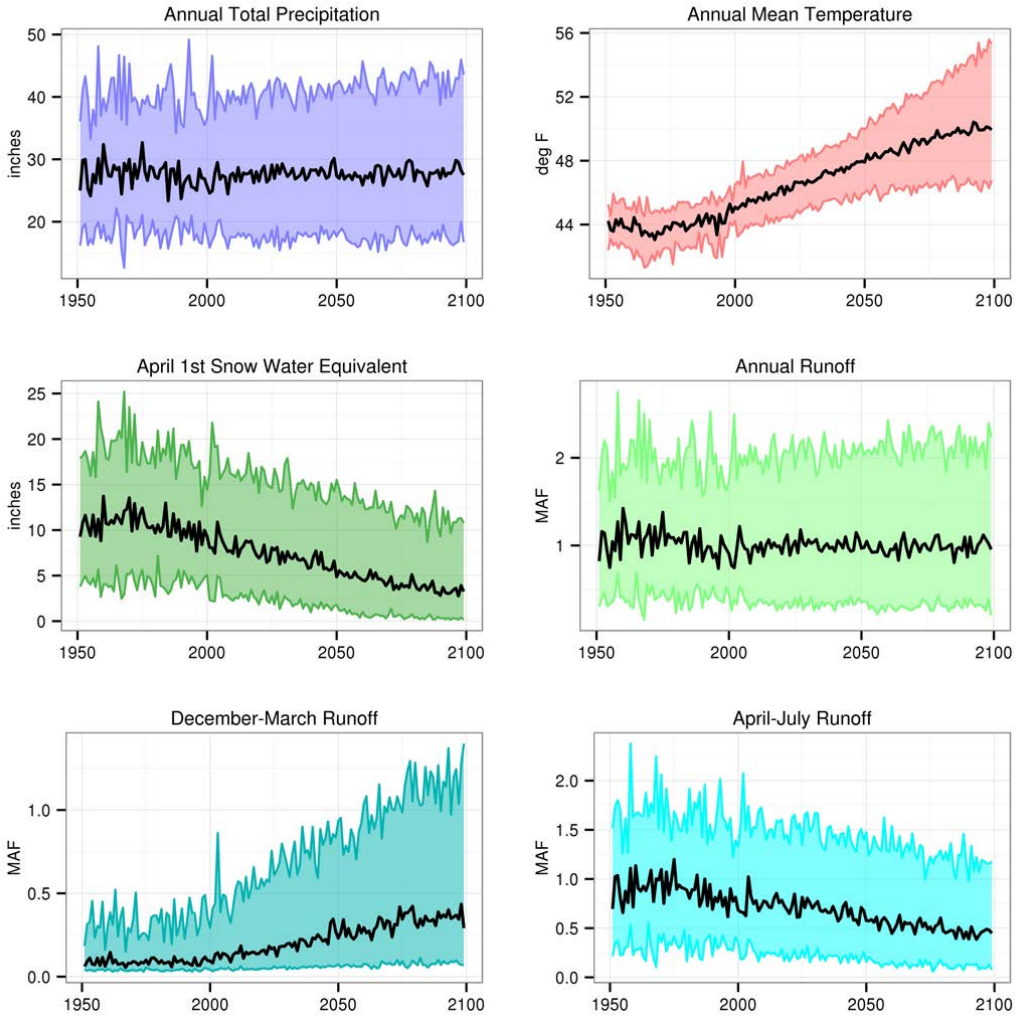

Figure 49. Truckee and Carson Basins – Projections for Six Hydroclimate Indicators

The heavy black line is the annual time series median value (i.e., median). The shaded area is the annual time series of 10^{h} to 90th percentiles.

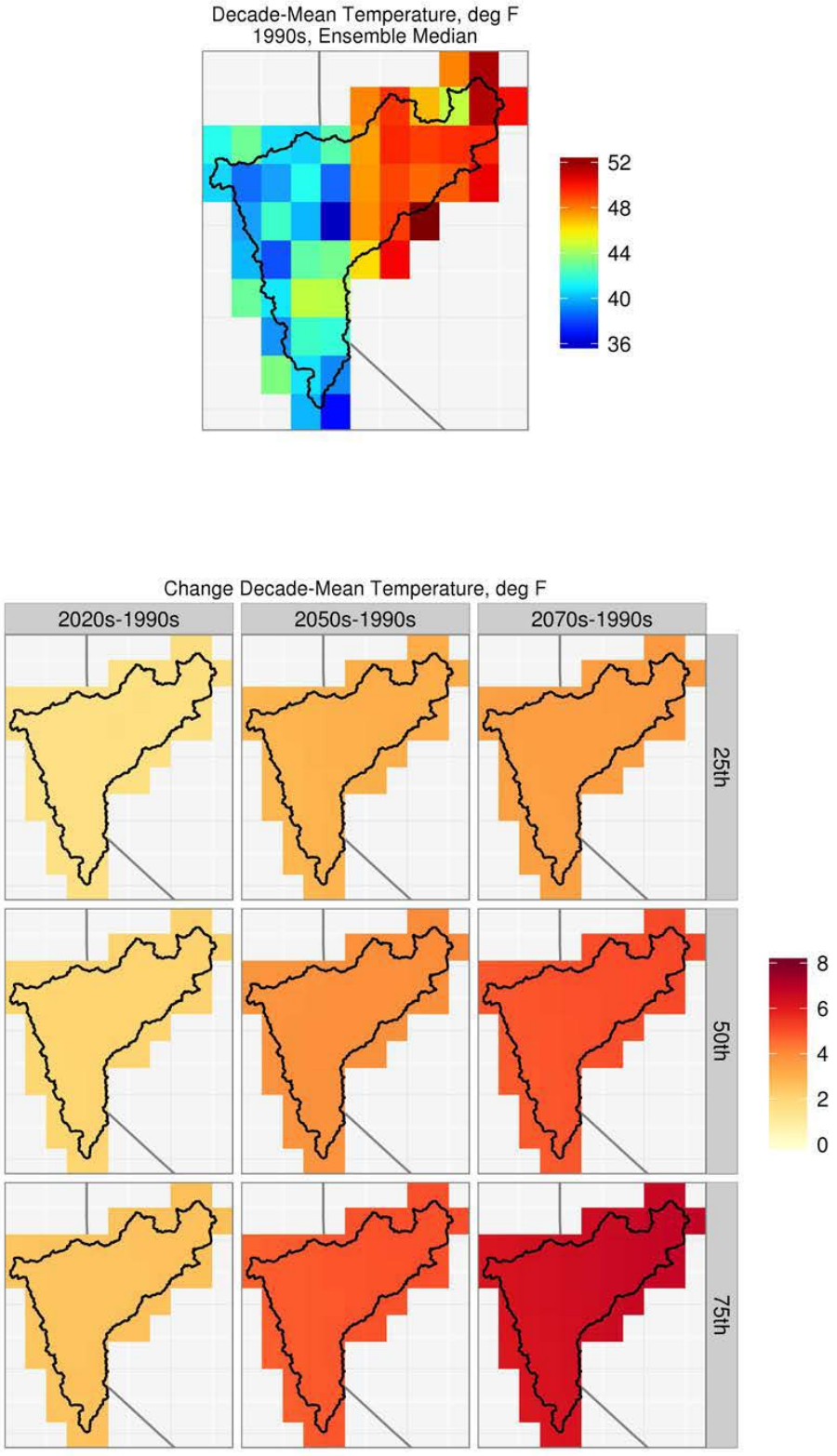

Figure 50. Truckee and Carson Basins – Spatial distribution of simulated decadal temperature

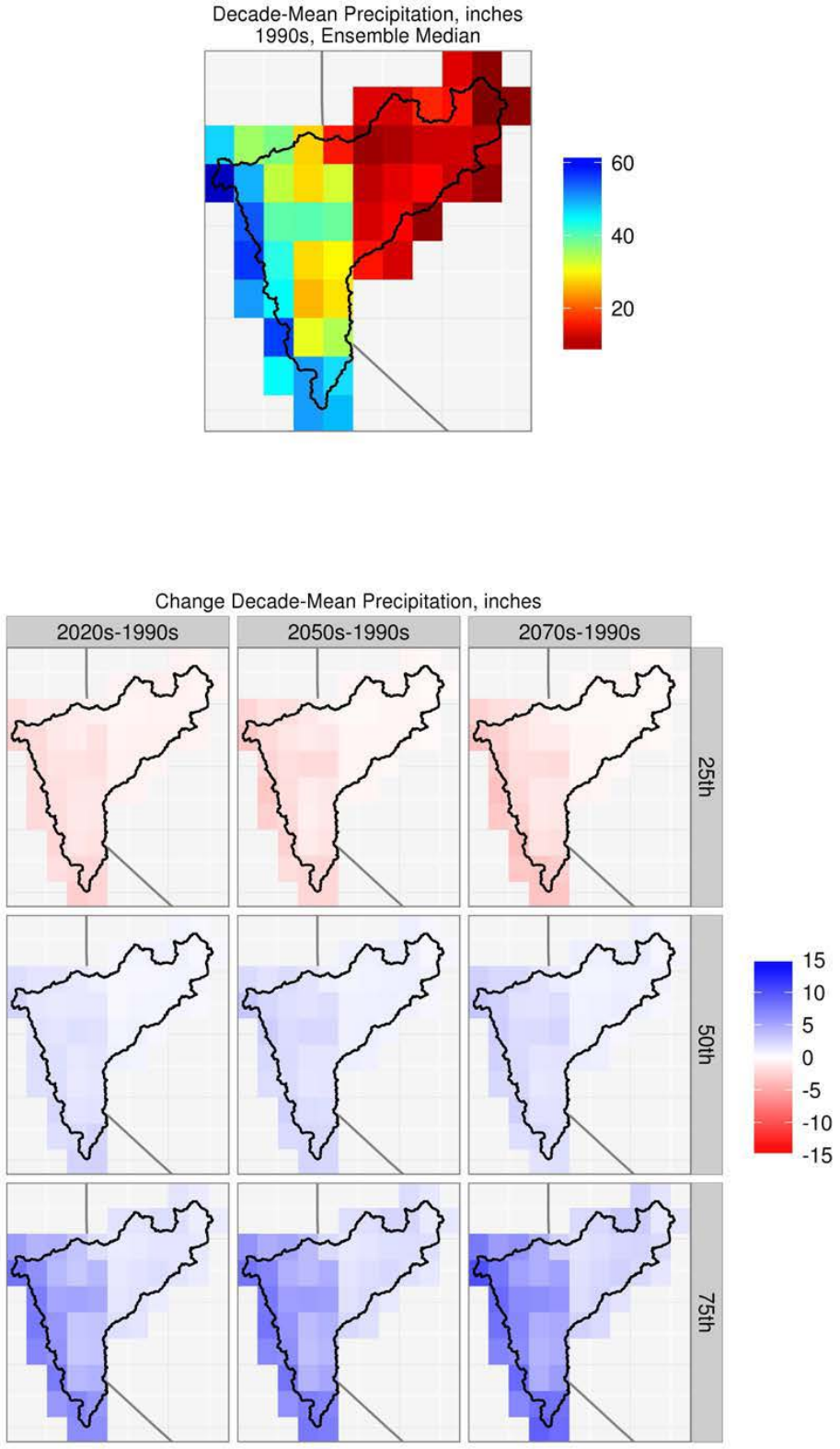

Figure 51. Truckee and Carson Basins – Spatial distribution of simulated decadal precipitation

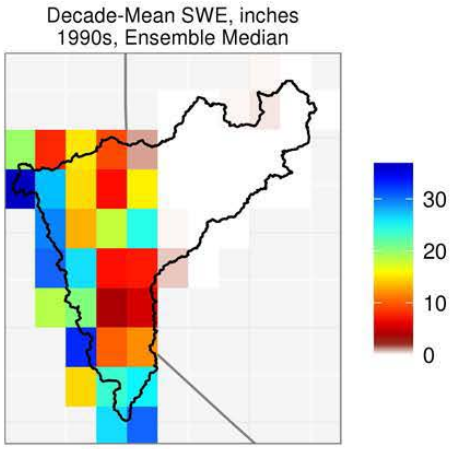

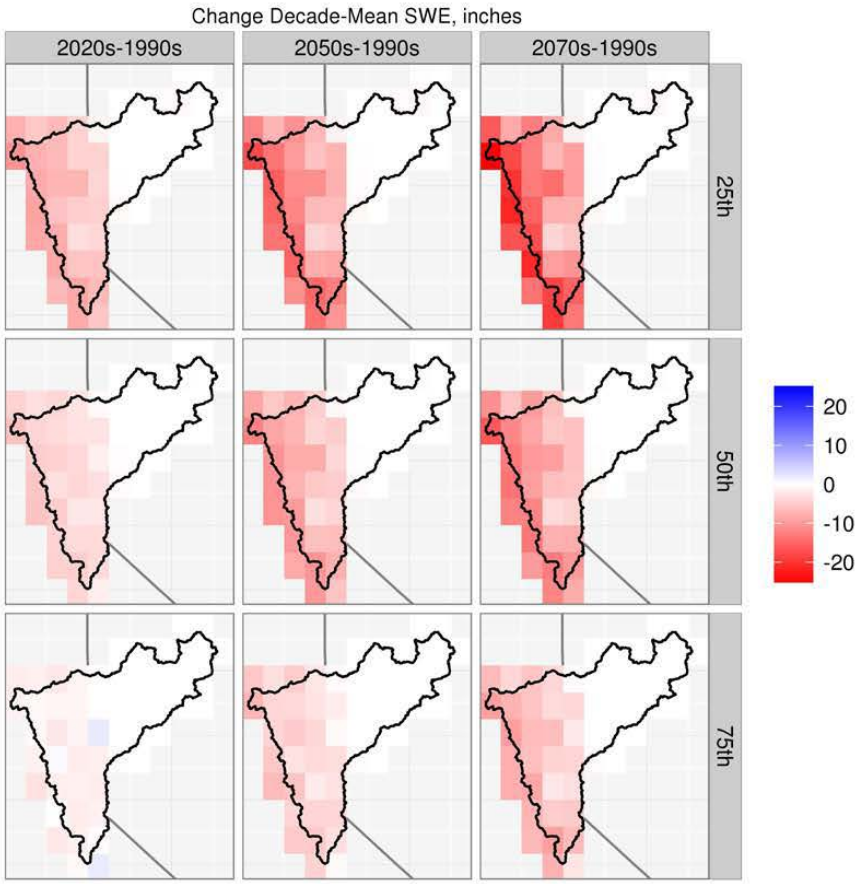

Figure 52. Truckee and Carson Basins – Spatial distribution of simulated decadal April 1st SWE

Figure 53 provides the distribution of April 1st SWE with elevation in the Truckee River Basin for the reference decade and the percentage change in this

distribution for the three future decades. The 25th and 75th percentile estimates provide a way to quantify the uncertainty in the calculated changes.

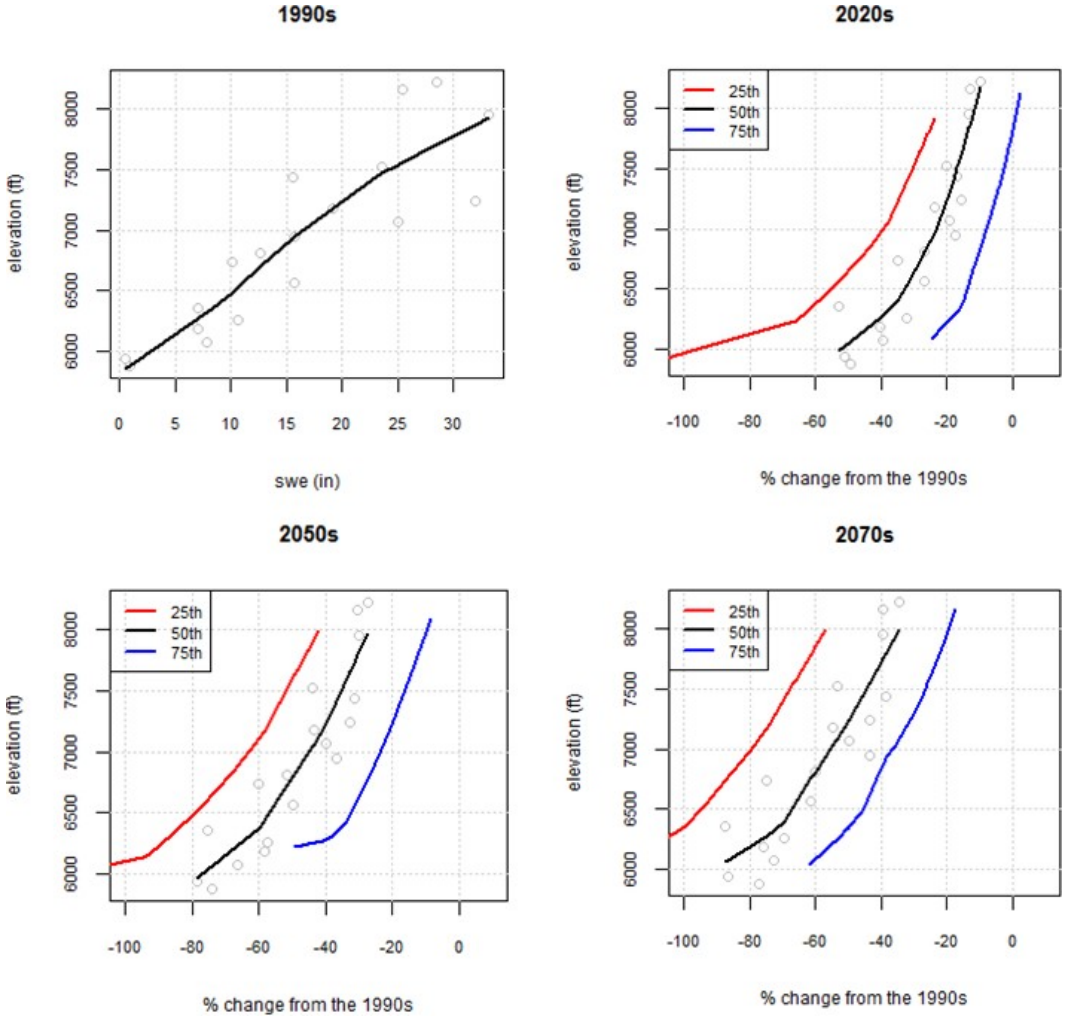

Figure 53. Truckee Basin – SWE distribution with elevation in the 1990s decade and future changes

The open light gray circles in this plot correspond to the median SWE values at each elevation with a fitted regression line is shown in black. The regression lines for the 25th and the 75th percentiles are presented in red and blue, respectively.

The SWE elevation range for the Truckee Basin (the elevation range of areas shown by the VIC model to have met the threshold April 1st SWE of at least 10 mm during the 1990s) was estimated to be approximately 6,000 to 8,000 feet. The 1990s decade-mean SWE distribution (top left panel plot) shows linear behavior, with greater snow amounts at higher elevations and the regression line attempting to optimally fit through the entire point scatter. The primary moisture source contributing to snowpack development for the Basin is wintertime precipitation. There appears to be substantial loss in SWE at all elevations throughout the Basin from the 1990s reference, and also moving forward from the 2020s to 2050s and from the 2050s to the 2070s decade.

3.8.2. Impacts on Runoff Annual and Seasonal Cycles

Figure 54 shows the mean monthly streamflow values for the 1990s, 2020s, 2050s, and 2070s in four Truckee River sub-basins and the Carson River Basin. There are noticeable shifts in the distribution of monthly flow in the future decades relative to the 1990s reference, but in all cases, there do not appear to be large shifts in the peak runoff timing.

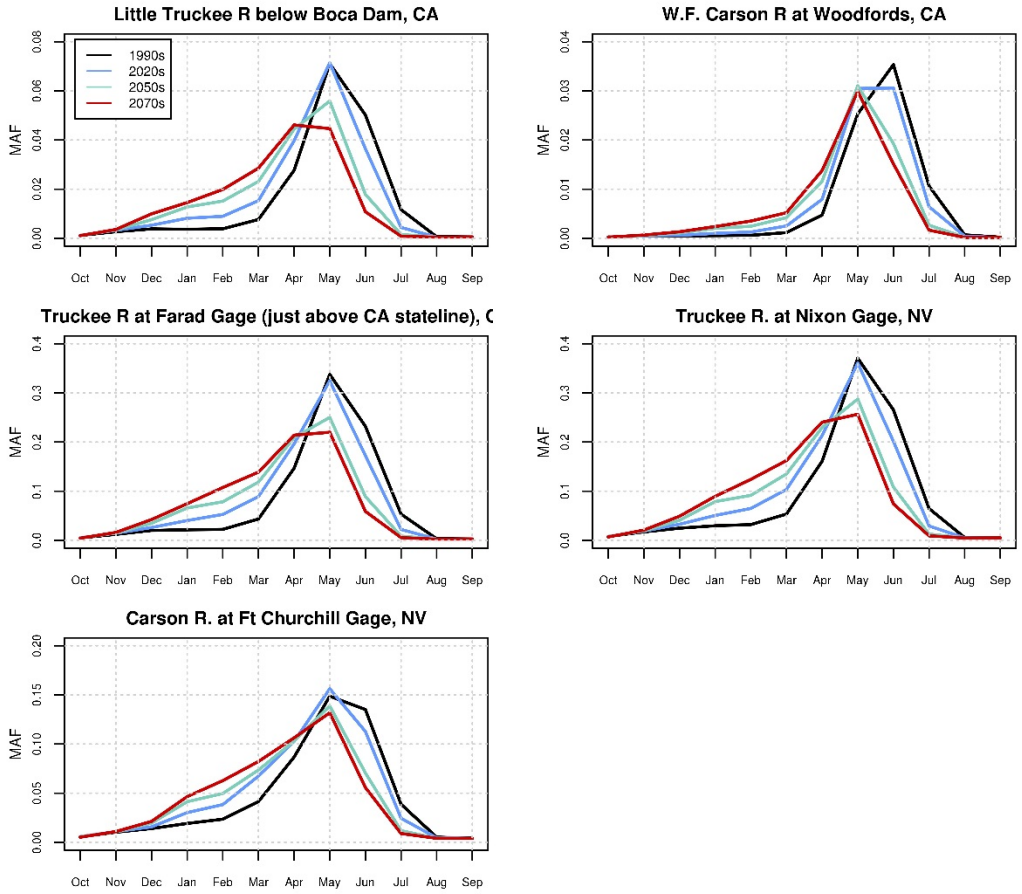

Figure 54. Truckee and Carson Basins – Simulated mean monthly runoff for various sub-basins

Figure 55 shows boxplots of the distribution of simulated changes in runoff magnitude for annual, December-through-March, and April-through-July runoff in the four Truckee River sub-basins and the Carson River Basin. Overall, the analysis shows that there is an increase in the ensemble-median December-through-March runoff and a decrease in the April-through-July runoff in all the three future decades, with nominal changes in the ensemble-median annual runoff magnitudes.

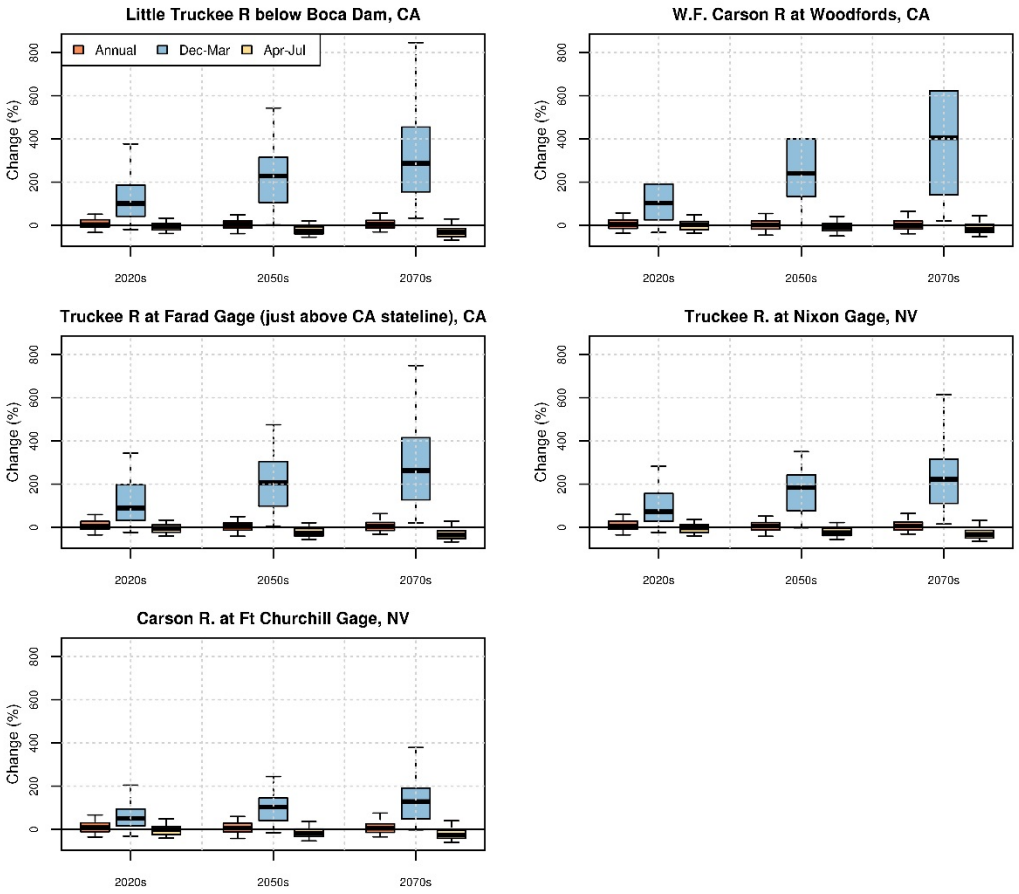

Figure 55. Truckee and Carson Basins – Simulated change in runoff magnitude for various sub-basins

Figure 56 shows the simulated shift in runoff timing for the various sub-basins. For all of the sub-basins, the shift represented by the ensemble median shows that half of the annual flow volume will occur earlier in the future decades relative to the 1990s decade. Also, it appears from the analysis that this earlier shift grows in the three future decades relative to the 1990s decade. For example, the Truckee River at the Nixon gage, the earlier shift is about, 9, 14, and 19 days, respectively, in the 2020s, 2050s and 2070s relative to the 1990s.

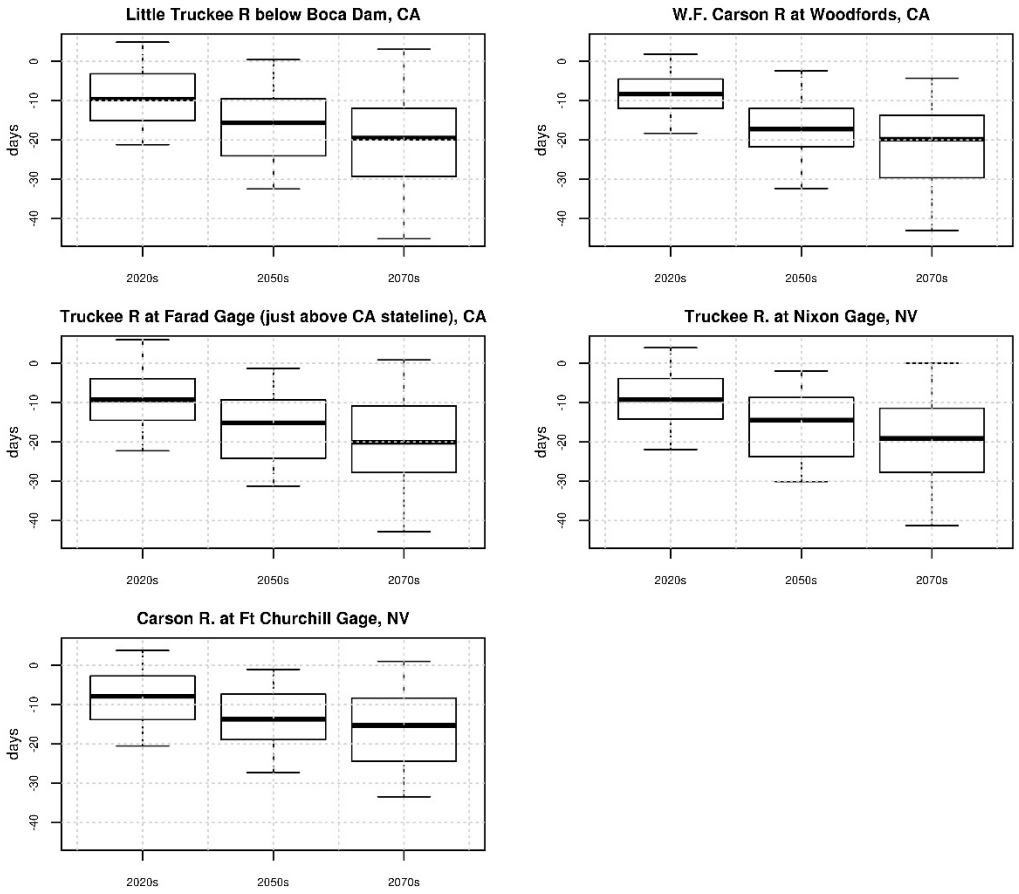

Figure 56. Truckee and Carson Basins –Simulated shift in runoff timing for various sub-basins

This page intentionally left blank.

4. West-wide Summary of Hydroclimate Changes

This chapter provides a West-wide summary of the findings from this hydroclimate analysis for the changes in precipitation, temperature, snow condition, and streamflow and runoff magnitude and runoff seasonality. For context of the BCSD-CMIP5 hydroclimate outputs, a comparison is provided to contemporary analysis, specifically BCSD-CMIP3 analysis from the 2011 WWCRA hydroclimate projections report (Reclamation, 2011b).

4.1. BCSD-CMIP5 Findings

4.1.1. Temperature

The U.S. average temperature has increased by 1.3° F to 1.9° F since record-keeping began in 1895; most of this increase has occurred since about 1970 (Melillo et al., 2014). The western U.S. has warmed roughly 2° F in the basins considered here and is projected to warm further during the 21st century. In many river basins, a warming trend has been noted since at least the 1970s (e.g., lower Colorado River basin), if not since the beginning of the 20th century (e.g., Columbia River Basin, Sacramento and San Joaquin River basins, the Rio Grande basin, and most of the Missouri River basin). This rise in temperature will continue trends already observed. Central estimates of this continued warming vary from roughly 5° F to 7° F depending on location.

4.1.2. Precipitation

Compared to projected changes in temperature, projected changes in precipitation are much less consistent among various climate models, and are characterized by greater uncertainty. While projected changes in average total annual precipitation are generally small in many areas, both wet and dry extremes (heavy precipitation events and length of dry spells) are expected to increase substantially throughout the West (Georgakakos et al. 2014). Overall precipitation is projected to remain variable, with no discernable trends in most basins.

4.1.3. Snowpack

Across most of the West, a trend toward more precipitation falling as rain and less as snow is already apparent. This is being observed both topographically (lower elevations receiving less precipitation in the form of snow) and seasonally (a shortening of the snow-accumulation period). In most areas, projections of future hydrology suggest that warming and associated loss of snowpack will persist over much of the western U.S. Trends toward decreasing snowpack are projected to continue across most of the West through the 21st century.

4.1.4. Runoff

Projected changes in temperature, precipitation, and snowpack are expected to change the magnitude and seasonality of runoff. Warming is expected to result in more rainfall-runoff during the cool season rather than snowpack accumulation, leading to increases in December-March runoff and decreases in April-July runoff. The area from the Southwest to the Southern Rockies is expected to experience gradual runoff declines during the 21st century. The area from the Northwest to north-central U.S. is expected to experience little change through mid-21st century, with increases projected for the late-21st century. Projected seasonal runoff trends are presented in Figure 57 and Figure 58 and are also summarized by river basin below.

- **Colorado River Basin:** Warmer conditions are projected to transition snowfall to rainfall, producing more December-March runoff and less April-July runoff. The median shift in the date of peak runoff is expected to be 12 days earlier by the end of the century.
- **Columbia River Basin:** Mean annual runoff is projected to increase by 2.9 percent by the 2050s. Moisture falling as rain instead of snow at lower elevations will increase the wintertime runoff and lead to decreased runoff during the summer.
- **Klamath River Basin:** By the 2050s, projected warming is expected to change runoff timing, with a 23 percent increase in rainfall-runoff during the winter (December through March) and a 33 percent decrease in runoff during the spring and summer (April through July).
- **Missouri River Basin:** Mean annual basin runoff is projected to increase as much as 15 percent, with higher variability in sub-basin runoff by mid-century. Moisture falling as rain instead of snow at lower elevations is expected to result in an increase of the wintertime runoff and a decrease in summer runoff.
- **Rio Grande Basin:** Mean annual runoff is projected to decrease by 3 percent by the 2050s, with higher variability in sub-basins. By mid-century, warmer conditions are projected to transition snowfall to rainfall, shifting the timing of runoff by up to 11 days in the upper basin tributaries.
- **Sacramento and San Joaquin River Basins:** Mean annual runoff is projected to increase as much as 5.4 percent in the Sacramento and San Joaquin Rivers Delta by the 2050s. Moisture falling as rain instead of snow at lower elevations will increase wintertime runoff by 22 percent (December through March) and decrease springtime runoff by 27 percent (April through July).

- **Truckee River Basin:** Mean annual runoff is projected to increase by 5.7 percent by the 2050s. Warmer conditions are projected to transition wintertime snow into rain, increasing December-through-March runoff and decreasing April-through-July runoff. The median date of peak runoff is expected to be 19 days earlier by the end of the century.

This page intentionally left blank.

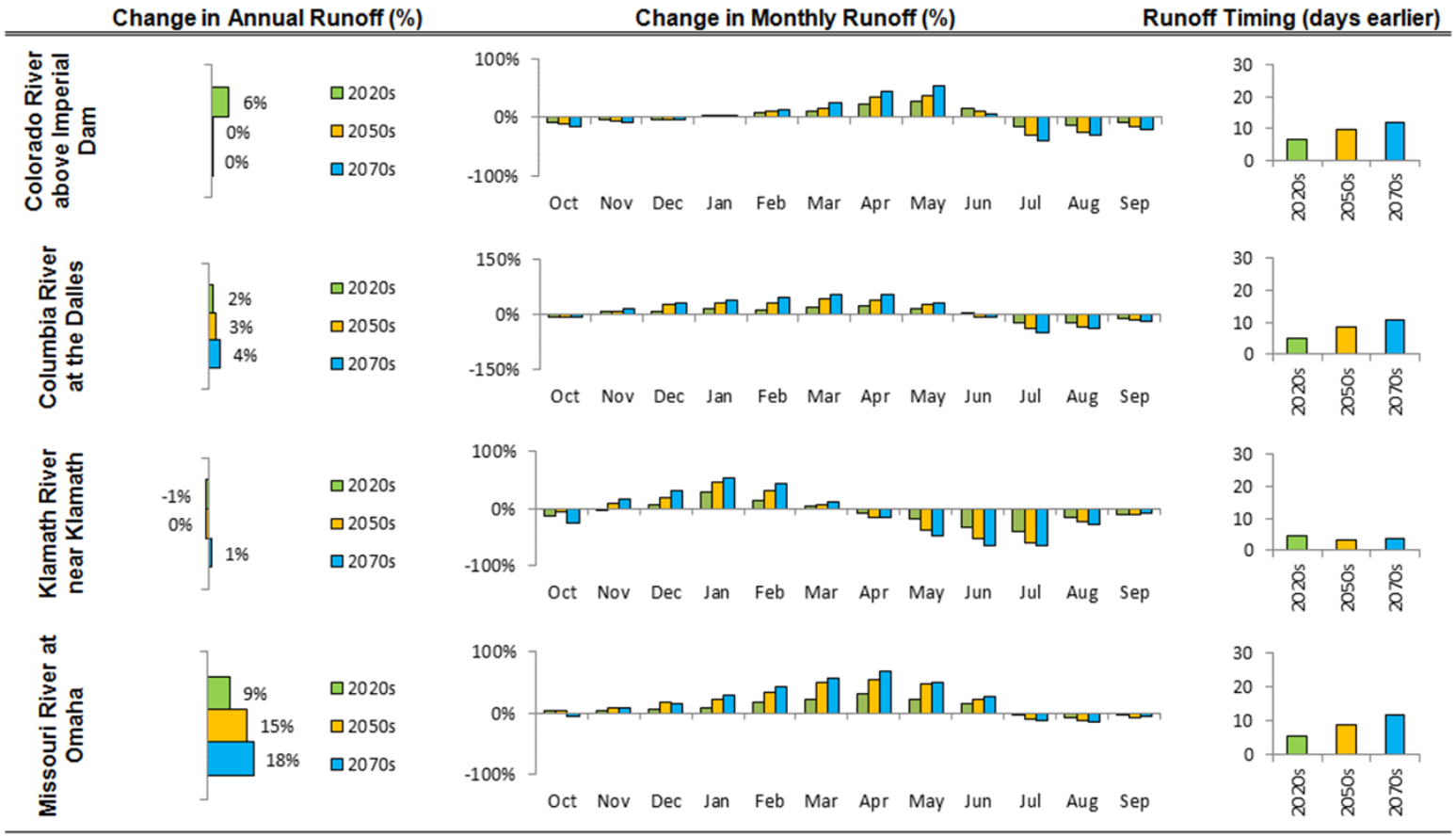

Figure 57. Projected shift in annual runoff, monthly runoff, and peak runoff date relative to the 1990s for the 2020s, 2050s, and 2070s in the major Reclamation river basins

In almost all cases, projections indicate an increase in cool-season runoff (November through April), and a decrease in warm-season runoff (May through September), as well as a shift to earlier peak runoff timing in every basin.

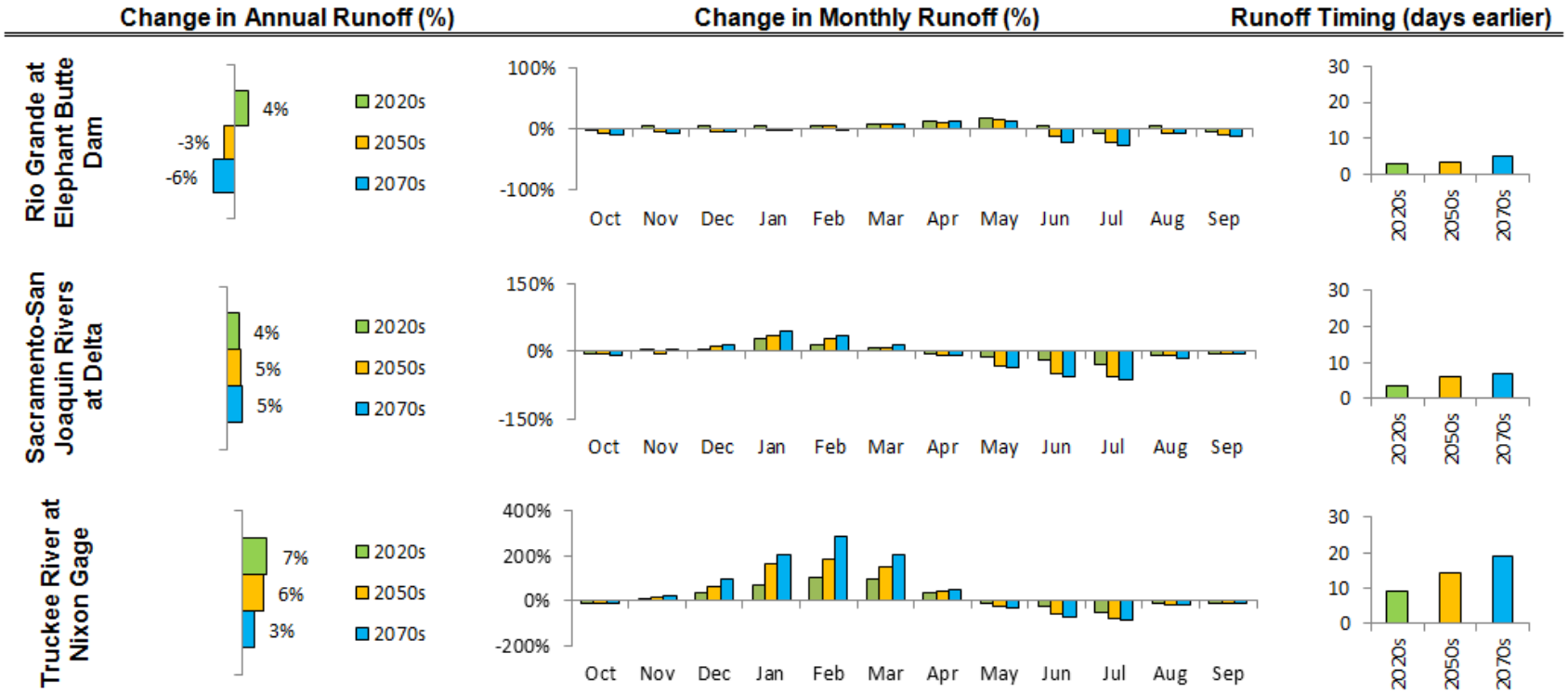

Figure 58. (Continued from Figure 57) Projected shift in annual runoff, monthly runoff, and peak runoff date relative to the 1990s for the 2020s, 2050s, and 2070s in the major Reclamation river basins

In almost all cases, projections indicate an increase in cool-season runoff (November through April), and a decrease in warm-season runoff (May through September), as well as a shift to earlier peak runoff timing in every basin.

To provide additional insights on the spatial distribution of runoff changes and to get a full West-wide coverage, the ensemble-median change in December-through-March and April-through-July runoff at the 416 locations (which includes 43 WWCRA locations used in this analysis, plus 152 HCDN locations and 221 locations used by NCAR to develop the CMIP5 hydrology projections) is shown in Figure 59 for the three future decades, 2020s, 2050s, and 2070s.

The underlying ensemble of projection information shows that there is significant variability and uncertainty, particularly with respect to precipitation. Changes in the frequency and intensity of extreme events have significant implications for the management of floods, other high flows, and storable water. As already noted, studies indicate a strong potential for the occurrence of more-intense precipitation events in most areas of the West. This, in turn, is expected to increase the frequency and/or magnitude of extreme runoff events. Evidence also suggests more year-to-year variability of surface water supplies in at least some areas. For example, the future of the Southwest may include longer, more-extreme dry and wet periods than previously observed (Georgakakos et al. 2014).

Where runoff is projected to increase relative to historical conditions, supplies available to meet delivery needs may increase, especially where adequate storage or other mechanisms exist for aligning the timing of water demands with runoff. Where runoff is projected to decrease, additional challenges for meeting water delivery needs can be anticipated. Impacts on water deliveries will vary from basin to basin and from year to year, depending on the timing and magnitude of water inflows and demands, available storage, and water delivery options.

4.1.5. Key Points

In summary, temperature increases are projected to continue, resulting in decreased snowpack, differences in the timing and volume of spring runoff, and an increase in peak flows for some western U.S. basins. The impacts to snowpack and runoff affect the timing and availability of water supplies. Precipitation changes are also expected to occur, interacting with warming to cause longer-term and more-frequent droughts and larger and more-numerous floods, varying by basin. These summary statements draw attention to mean projected changes in temperature and precipitation, characterized generally across the western U.S.

- Temperature increases have resulted in decreased snowpack, differences in the timing and volume of spring runoff, and an increase in peak flows for some western U.S. basins. The impacts to snowpack and runoff affect the timing and availability of water supplies.
- Warming is expected to continue, causing further impacts on supplies, increasing agricultural water demands, and affecting the seasonal demand for hydropower electricity.

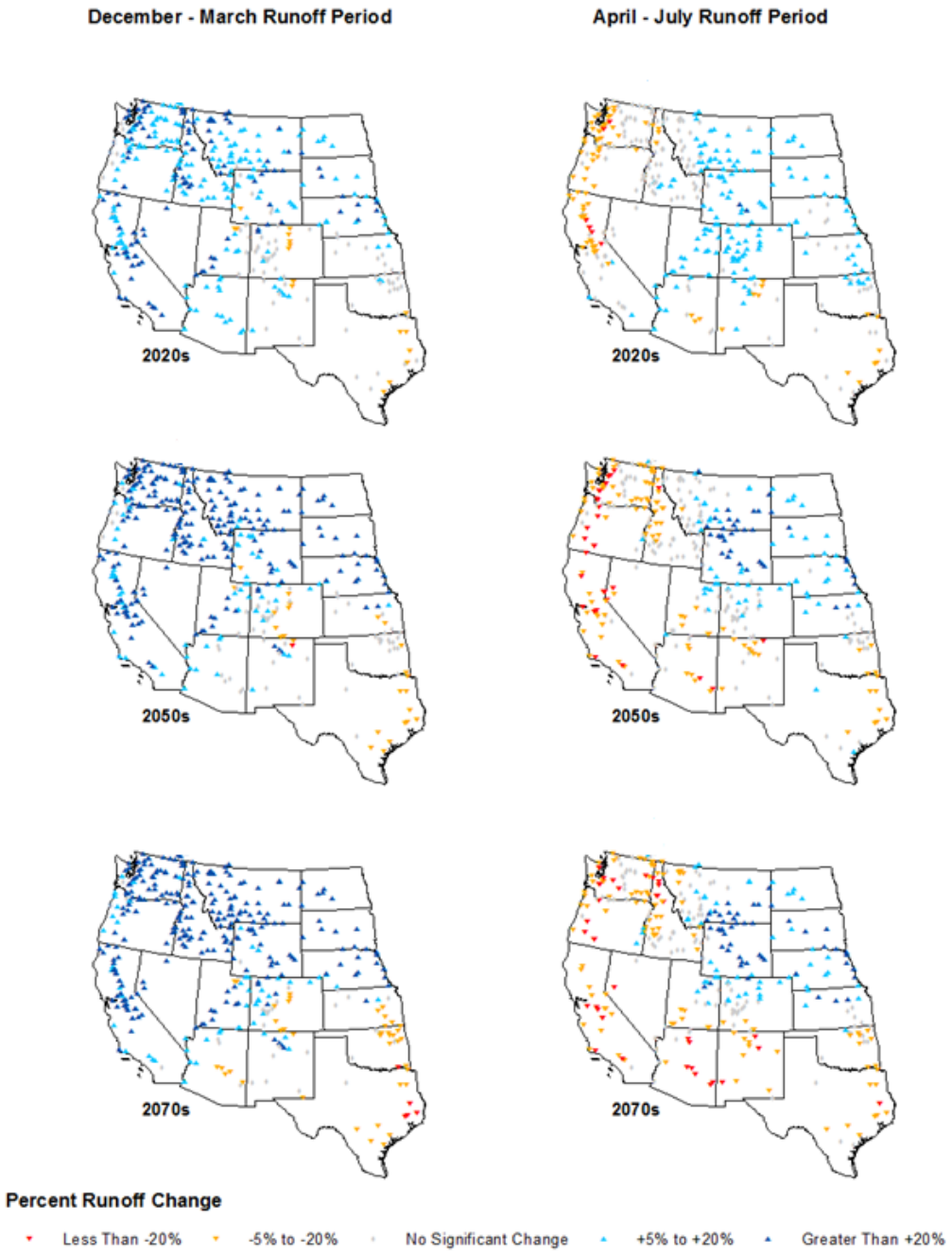

Figure 59. Projected change in December-March and April-July runoff relative to the 1990s for the 2020s, 2050s, and 2070s distributed over the West

Moisture falling as rain instead of snow at lower elevations is projected to increase wintertime runoff and decrease runoff during the summer.

- Precipitation changes are also expected to occur, interacting with warming to cause longer-term and more-frequent droughts and larger and more numerous floods, varying by basin.

- Cool-season runoff is projected to increase over the West Coast basins from California to Washington and over the north-central U.S., but little change to slight decreases are projected over the southwestern U.S. to Southern Rockies.
- Warm-season runoff is projected to decrease substantially over a region spanning southern Oregon, the southwestern U.S., and Southern Rockies. However, north of this region, warm-season runoff is projected to change little or to slightly increase.
- Projected increasing precipitation in the northern tier of the western U.S. could counteract warming-related decreases in warm-season runoff, whereas projected decreases in precipitation in the southern tier of the western U.S. could amplify warming-related decreases in warm-season runoff.

Collectively, the impacts of climate change to water resources give rise to difficult questions about how best to operate Reclamation facilities to meet growing demands for water and hydropower now and how to upgrade and maintain infrastructure to optimize operations in the future. More extreme variations in climate will make it difficult for Reclamation to meet competing demands for water. Warming is expected to continue, causing further impacts on supplies, increasing agricultural water demands, and affecting the seasonal demand for hydropower electricity. Increased intensity of droughts and floods also raises concerns about infrastructure safety, the resiliency of species and ecosystems to these changes, and the ability to maintain adequate levels of hydropower production.

4.1.6. National Climate Assessment

Reclamation's efforts to characterize likely changes in water supply, demand, and management constitute just one of many concurrent efforts to characterize the impacts of climate change on our water systems, as well as other critical systems, in the coming decades. Water supply and water management are critical areas projected to be impacted by future climate conditions. Results of this study indicate similar challenges for water resources in the West as those described in the Third National Climate Assessment (Melillo et al. 2014), which summarizes the impacts of climate change on the United States, now and in the future, based on a thorough review of the available literature. The Third National Climate Assessment, published in 2014, was prepared by a team of more than 300 experts guided by a 60-member Federal Advisory Committee. The report was extensively reviewed by the public and experts, including Federal agencies and a panel of the National Academy of Sciences. In meeting its mission, Reclamation's planning and operations rely on comprehensive assessments of present and future water supplies, such as the National Climate Assessment. Key observations related to this analysis from the Third National Climate Assessment include:

- **Changing Rain, Snow, and Runoff:** Very heavy precipitation events have increased nationally and are projected to increase in all regions. The length of dry spells is projected to increase in most areas, especially the southern and northwestern portions of the contiguous United States.
- **Droughts Intensify:** Short-term (seasonal or shorter) droughts are expected to intensify in most U.S. regions. Longer-term droughts are expected to intensify in large areas of the Southwest.
- **Increased Risk of Flooding in Many Parts of the U.S.:** Flooding may intensify in many U.S. regions, even in areas where total precipitation is projected to decline. Increasing flooding risk affects human safety and health, property, infrastructure, economies, and ecology in many basins across the United States.
- **Groundwater Availability:** Climate change is expected to affect water demand, groundwater withdrawals, and aquifer recharge, reducing groundwater availability in some areas.
- **Risks to Coastal Aquifers and Wetlands:** Sea-level rise, storms and storm surges, and changes in surface and groundwater use patterns are expected to compromise the sustainability of coastal freshwater aquifers and wetlands.
- **Water Quality Risks to Lakes and Rivers:** Increasing air and water temperatures, more-intense precipitation and runoff, and intensifying droughts can decrease river and lake water quality in many ways, including increases in sediment, nitrogen, and other pollutant loads.
- **Changes to Water Demand and Use:** Climate change affects water demand and the ways water is used within and across regions and economic sectors. The Southwest, Great Plains, and Southeast are particularly vulnerable to changes in water supply and demand.
- **Water Supply Availability:** Changes in precipitation and runoff, combined with changes in consumption and withdrawal, have reduced surface and groundwater supplies in many areas. These trends are expected to continue, increasing the likelihood of water shortages for many uses.
- **Water Resources Management:** In most U.S. regions, water resources managers and planners will encounter new risks, vulnerabilities, and opportunities that may not be properly managed within existing practices. In many places, competing demands for water create stress in local and regional watersheds.

4.1.7. Data Tables by Parameter

As a final component of this section, specific data for the 43 WWCRA runoff reporting locations is provided in Tables 2 through 7, which list projected changes

in temperature, precipitation, April 1st SWE, and annual and seasonal runoff at each location.

Table 2. Projected range of temperature change in the 2020s, 2050s, and 2070s relative to the 1990s, for the 43 WWCRA reporting locations

Basin*	Site Name and Description	Projected Range[1] of Temperature Change (°F)		
		2020s	2050s	2070s
Colorado	Colorado River at Lees Ferry	1.7 to 3.0	3.0 to 5.5	3.6 to 7.1
	Colorado River above Imperial Dam	1.7 to 2.9	3.0 to 5.3	3.6 to 6.9
	Green River near Greendale	1.7 to 3.1	3.1 to 5.7	3.5 to 7.5
	Colorado River near Cameo	1.6 to 3.0	3.0 to 5.2	3.5 to 6.8
	Gunnison River near Grand Junction	1.6 to 2.9	3.0 to 5.2	3.7 to 6.8
	San Juan River near Bluff, UT	1.7 to 2.9	3.2 to 5.1	3.5 to 7.1
Columbia	Snake River at Brownlee Dam	1.7 to 3.0	3.1 to 5.5	3.7 to 7.4
	Columbia River at Grand Coulee	1.6 to 2.9	2.9 to 5.3	3.5 to 7.0
	Columbia River at The Dalles	1.6 to 2.8	3.0 to 5.2	3.5 to 7.0
	Yakima River at Parker	1.5 to 2.6	2.7 to 5.0	3.3 to 6.4
	Deschutes River near Madras	1.5 to 2.6	2.6 to 4.7	3.1 to 6.4
	Snake River near Heise	1.6 to 3.1	3.1 to 5.6	3.4 to 7.5
	Flathead River at Columbia Falls	1.6 to 3.0	3.1 to 5.4	3.6 to 7.0
Klamath	Williamson R. below the Sprague River	1.5 to 2.6	2.7 to 4.8	3.3 to 6.4
	Klamath River below Iron Gate Dam	1.5 to 2.5	2.7 to 4.6	3.2 to 6.2
	Klamath River near Seiad Valley	1.4 to 2.5	2.7 to 4.5	3.2 to 6.2
	Klamath River at Orleans	1.4 to 2.4	2.7 to 4.5	3.2 to 6.1
	Klamath River near Klamath	1.4 to 2.4	2.6 to 4.4	3.2 to 6.0
Missouri	Missouri River at Canyon Ferry Dam	1.6 to 3.0	3.0 to 5.3	3.6 to 7.2

Basin*	Site Name and Description	Projected Range[1] of Temperature Change (°F)		
		2020s	2050s	2070s
	Milk River at Nashua	1.3 to 3.0	3.2 to 5.6	3.7 to 6.8
	South Platte River near Sterling	1.5 to 2.8	3.0 to 5.0	3.5 to 6.5
	Missouri River at Omaha	1.4 to 3.0	3.2 to 5.5	3.7 to 6.9
	Bighorn River at Yellowtail Dam	1.6 to 2.9	3.1 to 5.1	3.6 to 7.0
	North Platte River at Lake McConaughy	1.5 to 2.9	3.1 to 5.1	3.5 to 6.7
Rio Grande	Rio Grande near Lobatos	1.5 to 2.8	3.1 to 5.1	3.4 to 6.6
	Rio Chama near Abiquiu	1.6 to 2.9	3.1 to 5.0	3.4 to 6.6
	Rio Grande near Otowi	1.6 to 2.8	3.1 to 5.0	3.4 to 6.7
	Rio Grande at Elephant Butte Dam	1.6 to 2.8	3.1 to 5.0	3.3 to 6.6
	Pecos R at Damsite No. 3 near Carlsbad	1.6 to 2.7	3.2 to 4.8	3.5 to 6.5
Sacramento–San Joaquin	Sacramento River at Freeport	1.5 to 2.4	2.7 to 4.5	3.3 to 5.9
	Sacramento River at Bend Bridge near Red Bluff	1.6 to 2.5	2.7 to 4.6	3.5 to 6.2
	Feather River at Oroville	1.6 to 2.5	2.8 to 4.7	3.4 to 6.2
	San Joaquin River near Vernalis	1.6 to 2.4	2.7 to 4.6	3.2 to 6.0
	Stanislaus River at New Melones Dam	1.6 to 2.5	2.8 to 4.8	3.4 to 6.3
	Sacramento-San Joaquin Rivers at Delta	1.6 to 2.4	2.6 to 4.5	3.3 to 5.9
	San Joaquin River at Millerton Lake (Friant Dam)	1.6 to 2.5	2.9 to 5.0	3.3 to 6.3
	American River at Fair Oaks	1.6 to 2.5	2.8 to 4.7	3.4 to 6.1
	Tulare-Buena Vista Lakes	1.5 to 2.3	2.7 to 4.4	3.1 to 5.9
Truckee	Little Truckee River below Boca Dam	1.6 to 2.5	2.9 to 4.8	3.5 to 6.4
	W.F. Carson River at Woodfords	1.7 to 2.6	3.0 to 4.9	3.5 to 6.4

Basin*	Site Name and Description	Projected Range[1] of Temperature Change (°F)		
		2020s	2050s	2070s
	Truckee River at Farad Gage (just above CA stateline)	1.7 to 2.5	2.9 to 4.8	3.5 to 6.3
	Truckee River at Nixon Gage	1.7 to 2.6	3.0 to 4.9	3.5 to 6.5
	Carson River at Fort Churchill Gage	1.7 to 2.6	3.1 to 5.0	3.5 to 6.6

* Note – the Pecos, Tulare and Carson are not SWA Basins but are respectively included under the Rio Grande, Sacramento-San Joaquin, and Truckee as these locations are of interest from a water operations standpoint.

[1] Ranges of projected temperatures are the 25th to 75th percentile change of the 97 projections.

Table 3. Projected range of precipitation change in the 2020s, 2050s, and 2070s relative to the 1990s, for the 43 WWCRA reporting locations

Basin*	Site Name and Description	Projected Range[1] of Precipitation Change (%)		
		2020s	2050s	2070s
Colorado	Colorado River at Lees Ferry	–0.4 to 12.5	–0.5 to 12.7	1.2 to 16.3
	Colorado River above Imperial Dam	–0.4 to 13.3	–1.6 to 12.4	1.1 to 15.0
	Green River near Greendale	–1.4 to 14.2	0.9 to 16.7	3.7 to 19.6
	Colorado River near Cameo	–0.1 to 10.8	0.2 to 12.8	2.0 to 17.1
	Gunnison R. near Grand Junction	–0.5 to 11.0	–0.8 to 11.6	–0.3 to 14.0
	San Juan River near Bluff, UT	–1.8 to 13.4	–4.1 to 10.7	–2.0 to 12.3
Columbia	Snake River at Brownlee Dam	0.6 to 10.7	1.3 to 13.9	5.0 to 16.6
	Columbia River at Grand Coulee	–0.7 to 9.6	1.5 to 14.7	2.8 to 15.0
	Columbia River at The Dalles	0.2 to 7.8	2.6 to 12.5	4.3 to 13.9
	Yakima River at Parker	–1.9 to 9.1	1.1 to 9.8	1.7 to 13.5
	Deschutes River near Madras	–2.3 to 7.9	–2.8 to 9.6	–0.2 to 12.7
	Snake River near Heise	–0.6 to 11.5	2.8 to 15.1	4.4 to 20.4

Basin*	Site Name and Description	Projected Range[1] of Precipitation Change (%)		
		2020s	2050s	2070s
	Flathead River at Columbia Falls	0.5 to 11.7	1.7 to 14.9	2.1 to 16.9
Klamath	Williamson River below the Sprague River	–3.9 to 9.5	–4.7 to 12.7	–2.0 to 14.5
	Klamath River below Iron Gate Dam	–4.4 to 8.2	–4.1 to 11.5	–2.0 to 13.2
	Klamath River near Seiad Valley	–3.8 to 7.4	–4.0 to 11.1	–2.8 to 13.1
	Klamath River at Orleans	–3.2 to 6.9	–3.8 to 10.4	–3.8 to 12.3
	Klamath River near Klamath	–3.3 to 7.5	–4.1 to 10.5	–2.5 to 13.4
Missouri	Missouri River at Canyon Ferry Dam	0.0 to 9.1	1.9 to 12.9	2.8 to 15.6
	Milk River at Nashua	–2.0 to 13.3	–1.6 to 15.6	–1.3 to 19.2
	South Platte River near Sterling	0.1 to 9.7	0.8 to 9.4	2.2 to 12.7
	Missouri River at Omaha	–0.3 to 9.3	1.9 to 12.0	3.6 to 15.3
	Bighorn River at Yellowtail Dam	–0.1 to 13.6	4.4 to 15.1	3.6 to 20.5
	North Platte River at Lake McConaughy	–0.7 to 9.6	0.8 to 11.6	2.3 to 16.2
Rio Grande	Rio Grande near Lobatos	–1.8 to 10.6	–2.3 to 9.4	–1.1 to 12.8
	Rio Chama near Abiquiu	–1.4 to 11.1	–3.3 to 10.1	–3.0 to 9.9
	Rio Grande near Otowi	–1.6 to 9.8	–2.3 to 8.1	–2.2 to 10.6
	Rio Grande at Elephant Butte Dam	–3.2 to 9.4	–3.4 to 9.9	–4.5 to 9.0
	Pecos River at Damsite No. 3 near Carlsbad	–7.4 to 7.2	–8.0 to 9.0	–9.7 to 7.1
Sacramento–San Joaquin	Sacramento River at Freeport	–3.4 to 11.7	–4.9 to 14.0	–3.5 to 15.9
	Sacramento River at Bend Bridge near Red Bluff	–4.0 to 9.7	–4.5 to 13.4	–2.6 to 14.9
	Feather River at Oroville	–4.8 to 11.8	–5.5 to 15.1	–4.7 to 16.1

Basin*	Site Name and Description	Projected Range[1] of Precipitation Change (%)		
		2020s	2050s	2070s
	San Joaquin River near Vernalis	–2.8 to 16.1	–7.2 to 15.7	–6.0 to 17.9
	Stanislaus R. at New Melones Dam	–5.3 to 14.6	–4.6 to 16.5	–7.0 to 18.2
	Sacramento-San Joaquin Rivers at Delta	–3.0 to 13.1	–4.6 to 14.0	–4.7 to 16.4
	San Joaquin River at Millerton Lake (Friant Dam)	–2.3 to 18.2	–8.2 to 15.9	–6.8 to 18.9
	American River at Fair Oaks	–4.5 to 13.1	–4.6 to 13.6	–6.0 to 16.8
	Tulare-Buena Vista Lakes	–4.3 to 16.7	–12.4 to 15.6	–9.6 to 16.3
Truckee	Little Truckee R. below Boca Dam	–4.5 to 12.6	–4.6 to 14.9	–4.7 to 17.0
	W.F. Carson River at Woodfords	–5.7 to 13.3	–4.3 to 16.7	–6.2 to 17.6
	Truckee River at Farad Gage (just above CA stateline)	–4.7 to 13.2	–4.4 to 14.5	–5.5 to 16.4
	Truckee River at Nixon Gage	–5.7 to 12.6	–3.8 to 14.9	–5.4 to 16.7
	Carson River at Fort Churchill Gage	–6.3 to 13.8	–4.0 to 16.6	–5.2 to 18.9

* Note – the Pecos, Tulare and Carson are not SWA Basins but are respectively included under the Rio Grande, Sacramento-San Joaquin, and Truckee as these locations are of interest from a water operations standpoint.

[1] Ranges of projected precipitation are the 25th to 75th percentile change of the 97 projections.

Table 4. Projected range of April 1st SWE change in the 2020s, 2050s, and 2070s relative to the 1990s, by elevation band in each SECURE Water Act Basin

Basin (SWE elevation range)	Approximate Basin Elevation	Projected Range[1] of April 1st SWE (%)		
		2020s	2050s	2070s
Colorado (~6,000–12,000 ft)	~6,500 ft	–100 to 1	–100 to –26	–100 to –44
	~8,000 ft	–38 to 6	–58 to –10	–73 to –18
	~9,500 ft	–13 to 12	–25 to 5	–33 to 2
	~11,000 ft	–3 to 16	–7 to 15	–9 to 13
Columbia (~2,000–10,000 ft)	~3,000 ft	–70 to 26	–92 to –50	–99 to –55
	~5,000 ft	–27 to 5	–47 to –17	–60 to –23
	~7,000 ft	–14 to 6	–24 to 0	–33 to –4

Basin (SWE elevation range)	Approximate Basin Elevation	Projected Range[1] of April 1st SWE (%)		
		2020s	2050s	2070s
	~9,000 ft	–6 to 13	–9 to 12	–12 to 10
Klamath (~2,000–7,000 ft)	~3,000 ft	–100 to –35	–100 to –53	–100 to –63
	~4,000 ft	–71 to –25	–95 to –43	–100 to –53
	~5,000 ft	–49 to –14	–70 to –28	–83 to –39
	~6,500 ft	–24 to –3	–43 to –12	–56 to –18
Missouri (~4,500–11,500 ft)	~5,500 ft	–54 to –2	–72 to –20	–85 to –28
	~7,000 ft	–22 to 6	–37 to –5	–49 to –10
	~9,000 ft	–12 to 12	–19 to 8	–27 to 5
	~10,500 ft	–4 to 19	–4 to 20	–5 to 20
Rio Grande (~8,000–12,000 ft)	~8,500 ft	–73 to 6	–100 to –31	–100 to –48
	~9,500 ft	–37 to 14	–69 to –3	–81 to –18
	~10,500 ft	–15 to 21	–35 to 8	–43 to 2
	~11,500 ft	–4 to 19	–17 to 15	–20 to 12
Sacramento-San Joaquin (~3,000–11,000 ft)	~4,000 ft	–100 to –31	–100 to –50	–100 to –58
	~6,000 ft	–59 to –16	–83 to –35	–97 to –44
	~8,000 ft	–31 to 1	–50 to –10	–61 to –19
	~10,000 ft	–11 to 16	–21 to 13	–22 to 10
Truckee (~6,000–8,000 ft)	~6,000 ft	–74 to –22	–93 to –49	–100 to –57
	~7,000 ft	–47 to –11	–70 to –28	–87 to –42
	~7,500 ft	–33 to –4	–55 to –19	–71 to –29
	~8,000 ft	–24 to 1	–43 to –11	–58 to –21

[1] Ranges of projected April 1st SWE are the 25th to 75th percentile change of the 97 projections.

Table 5. Projected range of annual runoff change in the 2020s, 2050s, and 2070s relative to the 1990s, for the 43 WWCRA reporting locations

Basin*	Site Name and Description	Projected Range[1] of Annual Runoff Change (%)		
		2020s	2050s	2070s
Colorado	Colorado River at Lees Ferry	–6.9 to 18.0	–11.3 to 14.1	–12.2 to 19.0
	Colorado R. above Imperial Dam	–6.6 to 19.5	–11.0 to 15.9	–12.6 to 18.7
	Green River near Greendale	–10.7 to 22.9	–11.8 to 17.9	–9.0 to 24.7
	Colorado River near Cameo	–5.4 to 16.5	–9.5 to 14.4	–10.2 to 19.2
	Gunnison R. near Grand Junction	–8.6 to 20.9	–14.3 to 13.2	–15.6 to 13.1

Basin*	Site Name and Description	Projected Range[1] of Annual Runoff Change (%)		
		2020s	2050s	2070s
	San Juan River near Bluff, UT	–11.1 to 17.9	–19.2 to 5.4	–21.0 to 7.2
Columbia	Snake River at Brownlee Dam	–2.9 to 15.4	–1.9 to 18.1	0.2 to 19.6
	Columbia River at Grand Coulee	–4.5 to 10.8	–4.7 to 13.5	–2.3 to 10.6
	Columbia River at The Dalles	–2.5 to 8.7	–5.2 to 11.4	–2.2 to 11.0
	Yakima River at Parker	–7.0 to 8.4	–6.2 to 8.0	–5.1 to 10.3
	Deschutes River near Madras	–5.7 to 11.8	–7.1 to 13.8	–4.3 to 17.7
	Snake River near Heise	–10.2 to 16.7	–9.5 to 15.4	–8.7 to 21.1
	Flathead River at Columbia Falls	–4.5 to 11.2	–8.4 to 13.5	–8.0 to 12.8
Klamath	Williamson River below the Sprague River	–14.7 to 29.5	–14.8 to 30.0	–13.3 to 41.1
	Klamath R. below Iron Gate Dam	–13.4 to 22.4	–14.1 to 21.6	–13.2 to 25.4
	Klamath River near Seiad Valley	–11.2 to 20.7	–11.6 to 18.9	–10.6 to 24.5
	Klamath River at Orleans	–9.6 to 15.2	–9.7 to 14.3	–11.0 to 19.1
	Klamath River near Klamath	–9.8 to 14.7	–9.5 to 12.5	–8.5 to 18.2
Missouri	Missouri R. at Canyon Ferry Dam	–3.7 to 13.4	–3.6 to 17.7	–2.8 to 21.2
	Milk River at Nashua	–4.2 to 21.8	–3.1 to 29.8	–2.4 to 31.9
	South Platte River near Sterling	–6.8 to 17.3	–8.8 to 15.7	–10.0 to 26.0
	Missouri River at Omaha	2.6 to 18.6	6.5 to 25.1	7.0 to 34.5
	Bighorn River at Yellowtail Dam	–4.5 to 26.7	4.7 to 29.6	3.0 to 37.7
	North Platte River at Lake McConaughy	–2.9 to 22.6	0.4 to 28.7	6.4 to 43.3
Rio Grande	Rio Grande near Lobatos	–10.9 to 19.9	–19.2 to 7.9	–26.9 to 6.4
	Rio Chama near Abiquiu	–9.6 to 24.5	–16.6 to 16.0	–18.7 to 14.1
	Rio Grande near Otowi	–10.6 to 21.4	–17.9 to 9.0	–21.0 to 7.2

Basin*	Site Name and Description	Projected Range[1] of Annual Runoff Change (%)		
		2020s	2050s	2070s
	Rio Grande at Elephant Butte Dam	–7.8 to 17.6	–16.2 to 7.3	–20.5 to 8.9
	Pecos River at Damsite No. 3 near Carlsbad	–11.3 to 9.4	–13.2 to 13.8	–11.9 to 9.7
Sacramento–San Joaquin	Sacramento River at Freeport	–8.3 to 24.3	–11.5 to 24.1	–10.3 to 26.9
	Sacramento River at Bend Bridge near Red Bluff	–7.7 to 21.0	–10.2 to 22.5	–8.1 to 25.9
	Feather River at Oroville	–10.9 to 22.2	–13.1 to 22.4	–11.1 to 20.8
	San Joaquin River near Vernalis	–7.6 to 30.2	–16.0 to 28.5	–15.5 to 28.1
	Stanislaus River at New Melones Dam	–9.7 to 23.5	–13.1 to 20.7	–16.4 to 22.1
	Sacramento-San Joaquin Rivers at Delta	–8.2 to 24.8	–11.0 to 26.1	–12.0 to 24.6
	San Joaquin River at Millerton Lake (Friant Dam)	–8.8 to 32.2	–19.3 to 29.3	–16.6 to 31.2
	American River at Fair Oaks	–8.5 to 21.5	–12.7 to 17.9	–12.9 to 18.2
	Tulare-Buena Vista Lakes	–9.9 to 34.4	–21.8 to 31.4	–17.3 to 33.1
Truckee	Little Truckee R. below Boca Dam	–7.5 to 26.0	–12.6 to 21.1	–12.3 to 23.0
	W.F. Carson River at Woodfords	–14.3 to 25.0	–17.6 to 21.0	–17.3 to 20.8
	Truckee River at Farad Gage (just above CA stateline)	–7.6 to 27.6	–13.5 to 20.7	–14.2 to 22.7
	Truckee River at Nixon Gage	–8.1 to 28.7	–13.1 to 22.1	–13.0 to 24.2
	Carson R. at Fort Churchill Gage	–10.9 to 30.3	–13.0 to 27.3	–14.0 to 25.8

* Note – the Pecos, Tulare and Carson are not SWA Basins but are respectively included under the Rio Grande, Sacramento-San Joaquin, and Truckee as these locations are of interest from a water operations standpoint.

[1] Ranges of projected annual runoff are the 25th to 75th percentile change of the 97 projections.

Table 6. Projected range of December-through-March runoff change in the 2020s, 2050s, and 2070s relative to the 1990s, for the 43 WWCRA reporting locations

Basin*	Site Name and Description	Projected Range[1] of Dec–Mar Runoff Change (%)		
		2020s	2050s	2070s
Colorado	Colorado River at Lees Ferry	–5.5 to 16.6	–3.7 to 22.3	1.7 to 28.2
	Colorado River above Imperial Dam	–7.4 to 17.7	–6.3 to 22.9	–0.8 to 25.0
	Green River near Greendale	–11.2 to 17.5	–6.4 to 22.5	–2.4 to 30.7
	Colorado River near Cameo	–10.6 to 15.9	–6.9 to 15.1	–4.1 to 23.2
	Gunnison River near Grand Junction	–6.0 to 18.4	–4.4 to 17.9	2.3 to 25.1
	San Juan River near Bluff, UT	–10.0 to 18.8	–9.8 to 13.5	–14.8 to 20.8
Columbia	Snake River at Brownlee Dam	4.8 to 28.8	17.4 to 43.3	27.2 to 61.7
	Columbia R. at Grand Coulee	6.7 to 29.9	21.1 to 53.9	23.9 to 79.0
	Columbia River at The Dalles	5.5 to 28.0	21.7 to 45.4	23.6 to 68.8
	Yakima River at Parker	16.9 to 45.1	45.3 to 87.3	52.0 to 119.4
	Deschutes River near Madras	7.2 to 36.0	19.5 to 49.2	27.4 to 71.2
	Snake River near Heise	–2.7 to 20.9	7.8 to 40.0	11.9 to 81.7
	Flathead R. at Columbia Falls	7.1 to 40.8	21.7 to 85.1	31.4 to 112.4
Klamath	Williamson River below the Sprague River	3.0 to 58.2	12.8 to 73.0	18.0 to 95.9
	Klamath River below Iron Gate Dam	14.0 to 82.8	39.1 to 102.4	50.6 to 144.8
	Klamath River near Seiad Valley	10.1 to 56.5	22.6 to 73.0	32.6 to 101.5
	Klamath River at Orleans	7.5 to 45.9	15.3 to 55.6	26.6 to 77.5
	Klamath River near Klamath	2.0 to 31.1	10.3 to 43.4	16.0 to 54.4
Missouri	Missouri River at Canyon Ferry Dam	0.9 to 30.3	14.0 to 50.6	19.5 to 71.0

Basin*	Site Name and Description	Projected Range[1] of Dec–Mar Runoff Change (%)		
		2020s	2050s	2070s
	Milk River at Nashua	10.6 to 51.1	24.2 to 82.1	31.5 to 104.7
	South Platte River near Sterling	–13.7 to 16.4	–10.1 to 21.9	–11.9 to 28.8
	Missouri River at Omaha	2.2 to 26.5	15.6 to 44.6	13.8 to 59.0
	Bighorn River at Yellowtail Dam	–3.9 to 33.0	4.6 to 54.6	6.8 to 76.1
	North Platte River at Lake McConaughy	4.1 to 29.7	18.0 to 74.8	24.8 to 90.8
Rio Grande	Rio Grande near Lobatos	–18.1 to 9.0	–21.6 to 1.5	–29.3 to 2.0
	Rio Chama near Abiquiu	–0.2 to 37.8	3.2 to 45.8	1.5 to 54.8
	Rio Grande near Otowi	–11.0 to 16.7	–12.7 to 12.4	–14.1 to 15.4
	Rio Grande at Elephant Butte Dam	–8.2 to 16.0	–12.1 to 11.7	–15.4 to 15.0
	Pecos River at Damsite No. 3 near Carlsbad	–9.9 to 10.6	–10.5 to 10.5	–13.0 to 7.5
Sacramento–San Joaquin	Sacramento River at Freeport	–2.3 to 39.4	8.1 to 51.2	9.2 to 53.6
	Sacramento River at Bend Bridge near Red Bluff	–3.5 to 33.4	3.4 to 38.5	9.3 to 51.1
	Feather River at Oroville	4.1 to 43.5	16.8 to 62.1	22.6 to 71.1
	San Joaquin River near Vernalis	1.2 to 56.5	5.5 to 61.3	12.8 to 78.4
	Stanislaus River at New Melones Dam	5.1 to 53.9	15.4 to 66.7	21.8 to 89.4
	Sacramento-San Joaquin Rivers at Delta	–1.5 to 42.8	5.8 to 51.0	6.3 to 56.8
	San Joaquin River at Millerton Lake (Friant Dam)	8.8 to 71.7	25.5 to 94.6	29.6 to 117.9
	American River at Fair Oaks	–0.9 to 38.0	8.4 to 47.6	7.1 to 56.7
	Tulare-Buena Vista Lakes	–0.9 to 61.9	–6.2 to 60.9	–1.0 to 75.3

Basin*	Site Name and Description	Projected Range[1] of Dec–Mar Runoff Change (%)		
		2020s	2050s	2070s
Truckee	Little Truckee River below Boca Dam	42.0 to 186.6	105.8 to 314.8	155.3 to 454.8
	W.F. Carson R. at Woodfords	25.8 to 191.4	133.9 to 400.2	142.2 to 622.6
	Truckee River at Farad Gage (just above CA stateline)	31.3 to 197.2	98.7 to 304.7	127.5 to 414.6
	Truckee River at Nixon Gage	27.3 to 156.6	76.8 to 242.6	111.2 to 316.4
	Carson River at Fort Churchill Gage	15.6 to 94.6	40.5 to 144.8	48.6 to 191.4

* Note – the Pecos, Tulare and Carson are not SWA Basins but are respectively included under the Rio Grande, Sacramento-San Joaquin and Truckee as these locations are of interest from a water operations standpoint.

[1] Ranges of projected December-through-March runoff are the 25th to 75th percentile change of the 97 projections.

Table 7. Projected range of April-through-July runoff change in the 2020s, 2050s, and 2070s relative to the 1990s, for the 43 WWCRA reporting locations

Basin*	Site Name and Description	Projected Range[1] of Apr–Jul Runoff Change (%)		
		2020s	2050s	2070s
Colorado	Colorado River at Lees Ferry	–4.8 to 24.3	–9.2 to 19.3	–10.5 to 23.2
	Colorado River above Imperial Dam	–3.6 to 25.1	–8.4 to 21.2	–10.1 to 25.3
	Green River near Greendale	–6.4 to 30.3	–7.7 to 27.5	–4.0 to 32.4
	Colorado River near Cameo	–1.4 to 22.0	–6.6 to 19.9	–7.5 to 24.4
	Gunnison River near Grand Junction	–6.5 to 25.7	–17.7 to 18.1	–16.1 to 18.6
	San Juan River near Bluff, UT	–8.2 to 20.7	–18.4 to 13.2	–23.6 to 12.5
Columbia	Snake River at Brownlee Dam	–6.4 to 15.9	–9.5 to 14.4	–11.6 to 14.6
	Columbia River at Grand Coulee	–5.0 to 10.8	–8.5 to 11.5	–11.1 to 6.4
	Columbia River at The Dalles	–4.4 to 10.5	–7.6 to 9.9	–10.2 to 5.7

Basin*	Site Name and Description	Projected Range[1] of Apr–Jul Runoff Change (%)		
		2020s	2050s	2070s
	Yakima River at Parker	–15.8 to 0.2	–25.5 to –8.5	–35.1 to –12.8
	Deschutes River near Madras	–10.8 to 3.8	–21.1 to –0.1	–24.0 to –0.6
	Snake River near Heise	–9.6 to 19.1	–10.9 to 15.9	–14.0 to 16.1
	Flathead R. at Columbia Falls	–5.9 to 12.2	–13.2 to 6.3	–18.0 to 4.1
Klamath	Williamson River below the Sprague River	–28.3 to 13.7	–41.0 to 7.3	–43.2 to 3.2
	Klamath River below Iron Gate Dam	–26.4 to 0.6	–43.1 to –4.2	–51.9 to –16.5
	Klamath River near Seiad Valley	–28.7 to –3.7	–42.8 to –7.3	–50.6 to –16.9
	Klamath River at Orleans	–29.0 to –8.0	–46.1 to –13.1	–52.7 to –20.5
	Klamath River near Klamath	–27.5 to –11.2	–47.0 to –17.7	–54.9 to –22.9
Missouri	Missouri River at Canyon Ferry Dam	–4.2 to 17.4	–5.7 to 15.1	–9.3 to 18.6
	Milk River at Nashua	–4.8 to 22.3	–3.7 to 19.8	–6.6 to 24.2
	S. Platte River near Sterling	–1.4 to 26.1	–3.0 to 25.5	–5.0 to 37.7
	Missouri River at Omaha	4.5 to 22.7	8.6 to 32.0	13.1 to 41.7
	Bighorn River at Yellowtail Dam	0.2 to 31.8	9.7 to 36.9	9.8 to 48.6
	North Platte River at Lake McConaughy	–3.3 to 30.1	4.0 to 33.9	9.5 to 46.4
Rio Grande	Rio Grande near Lobatos	–8.5 to 28.4	–15.8 to 14.5	–19.8 to 14.9
	Rio Chama near Abiquiu	–10.8 to 22.3	–24.2 to 17.5	–29.5 to 3.7
	Rio Grande near Otowi	–9.6 to 26.3	–18.8 to 10.8	–22.7 to 11.5
	Rio Grande at Elephant Butte Dam	–9.2 to 25.1	–18.5 to 9.7	–22.2 to 11.2

Basin*	Site Name and Description	Projected Range[1] of Apr–Jul Runoff Change (%)		
		2020s	2050s	2070s
	Pecos River at Damsite No. 3 near Carlsbad	–11.6 to 10.4	–14.7 to 9.4	–17.6 to 3.4
Sacramento–San Joaquin	Sacramento River at Freeport	–28.4 to –5.6	–47.8 to –20.0	–52.2 to –19.9
	Sacramento River at Bend Bridge near Red Bluff	–26.3 to –4.3	–43.1 to –13.8	–48.0 to –16.3
	Feather River at Oroville	–34.6 to –9.1	–56.3 to –28.6	–65.8 to –30.2
	San Joaquin River near Vernalis	–18.6 to 15.8	–32.7 to 3.7	–33.7 to –2.2
	Stanislaus River at New Melones Dam	–23.9 to 3.7	–39.7 to –10.9	–46.7 to –16.5
	Sacramento-San Joaquin Rivers at Delta	–25.0 to –0.1	–40.9 to –14.0	–43.8 to –14.7
	San Joaquin River at Millerton Lake (Friant Dam)	–16.2 to 19.1	–34.5 to 12.3	–32.4 to 4.5
	American River at Fair Oaks	–29.1 to –3.5	–45.4 to –19.2	–53.8 to –20.4
	Tulare-Buena Vista Lakes	–17.8 to 25.7	–34.9 to 18.8	–32.4 to 10.4
Truckee	Little Truckee River below Boca Dam	–21.4 to 9.3	–39.5 to –6.5	–52.0 to –14.4
	W.F. Carson R. at Woodfords	–19.1 to 18.2	–25.3 to 8.9	–32.3 to 3.7
	Truckee River at Farad Gage (just above CA stateline)	–22.5 to 11.1	–39.9 to –6.0	–51.8 to –15.2
	Truckee R. at Nixon Gage	–22.8 to 11.8	–38.1 to –4.6	–49.9 to –13.8
	Carson River at Fort Churchill Gage	–23.4 to 13.3	–33.4 to 1.9	–41.8 to –5.7

* Note – the Pecos, Tulare and Carson are not SWA Basins but are respectively included under the Rio Grande, Sacramento-San Joaquin and Truckee as these locations are of interest from a water operations standpoint.

[1] Ranges of projected April-through-July runoff are the 25th to 75th percentile change of the 97 projections.

4.2. BCSD-CMIP5 Comparisons

The CMIP5 GCM climate simulations have served as the primary scientific basis for the IPCC's Fifth Assessment Report (IPCC 2014). The science and climate impacts assessment communities are evaluating the CMIP5 simulation and are comparing them with results from the CMIP3 archive. Sheffield et al. (2014), for example, developed a comparison of CMIP3/CMIP5 differences for North America. Brekke et al. (2013) summarizes the statistical downscaling steps and efforts towards developing the CMIP5 climate projections archive and also provides a comparison of results from the preceding CMIP3 archive.

The following section provides a comparison of the BCSD-CMIP5 hydroclimate analysis to the BCSD-CMIP3 results from the 2011 WWCRA hydroclimate projections report (Reclamation, 2011b). The WWCRA hydroclimate projections were designed to take advantage of best available datasets and modeling tools, follow methodologies documented in peer-reviewed literature, and update the consistent West-wide data developed for the 2011 SECURE Water Act Report to Congress.

This technical report's assessment updates the 2011 assessment using CMIP5 projections. The 2016 SECURE Water Act Report to Congress assessment was developed using the most current hydrologic projections featured in the IPCC Fifth Assessment and developed as part of the WCRP CMIP Phase 5. A summary of the comparison between BCSD CMIP5 and BCSD CMIP3 is given below.

- Temperature changes from the BCSD-CMIP5 and BCSD-CMIP3 are mostly of comparable magnitude, with a greater range in projected 2070s conditions with BCSD-CMIP5 than BCSD-CMIP3.
- Precipitation changes from the BCSD-CMIP5 indicate a similar pattern and range of precipitation estimated using BCSD-CMIP3. There is a slight shift of increasing precipitation within the Upper Colorado River Basin and Northern California compared to BCSD-CMIP3.
- The decreasing trend in April 1st SWE is somewhat lower for BCSD-CMIP5 in comparison to BCSD-CMIP3, but both analyses project declining snowpack across the western U.S.
- Changes to annual runoff are smaller in case of BCSD-CMIP5 in comparison to BCSD-CMIP3. When projected change is close to 0 percent, there may be a reversal of sign between the median estimates from these two projection sets, but the overall range of conditions is similar.
- Seasonal change in runoff (December through March and April through July) is generally greater in the case of BCSD-CMIP5 over BCSD-CMIP3.

Overall, the difference between BCSD-CMIP5 and BCSD-CMIP3 projections is relatively minor when assessing the range of basin-scale potential future climate and hydrologic conditions.

The BCSD-CMIP5 hydrology shows hydroclimate changes (i.e., temperature, precipitation, and runoff) that are generally similar to BCSD-CMIP3 across the contiguous U.S. However, in the BCSD-CMIP5 hydrology, there are some region-specific differences, including greater warming to the north, regions of more increased precipitation change in the West and Great Plains (although varying by season), and differences in runoff change that more closely follow those found for precipitation than for temperature (Reclamation 2013). A comparison of projected temperature and precipitation for both the BCSD-CMIP3 and BCSD-CMIP 5 projections is provided in Figure 60. The CMIP5 projections indicate a similar pattern for temperature and precipitation with CMIP5 projections indicating greater warming in the north and a slight shift of increasing precipitation into the Upper Colorado River Basin and Northern California.

Comparisons of six hydroclimate indicator variables used to estimate climate change impacts on the eight major Reclamation basins are presented in Table 8, Table 9, and Table 10, respectively for the three futures. The values in these tables correspond to the 25^{th} and 75^{th} percentiles of the hydroclimate indicator variables at the selected locations.

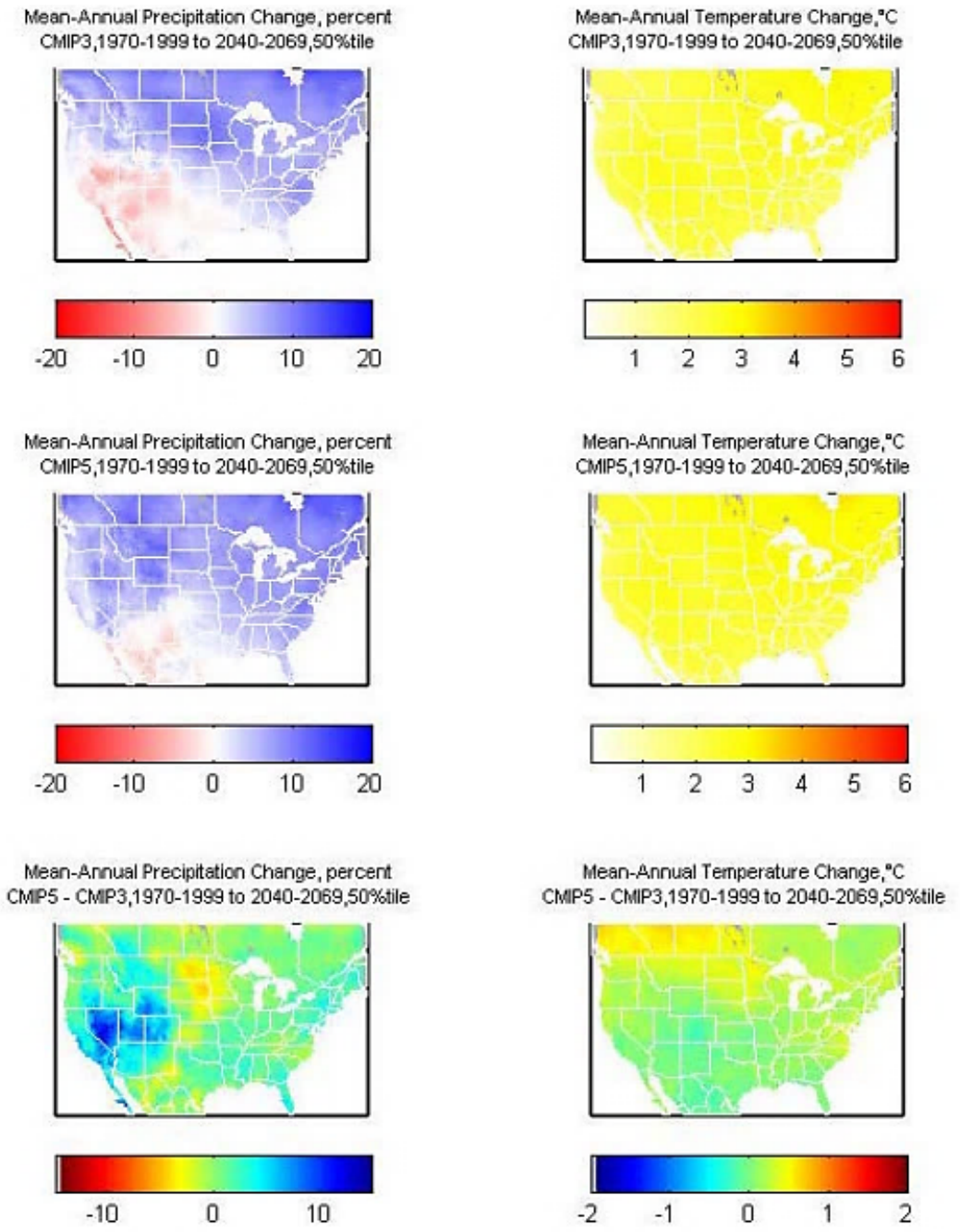

Figure 60. Central tendency changes in mean annual precipitation and temperature over the contiguous U.S. from 1970-1999 to 2040-2069 for BCSD-CMIP3 (top row), BCSD-CMIP5 (middle row), and the difference (bottom row). Source: Reclamation, 2013

Table 8. Comparison of CMIP5 with CMIP3 hydroclimate indicator variables for selected locations in the 2020s

SWA Basin	Location	BCSD	Temperature Change (°F)	Precipitation (%)	Annual Runoff (%)	December-through-March Runoff (%)	April-through-July Runoff (%)
Colorado	Colorado River at Lees Ferry	CMIP5	1.7 to 3.0	-0.4 to 12.5	-6.9 to 18.0	-5.5 to 16.6	-4.8 to 24.3
		CMIP3	1.3 to 2.6	-4.1 to 7.1	-14.5 to 8.6	-9.8 to 12.9	-16.0 to 9.2
	Colorado River at Imperial Dam	CMIP5	1.7 to 2.9	-0.4 to 13.3	-6.6 to 19.5	-7.4 to 17.7	-3.6 to 25.1
		CMIP3	1.3 to 2.4	-3.7 to 7.4	-14.0 to 11.5	-10.7 to 17.1	-14.5 to 12.2
Columbia	Columbia River at The Dalles	CMIP5	1.6 to 2.8	0.2 to 7.8	-2.5 to 8.7	2.0 to 31.1	-4.4 to 10.5
		CMIP3	0.9 to 2.1	-0.7 to 7.2	-3.8 to 8.4	-5.5 to 26.1	-3.3 to 9.5
Klamath	Klamath River near Klamath	CMIP5	1.4 to 2.4	-3.3 to 7.5	-9.8 to 14.7	5.5 to 28.0	-27.5 to -11.2
		CMIP3	0.7 to 1.8	-5.9 to 8.1	-11.8 to 17.0	2.9 to 18.6	-22.3 to 6.7
Missouri	Missouri River at Omaha	CMIP5	1.4 to 3.0	-0.3 to 9.3	2.6 to 18.6	2.2 to 26.5	4.5 to 22.7
		CMIP3	0.9 to 2.2	-2.6 to 8.1	-5.7 to 14.0	-5.2 to 17.9	-2.1 to 18.4
Rio Grande	Rio Grande at Elephant Butte Dam	CMIP5	1.6 to 2.8	-3.2 to 9.4	-7.8 to 17.6	-8.2 to 16.0	-9.2 to 25.1
		CMIP3	1.4 to 2.4	-6.6 to 6.8	-16.6 to 10.2	-11.9 to 10.7	-19.8 to 9.6

SWA Basin	Location	BCSD	Temperature Change (°F)	Precipitation (%)	Annual Runoff (%)	December-through-March Runoff (%)	April-through-July Runoff (%)
Sacramento-San Joaquin	Sacramento-San Joaquin Rivers at the Delta	CMIP5	1.6 to 2.4	-3.0 to 13.1	-8.2 to 24.8	-1.5 to 42.8	-25.0 to -0.1
		CMIP3	0.8 to 2.0	-6.8 to 11.3	-12.9 to 22.9	-8.8 to 32.0	-22.1 to 9.8
Truckee-Carson	Truckee River at Nixon Gage	CMIP5	1.7 to 2.6	-5.7 to 12.6	-8.1 to 28.7	27.3 to 156.6	-22.8 to 11.8
		CMIP3	0.8 to 2.2	-8.7 to 11.7	-16.4 to 26.3	2.5 to 82.9	-29.4 to 12.5

Table 9. Comparison of CMIP5 with CMIP3 hydroclimate indicator variables for selected locations in the 2050s

SWA Basin	Location	BCSD	Temperature Change (°F)	Precipitation (%)	Annual Runoff (%)	December-through-March Runoff (%)	April-through-July Runoff (%)
Colorado	Colorado River at Lees Ferry	CMIP5	3.0 to 5.5	–0.5 to 12.7	–11.3 to 14.1	–3.7 to 22.3	–9.2 to 19.3
		CMIP3	3.0 to 4.9	–6.1 to 8.1	–18.8 to 6.3	–10.0 to 13.5	–19.6 to 8.1
	Colorado River at Imperial Dam	CMIP5	3.0 to 5.3	–1.6 to 12.4	–11.0 to 15.9	–6.3 to 22.9	–8.4 to 21.2
		CMIP3	2.9 to 4.8	–7.4 to 7.3	–19.6 to 6.9	–12.5 to 11.5	–18.3 to 8.5
Columbia	Columbia River at The Dalles	CMIP5	3.0 to 5.2	2.6 to 12.5	–5.2 to 11.4	10.3 to 43.4	–7.6 to 9.9
		CMIP3	2.5 to 4.1	0.4 to 11.3	–3.2 to 13.3	–5.6 to 37.9	–6.3 to 12.6
Klamath	Klamath River near Klamath	CMIP5	2.6 to 4.4	–4.1 to 10.5	–9.5 to 12.5	21.7 to 45.4	–47.0 to –17.7
		CMIP3	2.3 to 3.6	–7.9 to 11.8	–16.4 to 23.0	8.1 to 29.9	–33.9 to –7.5
Missouri	Missouri River at Omaha	CMIP5	3.2 to 5.5	1.9 to 12.0	6.5 to 25.1	15.6 to 44.6	8.6 to 32.0
		CMIP3	2.6 to 4.3	0.2 to 12.7	–1.5 to 21.3	1.9 to 28.4	1.0 to 27.8
Rio Grande	Rio Grande at Elephant Butte Dam	CMIP5	3.1 to 5.0	–3.4 to 9.9	–16.2 to 7.3	–12.1 to 11.7	–18.5 to 9.7
		CMIP3	3.1 to 4.7	–8.5 to 4.7	–23.6 to –1.3	–19.4 to 0.9	–28.2 to 0.2

SWA Basin	Location	BCSD	Temperature Change (°F)	Precipitation (%)	Annual Runoff (%)	December-through-March Runoff (%)	April-through-July Runoff (%)
Sacramento-San Joaquin	Sacramento-San Joaquin Rivers at the Delta	CMIP5	2.6 to 4.5	–4.6 to 14.0	–11.0 to 26.1	5.8 to 51.0	–40.9 to –14.0
		CMIP3	2.3 to 3.9	–10.4 to 10.1	–18.9 to 18.5	–8.9 to 32.9	–37.1 to –2.6
Truckee-Carson	Truckee River at Nixon Gage	CMIP5	3.0 to 4.9	–3.8 to 14.9	–13.1 to 22.1	76.8 to 242.6	–38.1 to –4.6
		CMIP3	2.5 to 4.3	–10.9 to 12.1	–19.9 to 27.3	34.2 to 120.7	–43.9 to –2.0

Table 10. Comparison of CMIP5 with CMIP3 hydroclimate indicator variables for selected locations in the 2070s

SWA Basin	Location	BCSD	Temperature Change (°F)	Precipitation (%)	Annual Runoff (%)	December-through-March Runoff (%)	April-through-July Runoff (%)
Colorado	Colorado River at Lees Ferry	CMIP5	3.6 to 7.1	1.2 to 16.3	–12.2 to 19.0	1.7 to 28.2	–10.5 to 23.2
		CMIP3	4.2 to 6.7	–5.1 to 7.1	–20.2 to 5.2	–5.9 to 14.4	–23.4 to 7.8
	Colorado River at Imperial Dam	CMIP5	3.6 to 6.9	1.1 to 15.0	–12.6 to 18.7	–0.8 to 25.0	–10.1 to 25.3
		CMIP3	4.2 to 6.5	–7.8 to 7.6	–20.3 to 6.0	–7.6 to 13.8	–22.0 to 9.5
Columbia	Columbia River at The Dalles	CMIP5	3.5 to 7.0	4.3 to 13.9	–2.2 to 11.0	16.0 to 54.4	–10.2 to 5.7
		CMIP3	3.4 to 5.9	3.1 to 13.1	–1.5 to 14.4	–1.7 to 43.4	–4.8 to 15.5
Klamath	Klamath River near Klamath	CMIP5	3.2 to 6.0	–2.5 to 13.4	–8.5 to 18.2	23.6 to 68.8	–54.9 to –22.9
		CMIP3	3.2 to 5.2	–9.2 to 12.0	–16.8 to 22.6	20.0 to 46.1	–46.2 to –20.6
Missouri	Missouri River at Omaha	CMIP5	3.7 to 6.9	3.6 to 15.3	7.0 to 34.5	13.8 to 59.0	13.1 to 41.7
		CMIP3	3.7 to 5.9	2.1 to 14.6	0.1 to 24.8	6.6 to 39.7	3.3 to 31.5
Rio Grande	Rio Grande at Elephant Butte Dam	CMIP5	3.3 to 6.6	–4.5 to 9.0	–20.5 to 8.9	–15.4 to 15.0	–22.2 to 11.2
		CMIP3	4.1 to 6.4	–9.5 to 4.6	–29.9 to –5.6	–21.4 to –1.3	–36.7 to –5.5

SWA Basin	Location	BCSD	Temperature Change (°F)	Precipitation (%)	Annual Runoff (%)	December-through-March Runoff (%)	April-through-July Runoff (%)
Sacramento-San Joaquin	Sacramento-San Joaquin Rivers at the Delta	CMIP5	3.3 to 5.9	–4.7 to 16.4	–12.0 to 24.6	6.3 to 56.8	–43.8 to –14.7
		CMIP3	3.3 to 5.5	–11.0 to 12.7	–19.2 to 21.2	–12.0 to 38.0	–42.4 to –16.7
Truckee-Carson	Truckee River at Nixon Gage	CMIP5	3.5 to 6.5	–5.4 to 16.7	–13.0 to 24.2	111.2 to 316.4	–49.9 to –13.8
		CMIP3	3.5 to 5.8	–11.9 to 12.8	–21.2 to 24.2	36.6 to 148.7	–55.2 to –20.4

4.3. Data Visualization

Reclamation's Climate Change Adaptation Strategy acknowledges that Reclamation and its stakeholders will benefit from increased access to climate change and water resources data. Through the WaterSMART Basin Study Program, a data visualization site has been produced to accompany the release of this 2016 SECURE Water Act Report to Congress.[10] This tool allows users to walk through the SECURE Water Act Report and view changes in temperature, precipitation, and snowpack in major river basins and download supporting projection data sets. Screenshots from the data visualization tool are provided in Figure 61.

Fundamental to developing new information for adapting to climate change is assessing the current state of knowledge, identifying where gaps exist, and finding opportunities to address those gaps. Access to quality data on past and projected future hydrology, water use, land cover, and climate is essential if meaningful adaptation strategies are to be effectively evaluated and implemented. A key component of this report and the 2016 SECURE Water Act Report to Congress is creating open sets, such as those presented in this analysis.

[10] SECURE Water Act Report website: http://www.usbr.gov/climate/SECURE

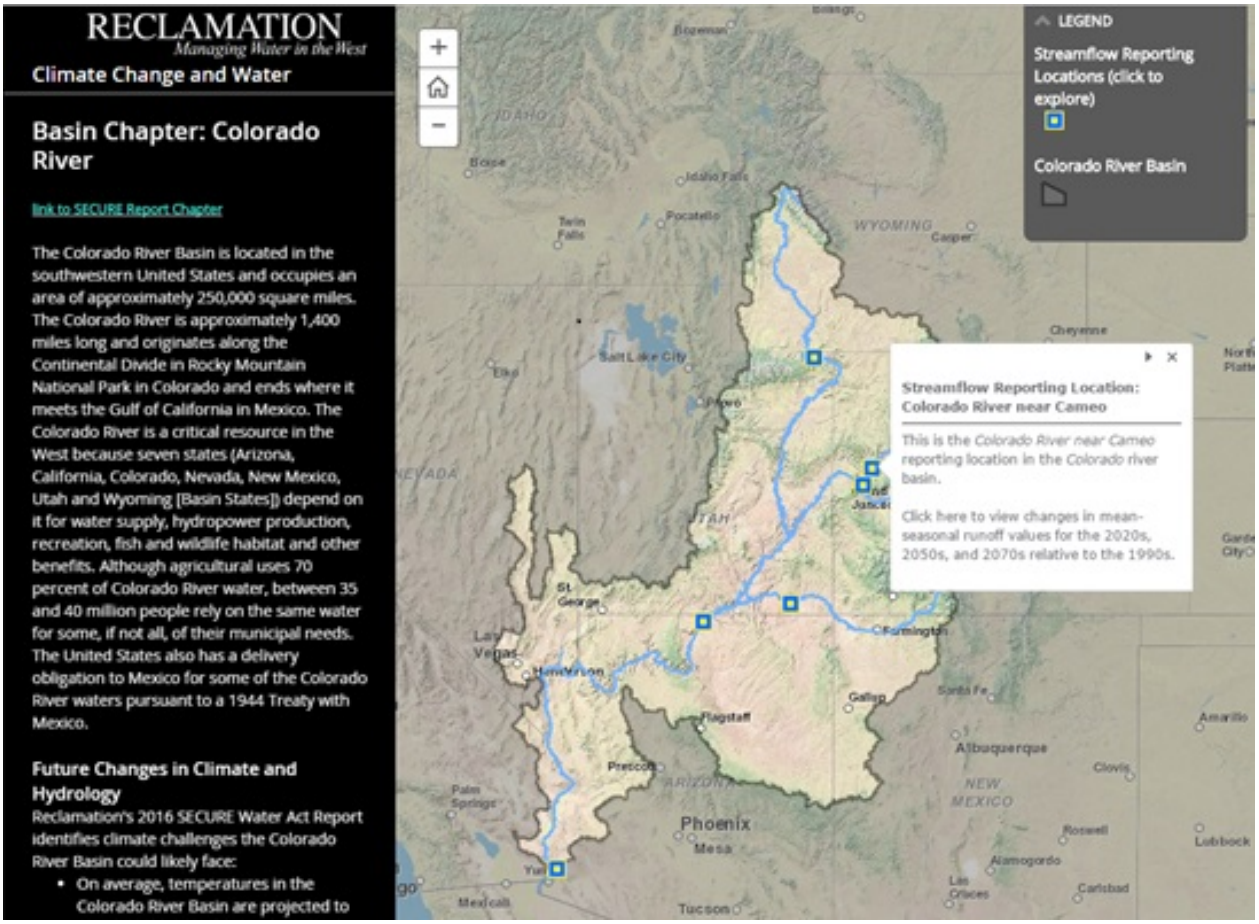

River basin information, routed streamflow locations, and links to download datasets

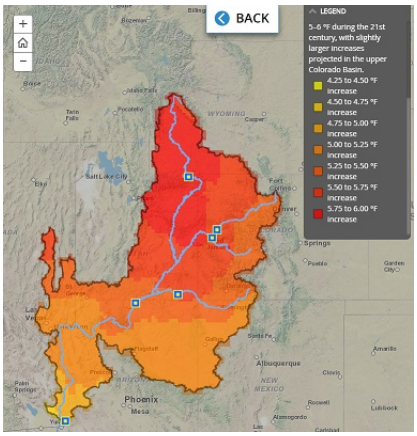

Projected Temperature

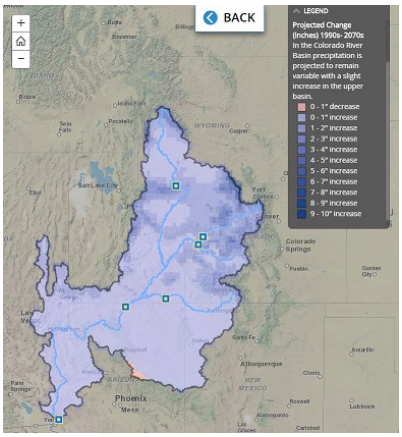

Projected Precipitation

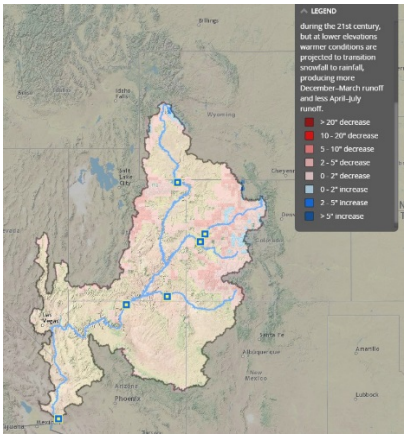

Projected April 1st SWE

Figure 61. SECURE Water Act Report data visualization and data access tool – Example projections for the Colorado River Basin

5. Uncertainties

This section of the report is included to provide perspective on potential sources of uncertainty in the report's hydrologic projection findings. The methods used in this report, which have been established through ongoing research spanning several decades, have provided many robust insights into hydroclimatic variability in the recent past and changes projected for the near future. A notable example is the simulation and diagnosis of the shift in precipitation regimes from snow to rainfall, with consequences for snowpack and associated water resources. Yet, the scientific and engineering knowledge base contributing to impact assessment methods is steadily evolving, and new research offers insights into the potential uncertainties of the methods used in this report, which should be considered as the findings are interpreted.

Uncertainties arise from [Clark et al. 2016a]:

- Choices in global climate forcing (e.g., emissions scenarios of GHGs)
- The choice of models used for global climate simulation
- Chaotic internal variability in the climate system
- The development of climate projection information at scales finer than the global climate model simulation scales (i.e., climate downscaling)
- The choice, configuration, and calibration of hydrologic models

The uncertainties from all these sources aggregate to the overall uncertainty in characterizing climate impacts. Subsequently, developing hydrologic projections from these climate projections through use of hydrologic models broadens the range of uncertainty. In the center part of Figure 62, we present the steps in developing the hydrologic projections, starting with global climate modeling, moving through climate downscaling, and finally applying hydrologic modeling. The conceptual range and distribution of considerations under each of these steps are depicted as probability density functions (PDFs) on the left and right sides of Figure 62.

The approach used to characterize uncertainty in this report and in the Reclamation (2011) study follows the process steps outlined in the left-hand column of Figure 62. Details on emissions scenarios, climate model simulations, the downscaling method, and hydrologic modeling were presented in Chapter 2 of this report. This approach to characterizing uncertainty does not fully reveal the uncertainty of the resulting projections. The right-hand column of Figure 62 provides a conceptual framework to fully characterize their uncertainties, illustrating an approach that would ideally be considered when generating information for water resources planning and management. However, some

elements of this approach remain an active area of research in which work is needed to understand how best to characterize these individual uncertainties and addressing them in a pragmatic manner.

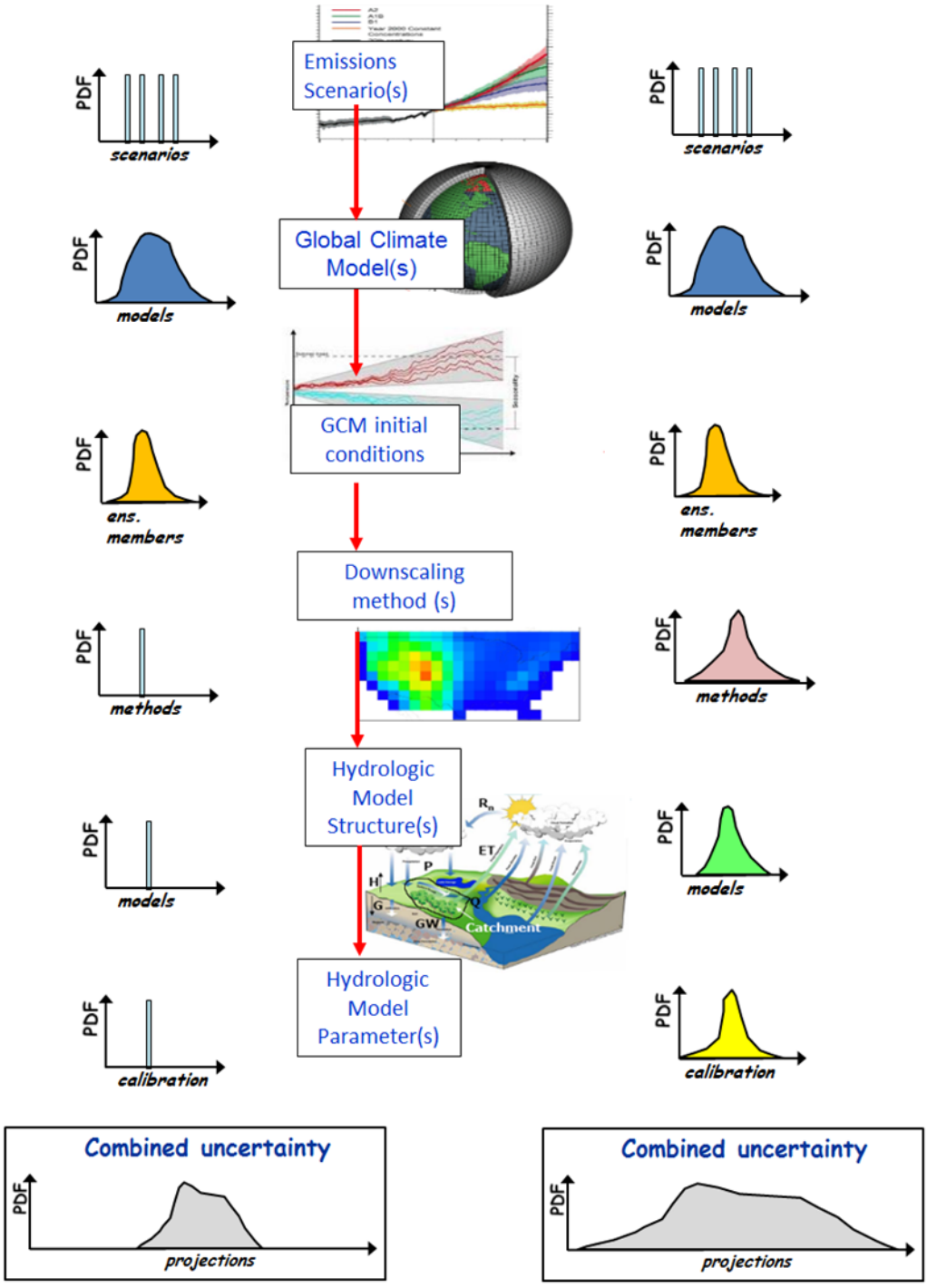

Figure 62. Characterizing uncertainty (PDF = probability density function); figure is modified from Clark et al. (2016a)

The next section provides an update on the three broad areas of science presented at the start of the chapter, namely (1) global climate modeling, (2) climate downscaling, and (3) hydrologic modeling with reference to ongoing research to fully reveal uncertainty.

5.1. Revealing Uncertainties

In recent years, the science community has substantially advanced a number of capabilities that characterize the range of possible futures for climate and hydrology. Some key developments have come in the areas of global climate modeling, climate downscaling, and hydrologic modeling.

5.1.1. Global Climate Modeling

A key source of uncertainty in climate impact assessments lies in the structure of global climate models. The climate research community continues to build models with more detailed representations of earth system processes; modern Earth System Models both have more spatial detail and explicitly resolve many more physical processes than their predecessors (Hurrell et al. 2013; Wehner et al. 2014; Clark et al. 2015a). Such advances in Earth System Modeling have increased the accuracy of climate model simulations (Knutti et al. 2013), yet the large number of differences among models still provide a wide range of possible climate futures (Bishop and Abramowitz 2013; Knutti et al. 2013; Knutti and Sedlácek 2013). Such diversity in climate models offer an information resource that can be used to define alternative climate change narratives for the water resources sector (Brekke et al. 2009). However, this resource has been termed an ensemble of opportunity, indicating that these narratives rely on an ad-hoc collection of models that are not deliberately designed to comprehensively characterize the myriad of uncertainties in climate modeling (Murphy et al. 2004; Stainforth et al. 2005; Knutti et al. 2010).

Another source of uncertainty stems from internal climate variability. It has long been recognized that the climate system evolves in a chaotic way (Lorenz 1963), meaning that small perturbations in atmospheric initial conditions cause large differences in the trajectory of future climate simulations (Deser et al. 2012a; Deser et al. 2012b). The differences among different initializations of the same model can be attributed to internal climate variability, as distinct from any model error (Tebaldi et al. 2011). In most climate impact assessments, internal climate variability is represented using the ensemble of opportunity described above. For example, the first ensemble member in this report was selected from each of the global climate models. In an effort to explore and understand the consequences of relying on such ensembles, some modeling groups are now working to characterize internal variability with much larger ensembles (Kay et al. 2014). This thrust may ultimately provide a path to explicitly characterize the

uncertainties associated with internal climate variability in subsequent climate impact assessments.

5.1.2. Climate Downscaling

Another major source of uncertainty stems from the methods used to derive hydrologically relevant forcing data from the course resolution climate model output. These methods, termed climate downscaling, can take a variety of forms. The methods traditionally used by the water resources sector in the United States, as in this report, have involved rescaling the precipitation and temperature outputs from the climate model using a statistical model (Wood et al. 2004; Hidalgo et al. 2008; Stoner et al. 2013). Such methods vary in the degree to which they preserve the change signal produced by the climate model itself (Pierce et al. 2015), which some users view as a requirement. Also, they often have weaknesses in their representation of hydrologically important meteorological features, such as the time-space scaling of storm characteristics (Maraun 2013; Gutmann et al. 2014).

A large variety of downscaling methods exist, including (1) statistical methods that make use of the climate model circulation patterns (Fowler et al. 2007; Wilby et al. 2014) or incorporate physically based dynamical considerations (Jarosch et al. 2012); (2) dynamical downscaling approaches (Giorgi 1990; Rasmussen et al. 2014), and most recently, (3) intermediate complexity dynamical methods (Gutmann et al. 2016). Such methods will produce a variety of downscaled climate projections that may vary, even in the sign of their climate change signal. Indeed, some methods even explicitly include a stochastically generated ensemble in an attempt to explicitly capture some of this uncertainty (Gangopadhyay et al. 2005; Langousis and Kaleris 2014). Even within the sophisticated dynamical downscaling approaches, different regional climate models provide different results when forced by the same parent global climate model (Takle et al. 1999; Christensen and Christensen 2007; Mearns et al. 2013). This is particularly problematic because often there are only sufficient resources to run a single regional climate model (Hay et al. 2002; Hay et al. 2006; Rasmussen et al. 2011), and for a limited time period relative to those that can be analyzed via statistical approaches. Furthermore, within a single regional climate model, substantial uncertainties may exist due to uncertainties in physical schemes, as investigated using the perturbed physics ensemble (PPE) approach (Yang and Arritt 2002; Murphy et al. 2007). With the advent of regional climate models of intermediate complexity, such an approach is now becoming computationally tractable for impact studies (Gutmann et al. 2016).

5.1.3. Hydrologic Modeling

An important result in research on the hydrologic impacts of climate change is that the portrayal of climate change impacts depends on the decisions made on the selection, configuration, and calibration of hydrologic models (Wilby 2005;

Miller et al. 2012; Vano et al. 2014; Mendoza et al. 2015). In one of the earliest studies, Wilby (2005) demonstrated that parameter uncertainties have a large impact on the portrayal of climate change impacts. Subsequent work has demonstrated that the portrayal of climate change impacts also depends on the choice of hydrologic models and on specific decisions made in model calibration (Miller et al. 2012; Vano et al. 2014; Mendoza et al., 2015). For a variety of reasons, hydrologic model calibration often receives inadequate attention in climate change impact assessments, with potential first-order effects on the estimation of future hydrologic responses.

The uncertainties in hydrologic modeling stem from both algorithmic simplifications of hydrologic theory and data limitations (Clark et al. 2016b). Considerations of parsimony may compel modelers to neglect specific processes (e.g., groundwater-surface water interactions, carbon fertilization). Moreover, data limitations constrain the extent that it is possible to adequately capture the details of the landscape, and especially, define appropriate model parameter values. Specifically, inter-model differences occur because different modelers have made model development decisions in different ways, as manifested in different spatial discretizations, process parameterizations, model parameter values, and time-stepping schemes (Clark et al. 2011). It is now possible to use multiple hypothesis-modeling frameworks to deliberately and systematically characterize uncertainties in physically motivated hydrologic models (Clark et al. 2015b; Clark et al. 2015c), and such work will be important to improve the realism of the portrayal of climate risk.

The problem confronting practitioners and decision-makers, and what is presented as the conceptual framework in the right-hand column of Figure 62, is that the projection uncertainty space (i.e., the combined uncertainty arising from uncertainties present at each step in the analysis) has expanded as research reveals a fuller range of uncertainties associated with the identified modeling steps. It is important to acknowledge that our current analytical approach provides only a limited view of the uncertainty space. For example, the trend toward using multiple hydrologic models rather than a single model (the standard approach for many prior studies, as well as this one) has confirmed that a single hydrologic model selection erroneously narrows the final projection uncertainty space by failing to represent the hydrologic sensitivities that would be estimated through different modeling choices. As the impact assessment community continues to formulate strategies toward reducing projection uncertainty, it is nonetheless critical now to gain a better understanding the full extent and sources of uncertainty, which likely are more significant than the present approach assumes.

This section has presented research highlights towards that goal. In the following section, we highlight research focused on reducing uncertainty.

5.2. Uncertainty Reduction

Uncertainty reduction is not always possible. For example, uncertainties due to climate system feedbacks and internal climate system variability (Deser et al. 2012a; 2012b; Knutti and Sedlácek 2013) likely include both those that cannot be represented due to technological limitations and others that arise from long-standing unknowns related to climate system behavior. Nevertheless, some practical approaches are being tried to reduce uncertainties in climate impact assessments. They are presented here in the same three areas of investigation used in the previous section.

5.2.1. Global Climate Modeling

Global climate modeling is inherently uncertain, due to climate system feedbacks and the chaotic evolution of system states. As such, inter-model differences are expected (Hawkins and Sutton 2009), and multi-model estimates of uncertainty are a critical component of many climate impact assessments (Brekke et al. 2009). Reducing uncertainty is possible by accepting that not all models are created equal and carefully rejecting or down-weighting models that have an inadequate representation of earth system processes or an inadequate representation of climate system dynamics (Knutti 2010). The selection and/or weighting of climate models is a challenging problem (Knutti 2010; Knutti et al. 2010). The research community is currently actively engaged in developing methods for meaningful multi-model combinations (Mote et al. 2011; Bishop and Abramowitz 2013; Evans et al. 2013), but this effort is a complicated and application-specific challenge because some models have more relevance and skill for some types of assessment questions.

5.2.2. Climate Downscaling

Likewise, reducing uncertainty in the downscaling process will be difficult, but progress can be made through improvements in computational power, systematic evaluation of existing downscaling methods, and the removal of poorly performing methods. For example, for an application that depends on the proper representation of precipitation in the mountains, it may be reasonable to remove methods that rely on climate model precipitation if that climate model does not have a representation of those mountains due to its coarse spatial resolution. If, in this case, multiple downscaling methods that provide a better representation of orographic effects all provide a similar answer, the resulting uncertainty can reasonably be reduced. Depending on the application, it is also possible to select methods for their ability to produce either unbiased information (Teutschbein and Seibert 2012), or a proper representation of extreme events or spatial scaling characteristics (Gutmann et al 2014). Improvements in computational capacity also have the potential to reduce uncertainties in regional climate modeling as these improvements lead to the ability to run models as convection permitting

scales (Kendon et al. 2014; Rasmussen et al. 2014). At these scales, it is possible to explicitly resolve convection, thus removing one source of uncertainty. Finally, one of the most important pieces to evaluate for any climate change assessment is the ability of the methods to represent the important changes.

5.2.3. Hydrologic Modeling

The opportunities to reduce uncertainty in hydrologic modeling relate to the selection, configuration, and calibration of hydrologic models. Reducing uncertainties associated with model selection requires that models appropriately represent dominant processes, because neglecting processes (e.g., groundwater-surface water interactions, or carbon fertilization) or over-simplifying the process representations (e.g., temperature index snow models, or temperature-based representations of potential evapotranspiration) can lead to biased portrayals of climate change impacts (Milly and Dunne 2011; Lofgren et al. 2013). For example, Sheffield et al. (2012) recently demonstrated that trends in global drought are exaggerated when using temperature-based representations of potential evapotranspiration. Efforts to reduce uncertainties through increases in model complexity may in fact increase inter-model differences. Such changes in the portrayal of uncertainty should not be viewed as an increase in uncertainty; rather, increases in inter-model differences simply reveal the uncertainties that have always been present.

The most accessible opportunity to reduce uncertainties is through the judicious selection of model parameter values (i.e., parameter values that are either specified a priori or inferred through model calibration). There are two challenges associated with this task, other than the investment of time and effort. The first issue is the realism of calibrated models for individual basins. Mendoza et al. (2016) demonstrated that even though model calibration may improve targeted aspects of a hydrologic simulation, decisions made during model calibration can nonetheless lead to appreciable differences in the portrayal of climate change impacts. These problems stem from parameter interactions and compensatory errors associated with traditional calibration objectives (e.g., a singular focus on daily streamflow errors), suggesting that more work should be focused on diagnostic, multivariate, and multi-objective approaches to parameter estimation so that models get the right answers for the right reasons (Gupta et al. 2008). The second issue is the difficulty in defining spatially consistent model parameters over large geographical domains (Archfield et al. 2016), in the face of a sparse hydrologic observations. In many continental domain applications, estimates of model parameters can be highly uncertain (Mizukami et al. 2015), where parameters are typically specified a priori to default values, or parameter maps are patched together from independent, uncoordinated calibration efforts. Such continental-domain parameter estimates can be improved substantially through the application of scale-aware parameter regionalization methodologies

(Samaniego et al. 2010). Attention to both individual basin calibration and large-domain parameter estimation can reduce uncertainties associated with inadequate representation of hydrologic processes.

5.3. Summary

Any climate change impacts assessment for the water sector must encompass the full suite of uncertainties associated with global climate modeling, climate downscaling, and hydrologic modeling (Wilby and Harris 2006; Davie et al. 2013; Addor et al. 2014; Schewe et al. 2014; Vano et al. 2014; Mendoza et al. 2015). However, the present analytical approach provides only a limited representation of the uncertainty space in particular, neglecting uncertainties in climate downscaling and hydrologic modeling. It is important to acknowledge this limitation in the current analysis and to make an initial effort to fully characterize and reveal that uncertainty space. We have summarized here ongoing research under a conceptual framework that would enable modelers to reach this goal (refer to right-hand column in Figure 62). Ongoing research should keep in perspective the computational requirements for such a framework, and the need for guidance to make specific methodological choices such that users are able to understand and communicate the implications of those choices for their respective applications.

We have also presented highlights from ongoing research that can help to reduce some of the uncertainties associated with global climate modeling, climate downscaling, and hydrologic modeling. Further progress toward this goal could be made by incorporating many of the findings from this research into applications to objectively meet climate impacts assessment needs.

The work presented in this report builds from community methods established during the prior decade for assessing potential climate change impacts on hydrology. Although these methods were widely accepted as a reasonable strategy toward this objective, the last decade of experience with such studies has also led to new possibilities and choices to each element in the assessment approach, coupled with a growing awareness that many of these choices would affect the assessment findings. Where once the field assessed changes based on a single GCM (e.g., Wood et al, 2004, and associated western US assessments such as Christensen et al, 2004), the recognition of uncertainty in the GCM choice has standardized the use of more than a dozen GCMs today.

Similarly, the approach taken in this study relies on a single downscaling method and a single hydrology model in which much of the domain is simulated using a priori parameter sets. Yet, the ongoing research described in this section makes clear that these choices narrow the depiction of uncertainties that would be manifested using multiple hydrology models, multiple downscaling methods, and improved model parameters. The field is currently progressing toward this new,

expanded uncertainty paradigm, just as it did in the past for the GCM element. At the time of this report, however, work is still underway to identify and/or develop pragmatic and scientifically sound strategies for doing so. The reader is thus encouraged to consider the findings of this report while bearing in mind that the projection uncertainties summarized herein are likely underestimated, for all of the reasons described earlier in this section.

This page intentionally left blank.

6. References

Addor, N., O. Rössler, N. Köplin, M. Huss, R. Weingartner, and J. Seibert, 2014: Robust changes and sources of uncertainty in the projected hydrological regimes of Swiss catchments. *Water Resources Research*, 50, 7541-7562.

Archfield, S. A., M. P. Clark, B. Arheimer, L. E. Hay, H. McMillan, J. E. Kiang, J. Seibert, K. Hakala, A. Bock, T. Wagener, W. H. Farmer, V. Andreassian, S. Attinger, A. Viglione, R. Knight, S. Markstrom, and T. Over, 2016: Accelerating advances in continental domain hydrologic modeling. Water Resources Research, doi: 10.1002/2015WR017498.

Bishop, C. H., and G. Abramowitz, 2013: Climate model dependence and the replicate Earth paradigm. *Climate Dynamics*, 41, 885-900

Brekke, L. D., E. P. Maurer, J. D. Anderson, M. D. Dettinger, E. S. Townsley, A. Harrison, and T. Pruitt, 2009: Assessing reservoir operations risk under climate change. *Water Resources Research*, 45, W04411, doi:10.1029/2008WR006941.

Brekke, L., B. L. Thrasher, E. P. Maurer, and T. Pruitt, 2013: Downscaled CMIP3 and CMIP5 climate projections: Release of downscaled CMIP5 climate projections, comparison with preceding information, and summary of user needs. Denver, CO: Bureau of Reclamation, *Technical Service Center*, 116 p. <http://gdo-dcp.ucllnl.org/downscaled_cmip_projections/techmemo/downscaled_climate.pdf>

Christensen, J. H., and O. B. Christensen, 2007: A summary of the PRUDENCE model projections of changes in European climate by the end of this century. Climatic change, 81, 7-30

Christensen, N. S., A. W. Wood, N. Voisin, D. P. Lettenmaier, and R. N. Palmer, 2004: The effects of climate change on the hydrology and water resources of the Colorado River basin. *Climatic Change*, 62, 337-363.

Clark, M. P., D. Kavetski, and F. Fenicia, 2011: Pursuing the method of multiple working hypotheses for hydrological modeling. Water Resources Research, 47, doi: 10.1029/2010WR009827.

Clark, M. P., Y. Fan, D. L. Lawrence, J. C. Adam, D. Bolster, D. Gochis, R. L. Hooper, M. Kumar, L. R. Leung, D. S. Mackay, R. M. Maxwell, C. Shen, S. C. Swenson, and X. Zeng, 2015a: Improving the representation of hydrologic processes in Earth System Models. Water Resources Research, doi: 10.1002/2015WR017096.

Clark, M. P., B. Nijssen, J. Lundquist, D. Kavetski, D. Rupp, R. Woods, E. Gutmann, A. Wood, L. Brekke, J. Arnold, D. Gochis, and R. Rasmussen,

2015b: A unified approach to process-based hydrologic modeling. Part 1: Modeling concept. Water Resources Research, 51, doi: 10.1002/2015WR017198.

Clark, M. P., B. Nijssen, J. Lundquist, D. Kavetski, D. Rupp, R. Woods, E. Gutmann, A. Wood, D. Gochis, R. Rasmussen, D. Tarboton, V. Mahat, G. Flerchinger, and D. Marks, 2015c: A unified approach for process-based hydrologic modeling: Part 2. Model implementation and example applications. Water Resources Research, 51, doi: 10.1002/2015WR017200.

Clark, M. P., R. L. Wilby, E. Gutmann, J. A. Vano, S. Gangopadhyay, A. Wood, H. Fowler, C. Prudhomme, J. Arnold, and L. Brekke, 2016a: Characterizing uncertainty of the hydrologic impacts of climate change. Climate Change Reports, (in press)

Clark, M. P., B. Schaefli, S. J. Schymanski, L. Samaniego, C. H. Luce, B. M. Jackson, J. E. Freer, J. R. Arnold, R. Dan Moore, E. Istanbulluoglu, and S. Ceola, 2016b: Improving the theoretical underpinnings of process-based hydrologic models. Water Resources Research, doi: 10.1002/2015WR017910.

Cleveland, W. S. (1981) LOWESS: A program for smoothing scatterplots by robust locally weighted regression. *The American Statistician* 35, 54.

Davie, J., P. Falloon, R. Kahana, R. Dankers, R. Betts, F. Portmann, D. Wisser, D. Clark, A. Ito, and Y. Masaki, 2013: Comparing projections of future changes in runoff from hydrological and biome models in ISI-MIP. *Earth System Dynamics*, 4, 359-374.

Deser, C., R. Knutti, S. Solomon, and A. S. Phillips, 2012a: Communication of the role of natural variability in future North American climate. Nature Climate Change, 2, 775-779.

Deser, C., A. Phillips, V. Bourdette, and H. Teng, 2012b: Uncertainty in climate change projections: the role of internal variability. Climate Dynamics, 38, 527-546

Evans, J. P., F. Ji, G. Abramowitz, and M. Ekström, 2013: Optimally choosing small ensemble members to produce robust climate simulations. *Environmental Research Letters*, 8, 044050.

Fowler, H., S. Blenkinsop, and C. Tebaldi, 2007: Linking climate change modelling to impacts studies: recent advances in downscaling techniques for hydrological modelling. International Journal of Climatology, 27, 1547-1578

Gangopadhyay, S., M. Clark, and B. Rajagopalan, 2005: Statistical downscaling using K-nearest neighbors. Water Resources Research, 41

Giorgi, F., 1990: Simulation of regional climate using a limited area model nested in a general circulation model. Journal of Climate, 3, 941-963

Georgakakos, A., P. Fleming, M. Dettinger, C. Peters-Lidard, T. C. Richmond, K. Reckhow, K. White, and D. Yates, 2014. Climate change impacts in the United States: the third National Climate Assessment. Water Resources. Pages 69–112 in J. M. Melillo, T. C. Richmond, and G. W. Yohe, editors. U.S. Global Change Research Program, Washington, D.C., USA.

Gupta, H. V., T. Wagener, and Y. Q. Liu, 2008: Reconciling theory with observations: elements of a diagnostic approach to model evaluation. Hydrological Processes, 22, 3802-3813, doi: 10.1002/hyp.6989.

Gutmann, E., T. Pruitt, M. P. Clark, L. Brekke, J. Arnold, D. Raff, and R. Rasmussen, 2014: An intercomparison of statistical downscaling methods used for water resource assessments in the United States. Water Resources Research, doi: 10.1002/2014WR015559.

Gutmann, E., I. Barstad, M. P. Clark, J. R. Arnold, and R. M. Rasmussen, 2016: The Intermediate Complexity Atmospheric Research Model. Journal of Hydrometeorology (in press)

Hawkins, E., and R. Sutton, 2009: The potential to narrow uncertainty in regional climate predictions. *Bulletin of the American Meteorological Society*, 90, 1095-1107

Hay, L. E., M. P. Clark, R. L. Wilby, W. J. Gutowski, G. H. Leavesley, Z. Pan, R. W. Arritt, and E. S. Takle, 2002: Use of regional climate model output for hydrologic simulations. Journal of Hydrometeorology, 3, 571-590, doi: 10.1175/1525-7541(2002)003<0571:uorcmo>2.0.co;2.

Hay, L. E., M. P. Clark, M. Pagowski, G. H. Leavesley, and W. J. Gutowski, 2006: One-way coupling of an atmospheric and a hydrologic model in Colorado. Journal of Hydrometeorology, 7, 569-589, doi: 10.1175/jhm512.1.

Hidalgo, H. G., M. D. Dettinger, and D. R. Cayan, 2008: Downscaling with constructed analogues: Daily precipitation and temperature fields over the United States. California Energy Commission PIER Final Project Report CEC-500-2007-123

Hurrell, J. W., M. Holland, P. Gent, S. Ghan, J. E. Kay, P. Kushner, J.-F. Lamarque, W. Large, D. Lawrence, and K. Lindsay, 2013: The community earth system model: a framework for collaborative research. Bulletin of the American Meteorological Society, 94, 1339-1360

Jarosch, A. H., F. S. Anslow, and G. K. Clarke, 2012: High-resolution precipitation and temperature downscaling for glacier models. Climate Dynamics, 38, 391-409

IPCC (Intergovernmental Panel on Climate Change), 2001: Climate Change 2001 — IPCC Third Assessment Report. Geneva. 4 volumes. <http://www.grida.no/publications/other/ipcc_tar/>

_____ 2007: Climate Change 2007 — IPCC Fourth Assessment Report. Geneva. 4 volumes. <http://www.ipcc.ch/report/ar4/>

_____ 2014: Climate Change 2014 — IPCC Fifth Assessment Report. IPCC, Geneva. 4 volumes. <http://www.ipcc.ch/report/ar5/>

Kay, J., C. Deser, A. Phillips, A. Mai, C. Hannay, G. Strand, J. Arblaster, S. Bates, G. Danabasoglu, and J. Edwards, 2014: The Community Earth System Model (CESM) large ensemble project: A community resource for studying climate change in the presence of internal climate variability. Bulletin of the American Meteorological Society

Kendon, E. J., N. M. Roberts, H. J. Fowler, M. J. Roberts, S. C. Chan, and C. A. Senior, 2014: Heavier summer downpours with climate change revealed by weather forecast resolution model. Nature Climate Change, 4, 570-576, doi: 10.1038/nclimate2258.

Knutti, R., D. Masson, and A. Gettelman, 2013: Climate model genealogy: Generation CMIP5 and how we got there. Geophysical Research Letters, 40, 1194-1199

Knutti, R., 2010: The end of model democracy? *Climatic Change*, 102, 395-404.

Knutti, R., and J. Sedlácek, 2013: Robustness and uncertainties in the new CMIP5 climate model projections. *Nature Climate Change*, 3, 369-373.

Knutti, R., R. Furrer, C. Tebaldi, J. Cermak, and G. A. Meehl, 2010: Challenges in combining projections from multiple climate models. *Journal of Climate*, 23, 2739-2758.

Langousis, A., and V. Kaleris, 2014: Statistical framework to simulate daily rainfall series conditional on upper-air predictor variables. Water Resources Research, 50, 3907-3932

Liang, X., D.P. Lettenmaier, E.F. Wood, and S.J. Burges. 1994. "A Simple Hydrologically Based Model of Land Surface Water and Energy Fluxes for General Circulation Models." *Journal of Geophysical Research*, 99, 14415-14428.

Liang, X., E.F. Wood, and D.P. Lettenmaier, 1996: Surface Soil Moisture Parameterization of the VIC-2L Model: Evaluation and Modification. *Global and Planetary Change*, 13(1-4), 195-206.

Lofgren, B. M., A. D. Gronewold, A. Acciaioli, J. Cherry, A. Steiner, and D. Watkins, 2013: Methodological Approaches to Projecting the Hydrologic Impacts of Climate Change. *Earth Interactions*, 17, 19, doi: 10.1175/2013ei000532.1.

Lorenz, E. N., 1963: Deterministic nonperiodic flow. Journal of the atmospheric sciences, 20, 130-141

Maraun, D., 2013: Bias correction, quantile mapping, and downscaling: Revisiting the inflation issue. Journal of Climate, 26, 2137-2143

E. P. Maurer, L. Brekke, T. Pruitt, B. Thrasher, J. Long, P. Duffy, M. Dettinger, D. Cayan, and J. Arnold, 2014: An Enhanced Archive Facilitating Climate Impacts and Adaptation Analysis. Bull. Amer. Meteor. Soc., 95, 1011–1019. doi: http://dx.doi.org/10.1175/BAMS-D-13-00126.1

Mearns, L., S. Sain, L. Leung, M. Bukovsky, S. McGinnis, S. Biner, D. Caya, R. Arritt, W. Gutowski, and E. Takle, 2013: Climate change projections of the North American regional climate change assessment program (NARCCAP). *Climatic Change*, 120, 965-975.

Melillo, J.M., T.C. Richmond, and G.W. Yohe, eds., 2014: *Climate Change Impacts in the United States: The Third National Climate Assessment*. Washington: U.S. Global Change Research Program, 841 p. <http://nca2014.globalchange.gov/report>

Mendoza, P. A., M. P. Clark, N. Mizukami, E. D. Gutmann, J. R. Arnold, L. D. Brekke, and B. Rajagopalan, 2016: How do hydrologic modeling decisions affect the portrayal of climate change impacts? Hydrological Processes, doi: 10.1002/hyp.10684.

Mendoza, P. A., M. P. Clark, N. Mizukami, A. J. Newman, M. Barlage, E. D. Gutmann, R. M. Rasmussen, B. Rajagopalan, L. D. Brekke, and J. R. Arnold, 2015: Effects of hydrologic model choice and calibration on the portrayal of climate change impacts. *Journal of Hydrometeorology*, 16, 762-780.

Miller, W. P., R. A. Butler, T. Piechota, J. Prairie, K. Grantz, and G. DeRosa, 2012: Water management decisions using multiple hydrologic models within the San Juan River basin under changing climate conditions. *Journal of Water Resources Planning and Management*, 138, 412-420.

Milly, P., and K. A. Dunne, 2011: On the hydrologic adjustment of climate-model projections: The potential pitfall of potential evapotranspiration. *Earth Interactions*, 15, 1-14.

Mizukami, N., M. P. Clark, E. Gutmann, P. A. Mendoza, A. J. Newman, B. Nijssen, B. Livneh, L. Hay, J. R. Arnold, and L. Brekke, 2015: Implications of the methodological choices for hydrologic portrayals of

climate change over the Contiguous United States: statistically downscaled forcing data and hydrologic models. *Journal of Hydrometeorology* (under review).

Monteith, J.L. 1965. "Evaporation and environment," Symposia of the Society for Experimental Biology 19: 205–224.

Mote, P., L. Brekke, P. B. Duffy, and E. Maurer, 2011: Guidelines for constructing climate scenarios. *Eos, Transactions American Geophysical Union*, 92, 257-258.

Murphy, J. M., B. B. Booth, M. Collins, G. R. Harris, D. M. Sexton, and M. J. Webb, 2007: A methodology for probabilistic predictions of regional climate change from perturbed physics ensembles. *Philosophical Transactions of the Royal Society of London A: Mathematical, Physical and Engineering Sciences*, 365, 1993-2028.

Murphy, J. M., D. M. Sexton, D. N. Barnett, G. S. Jones, M. J. Webb, M. Collins, and D. A. Stainforth, 2004: Quantification of modelling uncertainties in a large ensemble of climate change simulations. *Nature*, 430, 768-772.

Nijssen, B., D.P. Lettenmaier, X. Liang, S.W. Wetzel, and E.F. Wood. 1997: Streamflow Simulation for Continental-Scale River Basins. *Water Resources Research*, 33(4), 711-724.

Pierce, D. W., D. R. Cayan, E. P. Maurer, J. T. Abatzoglou, and K. C. Hegewisch, 2015: Improved Bias Correction Techniques for Hydrological Simulations of Climate Change*. Journal of Hydrometeorology, 16, 2421-2442

R Core Team (2015). R: A language and environment for statistical computing. R Foundation for Statistical Computing, Vienna, Austria. URL http://www.R-project.org/.

Rasmussen, R., C. H. Liu, K. Ikeda, D. Gochis, D. Yates, F. Chen, M. Tewari, M. Barlage, J. Dudhia, W. Yu, K. Miller, K. Arsenault, V. Grubisic, G. Thompson, and E. Gutmann, 2011: High-Resolution Coupled Climate Runoff Simulations of Seasonal Snowfall over Colorado: A Process Study of Current and Warmer Climate. Journal of Climate, 24, 3015-3048, doi: 10.1175/2010jcli3985.1.

Rasmussen, R., K. Ikeda, C. H. Liu, D. Gochis, M. P. Clark, A. Dai, E. Gutmann, J. Dudhia, F. Chen, M. Barlage, D. Yates, and G. Zhang, 2014: Climate Change Impacts on the Water Balance of the Colorado Headwaters: High-Resolution Regional Climate Model Simulations. Journal of Hydrometeorology, doi: 10.1175/JHM-D-13-0118.1.

Reclamation (Bureau of Reclamation), 2011a: *Reclamation, SECURE Water Act Section 9503(c) – Reclamation Climate Change and Water, Report to Congress, 2011*, Policy and Administration, Denver, CO, 206 p.

_____ 2011b: *West-Wide Climate Risk Assessments: Bias-Corrected and Spatially Downscaled Surface Water Projections*, Technical Memorandum No. 86-68210-2011-01, Technical Service Center, Denver, CO, 138 p.

_____ 2013: *Downscaled CMIP3 and CMIP5 Climate Projections: Release of Downscaled CMIP5 Climate Projections, Comparison with Preceding Information, and Summary of User Needs*. Downscaled CMIP3 and CMIP5 Climate and Hydrology Projections, U.S. Department of the Interior, Bureau of Reclamation, Technical Service Center, Denver, Colorado, 47 p.

Samaniego, L., R. Kumar, and S. Attinger, 2010: Multiscale parameter regionalization of a grid-based hydrologic model at the mesoscale. *Water Resources Research*, 46, W05523, doi:10.1029/2008WR007327.

Schewe, J., and Coauthors, 2014: Multimodel assessment of water scarcity under climate change. *Proc. Natl. Acad. Sci.*, U. S. A., 111, 3245-3250, doi: 10.1073/pnas.1222460110.

Sheffield, J., and others, 2014: *Regional Climate Processes and Projections for North America: CMIP3/CMIP5 Differences, Attribution and Outstanding Issue*, NOAA Technical Report OAR CPO-2.

Sheffield, J., E. F. Wood, and M. L. Roderick, 2012: Little change in global drought over the past 60 years. Nature, 491, 435-438

Stainforth, D. A., T. Aina, C. Christensen, M. Collins, N. Faull, D. J. Frame, J. A. Kettleborough, S. Knight, A. Martin, and J. Murphy, 2005: Uncertainty in predictions of the climate response to rising levels of greenhouse gases. *Nature*, 433, 403-406.

Stoner, A. M., K. Hayhoe, X. Yang, and D. J. Wuebbles, 2013: An asynchronous regional regression model for statistical downscaling of daily climate variables. International Journal of Climatology, 33, 2473-2494

Takle, E. S., W. J. Gutowski, R. W. Arritt, Z. Pan, C. J. Anderson, R. R. da Silva, D. Caya, S. C. Chen, F. Giorgi, and J. H. Christensen, 1999: Project to intercompare regional climate simulations (PIRCS): description and initial results. Journal of Geophysical Research: Atmospheres, 104, 19443-19461

Taylor, K. E., R. J. Stouffer, and G. A. Meehl, 2012: An Overview of CMIP5 and the Experiment Design. *Bulletin of the American Meteorological Society*, 93, 485–498, doi: http://dx.doi.org/10.1175/BAMS-D-11-00094.1.

Tebaldi, C., J. M. Arblaster, and R. Knutti, 2011: Mapping model agreement on future climate projections. *Geophysical Research Letters*, 38, L23701,doi:10.1029/2011GL049863.

Teutschbein, C., and J. Seibert, 2012: Bias correction of regional climate model simulations for hydrological climate-change impact studies: Review and evaluation of different methods. *Journal of Hydrology*, 456, 12-29.

Thornton, P.E., and S.W. Running, 1999: An improved algorithm for estimating incident daily solar radiation from measurements of temperature, humidity, and precipitation. *Agriculture and Forest Meteorology* 93, 211-228.

Thornton, P.E., H. Hasenauer, and M.A. White, 2000: Simultaneous estimation of daily solar radiation and humidity from observed temperature and precipitation: An application over complex terrain in Austria. *Agricultural and Forest Meteorology* 104 (4), 255–271.

Vano, J. A., B. Udall, D. R. Cayan, J. T. Overpeck, L. D. Brekke, T. Das, H. C. Hartmann, H. G. Hidalgo, M. Hoerling, and G. J. McCabe, 2014: Understanding uncertainties in future Colorado River streamflow. *Bulletin of the American Meteorological Society*, 95, 59-78.

Wehner, M. F., K. A. Reed, F. Li, J. Bacmeister, C. T. Chen, C. Paciorek, P. J. Gleckler, K. R. Sperber, W. D. Collins, and A. Gettelman, 2014: The effect of horizontal resolution on simulation quality in the Community Atmospheric Model, CAM5. 1. Journal of Advances in Modeling Earth Systems, 6, 980-997

Wilby, R. L., C. W. Dawson, C. Murphy, P. O'Connor, and E. Hawkins, 2014: The Statistical DownScaling Model - Decision Centric (SDSM-DC): conceptual basis and applications. Climate Research, 61, 259-276, doi: 10.3354/cr01254.

Wilby, R. L., 2005: Uncertainty in water resource model parameters used for climate change impact assessment. *Hydrological Processes*, 19, 3201-3219

Wilby, R. L., and I. Harris, 2006: A framework for assessing uncertainties in climate change impacts: Low-flow scenarios for the River Thames, UK. *Water Resources Research*, 42, W02419, doi: 10.1029/2005WR004065.

Wood, A. W., L. R. Leung, V. Sridhar, and D. Lettenmaier, 2004: Hydrologic implications of dynamical and statistical approaches to downscaling climate model outputs. Climatic change, 62, 189-216

Yang, Z., and R. W. Arritt, 2002: Tests of a perturbed physics ensemble approach for regional climate modeling. Journal of Climate, 15, 2881-2896